95 and 125 GeV Higgs boson excesses in the left-right supersymmetric standard model

Zhi-Chuan Wang,[1,2,*] Jin-Lei Yang,[1,2,3,†] Qi-Zhen Qin,[1,2,3,‡] Wen-Hui Zhang,[1,2,§] and Tai-Fu Feng[1,2,3,‖]

[1]*College of Physics Science and Technology, Hebei University, Baoding 071002, China*

[2]*Hebei Key Laboratory of High-precision Computation and Application of Quantum Field Theory, Baoding 071002, China*

[3]*Research Center for Computational Physics of Hebei Province, Baoding 071002, China*

(Received 9 February 2025; accepted 11 February 2026; published 24 March 2026)

This study investigates the excesses observed around 95 GeV in diphoton and $b\bar{b}$ experiments within the framework of the left-right supersymmetric model (LRSSM). Considering the one- and two-loop effective potential corrections to the Higgs masses, the model is able to describe the experimentally observed $\mu(h_{95})_{\gamma\gamma}$ and $\mu(h_{95})_{b\bar{b}}$ signal strengths. In addition, we also present the impacts of the LRSSM-specific parameters $\tan\beta_R$, v_R, and v_S on the theoretical predictions of the signal strengths for the 95 and 125 GeV neutral Higgs bosons.

DOI: 10.1103/t865-lq98

I. INTRODUCTION

In 2012, the Large Hadron Collider (LHC) discovered a Higgs boson with a mass of 125 GeV [1,2], marking a notable success for the standard model (SM). However, this discovery did not halt the quest for new physics (NP) at the LHC. Researchers have since focused on searching for lighter scalar particles, conducting experiments at facilities like the large electron positron (LEP) [3–5] and LHC. Notably, both the CMS and LEP experiments have reported an excess signal in a similar mass range. CMS, in particular, using a total integrated luminosity of 19.7 fb^{-1} at 8 TeV and 35.9 fb^{-1} at 13 TeV, searched for scalar diphoton resonances at 8 and 13 TeV [6–8]. These investigations reveal a local excess of 2.8σ at around 95.3 GeV [9]. This unexpected result has generated considerable interest and discussion within the scientific community regarding potential implications for NP models. Analyses in Refs. [10–22] demonstrate that, within the framework of the next-to-minimal supersymmetric standard model, the diphoton production rate for a scalar with a given mass can significantly exceed the rate predicted by the SM, sometimes by several multiples. In the two-Higgs-doublet model with an additional real singlet, Refs. [23–28] have explored the potential to account for the observed excess. In Ref. [29], the authors explore the feasibility of Higgs radion mixing at 125 GeV and the potential of a light radion to explain the CMS diphoton excess within the Higgs radion mixing model. Considering the one-loop corrections to the neutral scalar mass in the $\mu\nu$ supersymmetric standard model ($\mu\nu$SSM), the authors of Refs. [30,31] demonstrate how the $\mu\nu$SSM could simultaneously accommodate the two excesses observed at LEP and LHC at the 1σ level. Based on the analysis in Ref. [32], an extended scalar sector with an $SU(2)_L$ triplet (hypercharge $Y = 0$) can effectively explain the 95 GeV excess. References [33–36] reviewed whether certain model implementations could simultaneously explain both excesses while remaining consistent with all other Higgs-boson-related constraints and measurements.

In this paper, we investigate two possible scenarios in the left-right supersymmetric model (LRSSM) [37–54]. In the first scenario, the lightest Higgs boson is 125 GeV, analogous to the Higgs boson predicted by the SM. In the second scenario, the model contains both 95 and 125 GeV Higgs bosons, which could provide an explanation for the observed excesses of the 95 GeV in the LEP and LHC experiments. The LRSSM, based on the gauge group $SU(3) \times SU(2)_L \times SU(2)_R \times U(1)_{B-L}$, extends the minimal supersymmetric standard model (MSSM) by including triplet scalars that interact with leptons to generate the nonzero neutrino masses through the seesaw mechanism [55]. The observed neutrino flavor oscillations provide definite experimental evidence for physics beyond the SM. Furthermore, the LRSSM resolves some issues faced by the MSSM, such as the strong and electroweak *CP*

*Contact author: wangzc1020@163.com
†Contact author: jlyang@hbu.edu.cn
‡Contact author: 18403586107@163.com
§Contact author: zwh_0218@163.com
‖Contact author: fengtf@hbu.edu.cn

Published by the American Physical Society under the terms of the Creative Commons Attribution 4.0 International license. Further distribution of this work must maintain attribution to the author(s) and the published article's title, journal citation, and DOI. Funded by SCOAP³.

problems [56]. Moreover, in the LRSSM, the gauge structure naturally preserves R parity, ensuring the stability of the lightest supersymmetric particle (LSP), which is thus a natural dark-matter candidate. In this framework, there are two typical LSP candidates: a neutralinolike LSP or a right-handed sneutrino LSP. The neutralinolike LSP is a mixture of the gaugino and Higgsino states, and its relic density is often constrained by coannihilation processes with other supersymmetric particles. On the other hand, the right-handed sneutrino, being a Majorana particle, is another viable LSP candidate. The stability of the LSP in both cases is crucial for its role as dark matter. Furthermore, the relic density of these LSPs must comply with observational limits, and direct-detection experiments place additional constraints on their properties. The interplay between relic-density constraints and direct-detection limits determines the allowed parameter space of the LRSSM, which is crucial for understanding its implications for dark matter and particle physics [50,57]. This work is motivated by the rich Higgs sector in the LRSSM, in which a large number of Higgs bosons are introduced, including bidoublets, triplets, and the singlet Higgs bosons [58]. We propose that a real neutral scalar boson from this model, with the right properties, can explain the 95 GeV excess observed in the LHC and LEP data.

The structure of this paper is as follows. Section II provides a brief introduction to the LRSSM. In Sec. III, we investigate the 125 and 95 GeV excesses within the LRSSM. Section IV presents the numerical analysis, and Sec. V concludes with our findings.

II. THE LRSSM MODEL

The LRSSM is based on the $SU(3)\times SU(2)_L\times SU(2)_R\times U(1)_{B-L}$ gauge group. The model includes the additional local gauge group $SU(2)_R$, resulting in extra $W_R^{\pm}$ gauge bosons. Furthermore, it incorporates a $U(1)_{B-L}$ gauge group, which produces an additional Z_R^0 boson upon gauge symmetry breaking. Additionally, multiple types of Higgs bosons are introduced into the LRSSM, including bidoublets, triplets, and singlet Higgs bosons. The superpotential of the LRSSM is given by [59]

$$\begin{aligned} W = {} & Q_L^T Y_Q^i \Phi_i Q_R + L_L^T Y_L^i \Phi_i L_R + L_L^T h_{LL}\delta_L L_R \\ & + L_R^T h_{RR}\Delta_R L_R + \lambda_L S\mathrm{Tr}[\Delta_L\delta_L] + \lambda_R S\mathrm{Tr}[\Delta_R\delta_R] \\ & + \lambda_3 S\mathrm{Tr}[\tau_2\Phi_1^T\tau_2\Phi_2] + \lambda_4 S\mathrm{Tr}[\tau_2\Phi_1^T\tau_2\Phi_1] \\ & + \lambda_5 S\mathrm{Tr}[\tau_2\Phi_2^T\tau_2\Phi_2] + \lambda_S S^3 + \xi_F S, \end{aligned} \tag{1}$$

where the $Q_{L(R)}$ and $L_{L(R)}$ are quark and lepton superfields,

$$\begin{aligned} Q_L &= \begin{pmatrix} u_L \\ d_L \end{pmatrix} \sim \left(3,2,1,\frac{1}{3}\right), \qquad Q_R = \begin{pmatrix} d_R \\ -u_R \end{pmatrix} \sim \left(3,1,2,-\frac{1}{3}\right), \\ L_L &= \begin{pmatrix} \nu_L \\ e_L \end{pmatrix} \sim (1,2,1,-1), \qquad L_R = \begin{pmatrix} e_R \\ -\nu_R \end{pmatrix} \sim (1,1,2,1), \end{aligned} \tag{2}$$

and the $\Phi_{i(i=1,2)}, \Delta_{R(L)}, \delta_{R(L)}, S$ are Higgs fields [60].

$$\begin{aligned} \Phi_1 &= \begin{pmatrix} \Phi_{11}^+ & H_{11}^0 \\ H_{12}^0 & \Phi_{12}^- \end{pmatrix} \sim (1,2,2,0), \qquad \Phi_2 = \begin{pmatrix} \Phi_{21}^+ & H_{21}^0 \\ H_{22}^0 & \Phi_{22}^- \end{pmatrix} \sim (1,2,2,0), \\ \Delta_L &= \begin{pmatrix} \frac{\Delta_L^-}{\sqrt{2}} & H_{\Delta_L}^0 \\ \Delta_L^{--} & \frac{-\Delta_L^-}{\sqrt{2}} \end{pmatrix} \sim (1,3,1,-2), \qquad \delta_L = \begin{pmatrix} \frac{\delta_L^+}{\sqrt{2}} & \delta_L^{++} \\ H_{\delta_L}^0 & \frac{-\delta_L^+}{\sqrt{2}} \end{pmatrix} \sim (1,3,1,2), \\ \delta_R &= \begin{pmatrix} \frac{\delta_R^+}{\sqrt{2}} & \delta_R^{++} \\ H_{\delta_R}^0 & \frac{-\delta_R^+}{\sqrt{2}} \end{pmatrix} \sim (1,1,3,2), \qquad \Delta_R = \begin{pmatrix} \frac{\Delta_R^-}{\sqrt{2}} & H_{\Delta_R}^0 \\ \Delta_R^{--} & \frac{-\Delta_R^-}{\sqrt{2}} \end{pmatrix} \sim (1,1,3,-2), \\ S &= H_S^0 \sim (1,1,1,0), \end{aligned} \tag{3}$$

where we assume the $SU(2)_L$ triplets Δ_L and δ_L to be inert. The electroweak symmetry is broken when those Higgs fields acquire some nonzero vacuum expectation value (VEV) space.

$$\Phi_1 = \begin{pmatrix} 0 & \frac{1}{\sqrt{2}} v_1' e^{i\alpha_1} \\ \frac{1}{\sqrt{2}} v_1 & 0 \end{pmatrix}, \qquad \Phi_2 = \begin{pmatrix} 0 & \frac{1}{\sqrt{2}} v_2 \\ \frac{1}{\sqrt{2}} v_2' e^{i\alpha_2} & 0 \end{pmatrix},$$
$$\Delta_R = \begin{pmatrix} 0 & \frac{1}{\sqrt{2}} v_{R1} \\ 0 & 0 \end{pmatrix}, \qquad \delta_R = \begin{pmatrix} 0 & 0 \\ \frac{1}{\sqrt{2}} v_{R2} & 0 \end{pmatrix}, \qquad S = \frac{1}{\sqrt{2}} v_S e^{i\alpha_S}. \tag{4}$$

Within the framework of the LRSSM, the two Higgs doublets H_u and H_d from the MSSM are embedded into the bidoublet fields. Specifically, H_u can be expressed as a superposition of H_{12}^0 and H_{22}^0, while H_d is a superposition of H_{11}^0 and H_{21}^0. Furthermore, we introduce two parameters $\tan\beta = v_2/v_1$ and $\tan\beta_R = v_{R2}/v_{R1}$, where $v_1^2 + v_2^2 = 246\ \mathrm{GeV}^2$. The CP-violating mixing between $W_L^\pm$ and $W_R^\pm$ depends on terms proportional to $v_1 v_1' e^{i\alpha_1}$ and $v_2 v_2' e^{i\alpha_2}$. This mixing is tightly constrained to be small due to experimental limits from $K^0 - \overline{K^0}$ mixing data. To simplify the analysis and reduce the complexity of the parameter space, we adopt an assumed hierarchy,

$$v_{R1}, v_{R2}, v_S \gg v_1, v_2, v_1', v_2' \quad \text{and} \quad v_1' = v_2' = \alpha_1 = \alpha_2 = \alpha_S = 0. \tag{5}$$

In the supersymmetric limit, the F-terms and D-terms vanish, when $\lambda_R v_{R1} v_{R2} = \xi_F$ and $v_{R1} = v_{R2}$ [61]. On the other hand, the singlet VEV v_S is induced by the supersymmetry- (SUSY) breaking linear term ξ_S so that its natural scale is the supersymmetry-breaking scale. The right-hand symmetry-breaking scale is chosen larger than the SUSY-breaking scale, so the superpartner masses are lighter than the heavy $W_R^\pm$ and Z_R^0 gauge bosons [62–64]. For simplicity, the left-handed Δ_L and δ_L fields do not develop nonzero VEVs, and hence the neutrino masses do not get any contribution from type II seesaw. Then the soft supersymmetry-breaking Lagrangian of the LRSSM is generally given as

$$\begin{aligned} L_{\mathrm{soft}} = & -\frac{1}{2}\{M_1 \tilde{B}\cdot\tilde{B} + M_{2L}\tilde{W}_L^k \cdot \tilde{W}_{Lk} + M_{2R}\tilde{W}_R^k \cdot \tilde{W}_{Rk} + M_3 \tilde{g}^a \cdot \tilde{g}_a + \mathrm{H.c.}\} \\ & - \tilde{Q}_L^\dagger m_{Q_L}^2 \tilde{Q}_L - \tilde{Q}_R m_{Q_R}^2 \tilde{Q}_R^\dagger - \tilde{L}_L^\dagger m_{L_L}^2 \tilde{L}_L - \tilde{L}_R m_{L_R}^2 \tilde{L}_R^\dagger \\ & - (m_\Phi^2)^{f'f}\mathrm{Tr}(\Phi_f^\dagger \Phi_{f'}) - m_{\Delta_L}^2 \mathrm{Tr}(\Delta_L^\dagger \Delta_L) - m_{\delta_L}^2 \mathrm{Tr}(\delta_L^\dagger \delta_L) \\ & - m_{\Delta_R}^2 \mathrm{Tr}(\Delta_R^\dagger \Delta_R) - m_{\delta_R}^2 \mathrm{Tr}(\delta_R^\dagger \delta_R) - m_S^2 S^\dagger S \\ & - \{S[T_L \mathrm{Tr}(\Delta_L \delta_L) + T_R \mathrm{Tr}(\Delta_R \delta_R) + T_3 \mathrm{Tr}(\Phi_1^T \tau_2 \Phi_2 \tau_2) + T_4 \mathrm{Tr}(\Phi_1^T \tau_2 \Phi_1 \tau_2) \\ & + T_5 \mathrm{Tr}(\Phi_2^T \tau_2 \Phi_2 \tau_2) + T_S S^2 + \xi_S] + \mathrm{H.c.}\} + \{T_Q^1 (\tilde{Q}_L)^T \Phi_1 \tilde{Q}_R + T_Q^2 (\tilde{Q}_L)^T \Phi_2 \tilde{Q}_R \\ & + T_L^1 (\tilde{L}_L)^T \Phi_1 \tilde{L}_R + T_L^2 (\tilde{L}_L)^T \Phi_2 \tilde{L}_R + T_L^3 (\tilde{L}_L)^T \delta_L \tilde{L}_L + T_L^4 (\tilde{L}_R)^T \Delta_R \tilde{L}_R + \mathrm{H.c.}\}. \end{aligned} \tag{6}$$

We obtain the hierarchy $v_1, v_2 \gg v_1', v_2' \approx 0$ by setting small values for λ_4, λ_5, and the corresponding SUSY-breaking terms, which helps to reduce the mixing in the Higgs mass matrix and facilitates the calculation [59]. The D-term contribution to the scalar potential (neglecting the squark pieces) is given by

$$\begin{aligned} V_D = \sum_i \Big[& \frac{g_L^2}{8} |\mathrm{Tr}(2\Delta_L^\dagger \tau_i \Delta_L + 2\delta_L^\dagger \tau_i \delta_L + \Phi_1^\dagger \tau_i \Phi_1 + \Phi_2^\dagger \tau_i \Phi_2) + \tilde{L}_L^\dagger \tau_i \tilde{L}_L|^2 \\ & + \frac{g_R^2}{8} |\mathrm{Tr}(2\Delta_R^\dagger \tau_i \Delta_R + 2\delta_R^\dagger \tau_i \delta_R + \Phi_1^\dagger \tau_i \Phi_1 + \Phi_2^\dagger \tau_i \Phi_2) + \tilde{L}_R^\dagger \tau_i \tilde{R}_L|^2 \Big] \\ & + \frac{g_{B-L}^2}{2} [\mathrm{Tr}(-\Delta_L^\dagger \Delta_L + \delta_L^\dagger \delta_L - \Delta_R^\dagger \Delta_R + \delta_R^\dagger \delta_R) - \tilde{L}_L^\dagger \tilde{L}_L + \tilde{L}_R^\dagger \tilde{L}_R]. \end{aligned} \tag{7}$$

The F-term contribution to the scalar potential is given by

$$V_F = |\lambda_L \mathrm{Tr}(\Delta_L \delta_L) + \lambda_R \mathrm{Tr}(\Delta_R \delta_R) + \lambda_3 \mathrm{Tr}(\tau_2 \Phi_2^\dagger \tau_2 \Phi_2) + \lambda_4 \mathrm{Tr}(\tau_2 \Phi_1^\dagger \tau_2 \Phi_1) + \lambda_5 \mathrm{Tr}(\tau_2 \Phi_2^\dagger \tau_2 \Phi_2) + 3\lambda_S S^2 + \xi_F|^2 + \mathrm{Tr}(|\lambda_L S \delta_L|^2 + |\lambda_L S \Delta_L|^2 + |\lambda_R S \Delta_R|^2 + |\lambda_R S \delta_R|^2) + \mathrm{Tr}(|\lambda_3 S \Phi_2 + \lambda_4 S \Phi_1|^2 + |\lambda_3 S \Phi_1 + \lambda_5 S \Phi_2|^2). \quad (8)$$

The effective potential is

$$V_{\mathrm{eff}} = V_0 + \Delta V, \quad (9)$$

where

$$V_0 = -L_{\mathrm{soft}} + V_D + V_F, \qquad \Delta V = V_1 + V_2. \quad (10)$$

The V_1 is the one-loop-level effective potential and V_2 is the two-loop-level effective potential [65–68]. With the adoption of the dimensional reduction renormalization scheme, the effective Higgs potential up to the one-loop correction is presented in the Landau gauge, and the specific form of ΔV is given in [69,70]

$$\Delta V = \sum_i \frac{n_i}{64\pi^2} m_i^4(\phi_1, \phi_2, \phi_{\Delta_R}, \phi_{\delta_R}, \phi_s) \times \left(\log \frac{m_i^2(\phi_1, \phi_2, \phi_{\Delta_R}, \phi_{\delta_R}, \phi_s)}{Q^2} - \frac{3}{2} \right). \quad (11)$$

We denote the degrees of freedom for each mass eigenstate by n_i [-12 for quarks, -4 for leptons and charginos, -2 for neutralinos and neutrinos, 6 for squarks, 2 for sleptons and charged Higgs bosons, 3 and 6 for $Z(Z')$ and $W_1(W_2)$ bosons, and 1 for sneutrinos and the neutral Higgs scalars]. The specific potential for the one-loop correction is as follows:

$$\Delta V = V_t + V_b + V_\tau + V_{\nu_R} + V_{\tilde{u}_i} + V_{\tilde{d}_i} + V_{\tilde{e}_i} + V_{\tilde{\nu}_i} + V_{W_1,W_2} + V_{Z,Z'} + V_{\chi_i^0} + V_{H_i^\pm} + V_{\chi_i^\pm}. \quad (12)$$

Here, V_t, V_b, and V_τ represent the one-loop effective potential corrections from t, b, and τ. $V_{\tilde{u}_i}$ and $V_{\tilde{d}_i}$ represent the corrections from scalar up- and down-type quarks. $V_{\tilde{e}_i}$ represents the corrections from sleptons. $V_{\tilde{\nu}_i}$ represents the corrections from sneutrinos. V_{W_L,W_R}, V_{Z_L,Z_R}, V_{χ^0}, $V_{H^\pm}$, and $V_{\chi^\pm}$ represent the corrections from the $W_1(W_2)$ boson, $Z(Z')$ boson, neutralinos, charged Higgs bosons, and charginos, respectively. The two-loop effective potential is mainly contributed by top quarks, scalar top quarks, gluons, and gluinos, in units of $\alpha_s C_F N_c^f/(4\pi)^3$ where $C_F = 4/3$ and $N_c^f = 3$ are color factors. The V_2 reads [68]

$$V_2 = 2J(m_t^2, m_t^2) - 4m_t^2 I(m_t^2, m_t^2, 0) + \{2m_{\tilde{t}1}^2 I(m_{\tilde{t}1}^2, m_{\tilde{t}1}^2, 0) + 2L(m_{\tilde{t}1}^2, m_{\tilde{g}}^2, m_t^2) - 4m_t m_{\tilde{g}} s_{2\tilde{\theta}} c_{\varphi-\tilde{\varphi}} I(m_{\tilde{t}1}^2, m_{\tilde{g}}^2, m_t^2) + \frac{1}{2}(1 + c_{2\tilde{\theta}}^2) J(m_{\tilde{t}1}^2, m_{\tilde{t}1}^2) + \frac{s_{2\tilde{\theta}}^2}{2} J(m_{\tilde{t}1}^2, m_{\tilde{t}2}^2) + [m_{\tilde{t}1} \leftrightarrow m_{\tilde{t}2}, s_{2\tilde{\theta}} \to -s_{2\tilde{\theta}}]\}, \quad (13)$$

where m_t and m_b masses of the top and bottom quarks, $m_{\tilde{t}_i}$ and $m_{\tilde{b}_i}$ are the masses of the scalar top quarks and scalar bottom quarks, and $m_{\tilde{g}}$ is the gluino mass, respectively. The two-loop functions $I, J, s_{2\theta}, c_{\varphi-\tilde{\varphi}}$ in Eq. (13) can be found in Appendix D of Ref. [68]. The squared pole masses of a set of n scalar bosons that mix with each other are the real parts of the solutions for p^2 of the equation [68,71–75]

$$\det[\Gamma_{ij}(p^2)] = 0, \quad (14)$$

where $\Gamma_{ij}(p^2)$ is the $n \times n$ inverse propagator matrix and p denotes the incoming external momentum of the self-energies. Generally, $\Gamma_{ij}(p^2)$ can be decomposed as

$$-i\Gamma_{ij}(p^2) = p^2 \delta_{ij} - M_{ij,0}^2 - \Delta M_{ij}^2(p^2), \quad (15)$$

where $M_{ij,0}^2$ is the tree-level squared mass matrix, and $\Delta M_{ij}^2(p^2)$ are the radiative corrections to the squared matrix, respectively.

In the limit of vanishing external momentum, tadpole and self-energy diagrams can be obtained through the derivatives of the effective potential; thus, one has

$$T_i = -\left.\frac{\partial V_{\mathrm{eff}}}{\partial \phi_i}\right|_{\mathrm{min}}, \qquad \Pi_{ij}(0) = -\left.\frac{\partial^2 \Delta V}{\partial \phi_i \partial \phi_j}\right|_{\mathrm{min}}, \qquad \Delta M_{ij}^2(p^2) = \Pi(p^2) - \Pi_{ij}(0) - \frac{\partial^2 \Delta V}{\partial \phi_i \partial \phi_j}, \quad (16)$$

where the detailed calculations of the contributions from $\Delta M_{ij}^2(p^2)$ in Eq. (16) are collected in Appendix D. In the basis $(\mathrm{Re}[H_{12}^0], \mathrm{Re}[H_{21}^0], \mathrm{Re}[H_{\Delta_R}^0], \mathrm{Re}[H_{\delta_R}^0], \mathrm{Re}[H_S^0])$, the tree-level squared mass matrix of the CP-even Higgs fields is written as [refer to Eq. (3) for the notation]

$$m^2_{H_3} = \begin{pmatrix} m^2_{H^0_{12}H^0_{12}} & m^2_{H^0_{12}H^0_{21}} & m^2_{H^0_{12}H^0_{\Delta_R}} & m^2_{H^0_{12}H^0_{\delta_R}} & m^2_{H^0_{12}H^0_S} \\ m^2_{H^0_{21}H^0_{12}} & m^2_{H^0_{21}H^0_{21}} & m^2_{H^0_{21}H^0_{\Delta_R}} & m^2_{H^0_{21}H^0_{\delta_R}} & m^2_{H^0_{21}H^0_S} \\ m^2_{H^0_{\Delta_R}H^0_{12}} & m^2_{H^0_{\Delta_R}H^0_{21}} & m^2_{H^0_{\Delta_R}H^0_{\Delta_R}} & m^2_{H^0_{\Delta_R}H^0_{\delta_R}} & m^2_{H^0_{\Delta_R}H^0_S} \\ m^2_{H^0_{\delta_R}H^0_{12}} & m^2_{H^0_{\delta_R}H^0_{21}} & m^2_{H^0_{\delta_R}H^0_{\Delta_R}} & m^2_{H^0_{\delta_R}H^0_{\delta_R}} & m^2_{H^0_{\delta_R}H^0_S} \\ m^2_{H^0_SH^0_{12}} & m^2_{H^0_SH^0_{21}} & m^2_{H^0_SH^0_{\Delta_R}} & m^2_{H^0_SH^0_{\delta_R}} & m^2_{H^0_SH^0_S} \end{pmatrix}. \tag{17}$$

The matrix elements are defined as

$$\begin{aligned}
m^2_{H^0_{12}H^0_{12}} &= \frac{1}{8}(8m_1^2 + 3g_R^2v_1^2 - g_R^2v_2^2 + g_L^2(3v_1^2 - v_2^2) + 2g_R^2v_{R2}^2 + 4\lambda_3^2v_2^2 + 4\lambda_3^2v_S^2), \\
m^2_{H^0_{12}H^0_{21}} &= \frac{1}{4}(-g_L^2v_1v_2 - g_R^2v_1v_2 - 2(\sqrt{2}T_3v_S + \lambda_3(-2\lambda_3v_1v_2 + \lambda_Rv_{R1}v_{R2} + 3\lambda_Sv_S^2 + 2\xi_F))), \\
m^2_{H^0_{12}H^0_{\Delta_R}} &= \frac{1}{2}(g_R^2v_1v_{R1} - \lambda_3\lambda_Rv_2v_{R2}), \qquad m^2_{H^0_{12}H^0_{\delta_R}} = \frac{1}{2}(-g_R^2v_1v_{R2} - \lambda_3\lambda_Rv_2v_{R1}), \\
m^2_{H^0_{12}H^0_S} &= -\frac{T_3v_2}{\sqrt{2}} + \lambda_3v_S(\lambda_3v_1 - 3\lambda_Sv_2), \qquad m_{H^0_{21}H^0_S} = \frac{1}{2}(g_R^2v_2v_{R2} - \lambda_3\lambda_Rv_1v_{R1}), \\
m^2_{H^0_{21}H^0_{21}} &= \frac{1}{8}(8m_2^2 - g_R^2v_1^2 + 3g_R^2v_2^2 - g_L^2(v_1^2 - 3v_2^2) - 2g_R^2v_{R1}^2 + 2g_R^2v_{R2}^2 + 4\lambda_3^2v_1^2 + 4\lambda_3^2v_S^2), \\
m^2_{H^0_{21}H^0_{\Delta_R}} &= \frac{1}{2}(-g_R^2v_2v_{R1} - \lambda_3\lambda_Rv_1v_{R2}), \qquad m^2_{H^0_{21}H^0_{\delta_R}} = \frac{1}{2}(g_R^2v_2v_{R2} - \lambda_3\lambda_Rv_1v_{R1}), \\
m^2_{H^0_{\Delta_R}H^0_{\Delta_R}} &= \frac{1}{4}(4m^2_{\Delta_R} + g_R^2(v_1^2 - v_2^2 + 6v_{R1}^2 - 2v_{R2}^2) + 2g_B^2(3v_{R1}^2 - v_{R2}^2) + 2\lambda_R^2(v_{R2}^2 + v_S^2)), \\
m^2_{H^0_{\Delta_R}H^0_{\delta_R}} &= -g_B^2v_{R1}v_{R2} - g_R^2v_{R1}v_{R2} + \frac{T_Rv_S}{\sqrt{2}} - \frac{1}{2}\lambda_3\lambda_Rv_1v_2 + \lambda_R^2v_{R1}v_{R2} + \frac{3}{2}\lambda_S\lambda_Rv_S^2 + \lambda_R\xi_F, \\
m^2_{H^0_{\Delta_R}H^0_S} &= \frac{T_Rv_{R2}}{\sqrt{2}} + \lambda_Rv_S(\lambda_Rv_{R1} + 3\lambda_Sv_{R2}), \qquad m^2_{H^0_{\delta_R}H^0_S} = \frac{T_Rv_{R1}}{\sqrt{2}} + \lambda_Rv_S(\lambda_Rv_{R2} + 3\lambda_Sv_{R1}), \\
m^2_{H^0_{\delta_R}H^0_{\delta_R}} &= \frac{1}{4}(4m^2_{\delta_R} - 2g_B^2v_{R1}^2 + 6g_B^2v_{R2}^2 + g_R^2(-v_1^2 + v_2^2 - 2v_{R1}^2 + 6v_{R2}^2) + 2\lambda_R^2v_{R1}^2 + 2\lambda_R^2v_S^2), \\
m^2_{H^0_SH^0_S} &= \frac{1}{2}(2m_S^2 + 6\sqrt{2}T_Sv_S + \lambda_3^2(v_1^2 + v_2^2 + v_{R1}^2 + v_{R2}^2) - 6\lambda_3\lambda_S(v_1v_2 + v_{R1}v_{R2}) \\
&\quad + 54\lambda_S^2v_S^2 + 12\lambda_S\xi_F).
\end{aligned} \tag{18}$$

This mass matrix can be diagonalized by the rotation matrix Z^H as $Z^H m_H^2 Z^{H^\dagger} = m^2_{H,\mathrm{diag}}$, and the relationship between the Higgs bosons H_i (with $i = 1$–5) in the mass eigenstates and the gauge eigenstates $\phi_{a(a=1,2,\Delta_R,\delta_R,S)}$ are given by $H_i = \sum_a Z^H_{ia}\phi_a$. The squared mass matrix of other Higgs fields is given in Appendix A. In our calculation, we consider the radiative corrections originating from the third generation quarks and scalar quarks up to two-loop level [58]. Although we have considered the one-loop effective potential and partial contributions from the two-loop effective potential, the portions of the two-loop effective potential not included may introduce some uncertainty. The experimental uncertainty in the top quark mass, $m_t = 173.2 \pm 0.9$ GeV, has a direct impact on the Higgs mass calculation; therefore, this error range has been included in our results. Furthermore, QCD effects and the choice of the renormalization scale may also lead to variations in the calculated results, making these scale uncertainties another source of error. So, the theoretical error in the SM-like Higgs boson mass calculation allows for a mass range of 122–128 GeV [76–80].

III. HIGGS-BOSON SIGNALS IN THE LRSSM

At the LHC, h^0 is produced chiefly from the gluon fusion ($gg \to h^0$). The one-loop diagrams with virtual top quarks have the most significant contribution to the leading order (LO). In the LRSSM, the LO contributions need to be

added by the Higgs-new-particle couplings, whose effects are significant. So the decay width of $h^0 \to gg$ can be shown as [81–83]

$$\Gamma_{\rm NP}(h^0 \to gg) = \frac{G_F \alpha_s^2 m_{h^0}^3}{64\sqrt{2}\pi^3}\left|\sum_q g_{h^0 qq} A_{\frac{1}{2}}^H(x_q) + \sum_{\tilde{q}} g_{h^0 \tilde{q}\tilde{q}} \frac{m_Z^2}{m_{\tilde{q}}^2} A_0^H(x_{\tilde{q}})\right|^2, \tag{19}$$

with $x_a = m_{h^0}^2/(4m_a^2)$. Here, q and $\tilde{q}$ are quarks and squarks. The LO contributions for decay $h^0 \to \gamma\gamma$ also originate from one-loop diagrams. In the SM, the concrete contributions are mainly derived from top quark and charged gauge bosons $W_1^{\pm}$. Because of the Higgs-new-particle couplings in the LRSSM, the decay width of $h^0 \to \gamma\gamma$ can be expressed as [81–85]

$$\begin{aligned}\Gamma_{\rm NP}(h^0 \to \gamma\gamma) = \frac{G_F \alpha_s^2 m_{h^0}^3}{128\sqrt{2}\pi^3}\Bigg|&\sum_f N_c Q_f^2 g_{h^0 ff} A_{\frac{1}{2}}^H(x_f) + \sum_f g_{h^0 \tilde{f}\tilde{f}} \frac{m_Z^2}{m_{\tilde{f}}^2} A_0^H(x_{\tilde{f}}) \\ &+ \sum_{i=1}^{2} g_{h^0 H_i^+ H_i^-} \frac{m_Z^2}{m_{h_i^{\pm}}^2} A_0^H(x_{H_i^{\pm}}) + \sum_{j=1}^{2} g_{h^0 H_j^{++} H_j^{--}} \frac{m_Z^2}{m_{h_j^{\pm\pm}}^2} A_0^H(x_{H_j^{\pm\pm}}) \\ &+ \sum_{k=1}^{2} g_{h^0 \chi_k^+ \chi_k^-} \frac{m_Z^2}{m_{\chi_k^{\pm}}^2} A_{\frac{1}{2}}^H(x_{\chi_k^{\pm}}) + g_{h\chi^{++}\chi^{--}} \frac{m_Z^2}{m_{\chi^{\pm\pm}}^2} A_{\frac{1}{2}}^H(x_{\chi^{\pm\pm}}) \\ &+ g_{h^0 WW} A_1^H(x_W)\Bigg|^2,\end{aligned} \tag{20}$$

with $\chi_i^{\pm}$ denoting the charginos and $\chi_i^{\pm\pm}$ denoting the doubly charged charginos. The functions $A_1^H(x)$, $A_{1/2}^H(x)$, $A_0^H(x)$, and $g(x)$ are given by

$$\begin{aligned} A_1^H(x) &= -(2x^2 + 3x + 3(2x-1)g(x))/x^2, \\ A_{\frac{1}{2}}^H(x) &= 2(x + (x-1)g(x))/x^2, \\ A_0^H(x) &= -(x - g(x))/x^2, \\ g(x) &= \begin{cases} \arcsin^2\sqrt{x}, & x \le 1, \\ -\frac{1}{4}\left[ln\frac{1+\sqrt{1-1/x}}{1-\sqrt{1-1/x}} - i\pi\right]^2, & x > 1. \end{cases} \end{aligned} \tag{21}$$

The decay width for $h^0 \to VV^*(V = W_1, Z)$ is given by [86,87]

$$\Gamma_{\rm NP}(h^0 \to W_1 W_1^*) = \frac{g_2^4 m_{h^0}}{3072\pi^3} |g_{h^0 W_1 W_1}|^2 F(\epsilon), \tag{22}$$

$$\Gamma_{\rm NP}(h^0 \to ZZ^*) = \frac{g_2^4 m_{h^0}}{2048\pi^3 c_W^4}\left(7 - \frac{40 s_W^2}{3} + \frac{160 s_W^4}{9}\right)|g_{h^0 ZZ}|^2 F(\epsilon'), \tag{23}$$

where

$$\begin{aligned} F(x) = &\frac{3(1 - 8x^2 + 20x^4)}{(4x^2-1)^2}\arccos\left(\frac{3x^2-1}{2x^3}\right) - (1-x^2)\left(\frac{47x^2}{2} - \frac{13}{2} + \frac{1}{x^2}\right) \\ &- 3(1 - 6x^2 + 4x^4)\ln x \end{aligned} \tag{24}$$

and $\epsilon = m_W/m_h$, $\epsilon' = m_Z/m_h$. In the Born approximation, the partial decay widths of CP-even Higgs bosons decaying into fermion pairs are given by [88]

$$\Gamma_{\rm NP}(h^0 \to f\bar{f}) = \frac{N_c G_F m_f^2 m_{h^0}}{4\sqrt{2}\pi} |g_{h^0 ff}|^2 \left(1 - \frac{4m_f^2}{m_{h^0}^2}\right)^{\frac{3}{2}}. \tag{25}$$

The total decay width of the light CP-even Higgs boson in the LRSSM can be written as

$$\Gamma_{\rm tot}^{\rm NP} = \Gamma_{\rm NP}(h^0 \to gg) + \Gamma_{\rm NP}(h^0 \to \gamma\gamma) + \sum_{V=W,Z} \Gamma_{\rm NP}(h^0 \to VV^*) + \sum_{f=\tau,b,c} \Gamma_{\rm NP}(h^0 \to f\bar{f}). \tag{26}$$

Normalized to the SM expectation, the signal strengths for the Higgs decay channels are quantified by the ratios [89]

$$\mu_{\gamma\gamma,VV^*}^{\rm ggF} = \frac{\sigma_{\rm NP}({\rm ggF})}{\sigma_{\rm SM}({\rm ggF})} \frac{{\rm BR}_{\rm NP}(h \to \gamma\gamma, VV^*)}{{\rm BR}_{\rm SM}(h \to \gamma\gamma, VV^*)}, \quad (V = Z, W),$$
$$\mu_{ff}^{\rm VBF} = \frac{\sigma_{\rm NP}({\rm VBF})}{\sigma_{\rm SM}({\rm VBF})} \frac{{\rm BR}_{\rm NP}(h \to f\bar{f})}{{\rm BR}_{\rm SM}(h \to f\bar{f})}, \quad (f = b, \tau), \tag{27}$$

where ggF, VBF, and BR stand for gluon-gluon fusion, vector boson fusion, and branching ratio, respectively. Normalized to the SM values, one can evaluate the Higgs production cross sections

$$\frac{\sigma_{\rm NP}({\rm ggF})}{\sigma_{\rm SM}({\rm ggF})} \simeq \frac{\Gamma_{\rm NP}(h \to gg)}{\Gamma_{\rm SM}(h \to gg)} = \frac{\Gamma_{\rm NP}^h}{\Gamma_{\rm SM}^h} \frac{{\rm BR}_{\rm NP}(h \to gg)}{{\rm BR}_{\rm SM}(h \to gg)},$$
$$\frac{\sigma_{\rm NP}({\rm VBF})}{\sigma_{\rm SM}({\rm VBF})} \simeq \frac{\Gamma_{\rm NP}(h \to VV^*)}{\Gamma_{\rm SM}(h \to VV^*)} = \frac{\Gamma_{\rm NP}^h}{\Gamma_{\rm SM}^h} \frac{{\rm BR}_{\rm NP}(h \to VV^*)}{{\rm BR}_{\rm SM}(h \to VV^*)}, \tag{28}$$

where we have neglected the contributions from the rare or invisible decays, and $\Gamma_{\rm SM}^h$ denotes the SM Higgs total decay width. Through Eqs. (27) and (28), we can quantify the signal strengths for the Higgs decay channels in the LRSSM,

$$\begin{aligned}
\mu_{\gamma\gamma}^{\rm ggF} &\approx \frac{\Gamma_{\rm NP}(h \to gg)}{\Gamma_{\rm SM}(h \to gg)} \frac{\Gamma_{\rm NP}(h \to \gamma\gamma)/\Gamma_{\rm NP}^h}{\Gamma_{\rm SM}(h \to \gamma\gamma)/\Gamma_{\rm SM}^h} \\
&= \frac{\Gamma_{\rm SM}^h}{\Gamma_{\rm NP}^h} \frac{\Gamma_{\rm NP}(h \to gg)}{\Gamma_{\rm SM}(h \to gg)} \frac{\Gamma_{\rm NP}(h \to \gamma\gamma)}{\Gamma_{\rm SM}(h \to \gamma\gamma)}, \\
\mu_{VV^*}^{\rm ggF} &\approx \frac{\Gamma_{\rm NP}(h \to gg)}{\Gamma_{\rm SM}(h \to gg)} \frac{\Gamma_{\rm NP}(h \to VV^*)/\Gamma_{\rm NP}^h}{\Gamma_{\rm SM}(h \to VV^*)/\Gamma_{\rm SM}^h} \\
&= \frac{\Gamma_{\rm SM}^h}{\Gamma_{\rm NP}^h} \frac{\Gamma_{\rm NP}(h \to gg)}{\Gamma_{\rm SM}(h \to gg)} |g_{hVV}|^2, \\
\mu_{ff}^{\rm VBF} &\approx \frac{\Gamma_{\rm NP}(h \to VV^*)}{\Gamma_{\rm SM}(h \to VV^*)} \frac{\Gamma_{\rm NP}(h \to f\bar{f})/\Gamma_{\rm NP}^h}{\Gamma_{\rm SM}(h \to f\bar{f})/\Gamma_{\rm SM}^h} \\
&= \frac{\Gamma_{\rm SM}^h}{\Gamma_{\rm NP}^h} |g_{hVV}|^2 |g_{hff}|^2 \qquad (V = Z, W_1; f = b, \tau),
\end{aligned} \tag{29}$$

with

$$\frac{\Gamma_{\rm NP}(h \to VV^*)}{\Gamma_{\rm SM}(h \to VV^*)} = |g_{hVV}|^2 = |g_{hZZ}|^2 = |g_{hW_1W_1}|^2,$$
$$\frac{\Gamma_{\rm NP}(h \to f\bar{f})}{\Gamma_{\rm SM}(h \to f\bar{f})} = |g_{hff}|^2 = |g_{hbb}|^2 \simeq |g_{h\tau\tau}|^2. \tag{30}$$

Therefore, we could just analyze the signal strengths $\mu_{\gamma\gamma}^{\rm ggF}$, $\mu_{VV^*}^{\rm ggF}$, and $\mu_{ff}^{\rm VBF}$ in the following. In the LRSSM, the concrete expressions for $g_{h^0qq}, g_{h^0\tilde{q}\tilde{q}}, g_{h^0ff}, g_{h^0\tilde{f}\tilde{f}}$, $g_{h^0H^+H^-}, g_{h^0\chi^+\chi^-}, g_{h^0WW}$, and g_{h^0ZZ} have been discussed in Appendix C. It is intriguing to note that the CMS Collaboration has reported a 2.9σ global (1.9σ local) excess in the diphoton channel with an invariant mass of 95.4 GeV [7,8]. A similar analysis by the ATLAS Collaboration has found a 1.7σ local excess at the same mass [90]. In addition, CMS has reported another excess in the $\tau^+\tau^-$ channel around 100 GeV with 2.6σ local (2.3σ global) [91–100] significance. Observed signal rates and the local (global) significance for the 95 GeV excess in different channels are presented in Table I [101]. As analyzed in Ref. [102], the light CP-even Higgs does suffer strict constraints from the LHC search for the top quark associated production of the SM Higgs boson that decays into $\tau\bar{\tau}$, and the possibility to explain the di-τ excess by the CP-even scalar is excluded according to the analysis in Ref. [103]. However, they consider the 1σ range of $\mu(\Phi_{95})_{\tau\tau}$ in the analysis, and it is found that this constraint can be relaxed if the 2σ of $\mu(\Phi_{95})_{\tau\tau}$ is considered. We have therefore decided to focus on the $\gamma\gamma$ and $b\bar{b}$ channels, which are subject to weaker constraints and exhibit cleaner signals, providing a clearer window for probing our model.

For the Higgs boson at about 95 GeV, we have

$$\mu(H_{95})_X = \frac{\sigma(h_{95}) \times {\rm Br}^{\rm NP}(h_{95} \to X)}{\sigma^{\rm SM}(h_{95}) \times {\rm Br}^{\rm SM}(h_{95} \to X)}. \tag{31}$$

The process measured at LEP was reported as a 2.3σ local excess in the $b\bar{b}$ final state searches, with the scalar mass at ~96 GeV. We consider the production of a Higgs boson via Higgstrahlung associated with the Higgs boson decaying to bottom quarks. In the LRSSM, we use $\mu_{\rm NP}^{bb}$ and $\mu_{\rm NP}^{\gamma\gamma}$ to describe the signal strengths [30,105,106]

TABLE I. Observed signal rates for a possible new 95 GeV scalar particle.

Channel	Signal strength	Local (global) sig.
$gg \to h_{95} \to \gamma\gamma$	$0.33^{+0.19}_{-0.12}$	$2.9(1.3)\sigma$ [104]
$gg \to h_{95} \to \tau^+\tau^-$	$1.23^{+0.61}_{-0.49}$	$2.6(2.3)\sigma$ [100]
$e^+e^- \to Zh_{95} \to Zb\bar{b}$	0.117 ± 0.057	$2.3(< 1)\sigma$ [4]

$$\begin{aligned}\mu_{\mathrm{NP}}^{bb} &= \frac{\sigma^{\mathrm{NP}}(Z^* \to Z h_1)}{\sigma^{\mathrm{SM}}(Z^* \to Z h_1)} \times \frac{\mathrm{Br}^{\mathrm{NP}}(h_1 \to b\bar{b})}{\mathrm{Br}^{\mathrm{SM}}(h_1 \to b\bar{b})} \\ &\approx |C_{h_1 VV}|^2 \times \frac{\Gamma^{\mathrm{NP}}_{h_1 \to b\bar{b}}}{\Gamma^{\mathrm{SM}}_{h_1 \to b\bar{b}}} \times \frac{\Gamma^{\mathrm{SM}}_{\mathrm{tot}}}{\Gamma^{\mathrm{NP}}_{\mathrm{tot}}} \\ &\approx \frac{|C_{h_1 VV}|^2 \times |C_{h_1 dd}|^2}{|C_{h_1 dd}|^2(\mathrm{Br}^{\mathrm{SM}}_{h_1 \to b\bar{b}} + \mathrm{Br}^{\mathrm{SM}}_{h_1 \to \gamma\gamma}) + |C_{h_1 uu}|^2(\mathrm{Br}^{\mathrm{SM}}_{h_1 \to gg} + \mathrm{Br}^{\mathrm{SM}}_{h_1 \to c\bar{c}})},\end{aligned} \tag{32}$$

$$\begin{aligned}\mu_{\mathrm{NP}}^{\gamma\gamma} &= \frac{\sigma^{\mathrm{NP}}(gg \to h_1)}{\sigma^{\mathrm{SM}}(gg \to h_1)} \times \frac{\mathrm{Br}^{\mathrm{NP}}(h_1 \to \gamma\gamma)}{\mathrm{Br}^{\mathrm{SM}}(h_1 \to \gamma\gamma)} \\ &\approx \frac{\Gamma^{\mathrm{NP}}_{h_1 \to gg}}{\Gamma^{\mathrm{SM}}_{h_1 \to gg}} \times \frac{\Gamma^{\mathrm{NP}}_{h_1 \to \gamma\gamma}}{\Gamma^{\mathrm{SM}}_{h_1 \to \gamma\gamma}} \times \frac{\Gamma^{\mathrm{SM}}_{\mathrm{tot}}}{\Gamma^{\mathrm{NP}}_{\mathrm{tot}}} \\ &\approx \frac{|C_{h_1 uu}|^2 \times |C_{h_1 \gamma\gamma}|^2}{|C_{h_1 dd}|^2(\mathrm{Br}^{\mathrm{SM}}_{h_1 \to b\bar{b}} + \mathrm{Br}^{\mathrm{SM}}_{h_1 \to \tau\tau}) + |C_{h_1 uu}|^2(\mathrm{Br}^{\mathrm{SM}}_{h_1 \to gg} + \mathrm{Br}^{\mathrm{SM}}_{h_1 \to c\bar{c}})},\end{aligned} \tag{33}$$

where [30]

$$|C_{h_1\gamma\gamma}|^2 = \frac{|\frac{4}{3} C_{h_1 tt} A_{1/2}(\tau_t) + C_{h_1 VV} A_1(\tau_W)|^2}{|\frac{4}{3} A_{1/2}(\tau_t) + A_1(\tau_W)|^2} \tag{34}$$

with $\tau_t = \frac{m_{h_1}^2}{4m_t^2} < 1$ and $\tau_W = \frac{m_{h_1}^2}{4m_W^2} < 1$. The form factors $A_{1/2}$ and A_1 are given by [107]

$$\begin{aligned} A_{1/2}(x) &= 2(x + (x-1)\mathrm{arcsin}^2\sqrt{x})x^{-2}, \qquad x \le 1, \\ A_1(x) &= -(2x^2 + 3x + 3(2x-1)\mathrm{arcsin}^2\sqrt{x})x^{-2}, \qquad x \le 1. \end{aligned} \tag{35}$$

$C_{h_1 VV}$ is the ratio of vertices in the SM and LRSSM related to the coupling vertex between the h_1 and the gauge boson $W_L^{\pm}$, while $C_{h_1 u\bar{u}(h_1 d\bar{d})}$ is the ratio of vertices between h_1 and up-type quarks as well as down-type quarks. The specific form of the couplings are given by

$$\begin{aligned} C_{h_1 d\bar{d}} &= \frac{Z_{11}^H}{\cos\beta}, \qquad C_{h_1 u\bar{u}} = \frac{Z_{12}^H}{\sin\beta}, \\ C_{h_1 VV} &= Z_{11}^H \cos\beta + Z_{12}^H \sin\beta. \end{aligned} \tag{36}$$

Here, Z_H is the unitary matrix of the CP-even Higgs field mass matrix.

IV. NUMERICAL ANALYSIS

In this section, we conduct a detailed exploration of two different scenarios. In the first scenario, we consider only the 125 GeV SM-like Higgs boson, serving as a benchmark model for comparative analysis. The second scenario expands to include two scalar particles with masses of 95 and 125 GeV [108]. The measured SM-like Higgs mass is [109]

$$m_h = 125.09 \pm 0.24 \text{ GeV}. \tag{37}$$

The SM input parameters we used are $m_W = 80.377$ GeV, $m_Z = 91.1876$ GeV, $\sin^2\theta_W(m_Z) = 0.2312$, $\alpha_s(m_Z) = 0.118$, and the fermion coupling constant $G_F = 1.1664 \times 10^{-5}$ GeV^{-2}. The masses of SM fermions are taken as $m_\tau = 1.78$, $m_c = 1.28$, $m_t = 173.5$, and $m_b = 4.65$ GeV from the Particle Data Group (PDG) [109]. Furthermore, we take $\lambda_4 = \lambda_5 = T_L = T_4 = T_5 = 0$ for simplicity. It is important to note that, while the model framework adopted here is similar to that in Ref. [59], our analysis incorporates one- and two-loop effective potential corrections to the Higgs mass matrices and explores a significantly extended parameter space through a comprehensive rescan. The choice to fix the specific parameters mentioned above is a decision informed by the numerical results and feedback obtained from our scanning procedure. This approach simplifies the numerical calculation without loss of generality.

A. Signal strengths of the 125 GeV Higgs bosons

In order to globally fit the electroweak experimental data [59], we adopt the following:

$$\begin{aligned} T_S &= -5500 \text{ GeV}, \qquad T_R = -5000 \text{ GeV}, \\ T_3 &= -2500 \text{ GeV}, \qquad T_Q^1 = T_Q^2 = -1000 \text{ GeV}, \\ M_1 &= 1000 \text{ GeV}, \qquad M_{2L} = M_{2R} = 5000 \text{ GeV}, \\ m_{Q_R}^2 &= m_{Q_L}^2 = 4 \times 10^6 \text{ GeV}^2, \qquad \xi_F = -5500 \text{ GeV}^2, \\ m_{L_R}^2 &= m_{L_L}^2 = 4 \times 10^6 \text{ GeV}^2. \end{aligned} \tag{38}$$

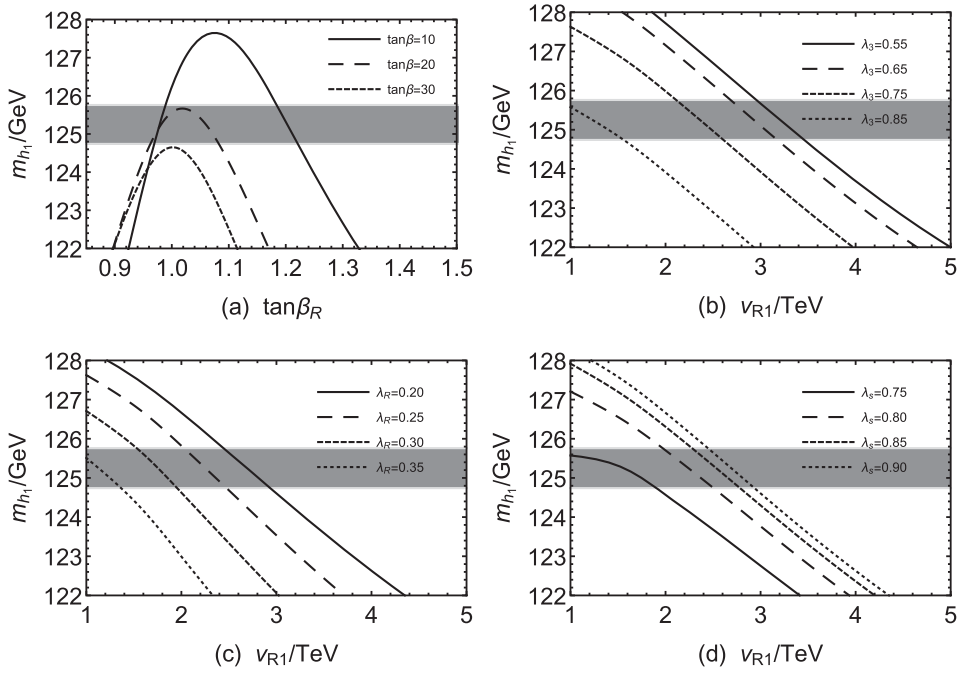


FIG. 1. (a) The mass of the CP-even Higgs boson m_{h_1} varies with $\tan\beta_R$ and different values of $\tan\beta$ are taken. (b)–(d) Display m_{h_1} varies with v_{R1} with taking the different values of $\lambda_3, \lambda_R, \lambda_S$, respectively. The horizontal gray band represents the 3σ interval of Eq. (37).

In the numerical analyses, we mainly focus on the impact from the following parameters on the Higgs masses and couplings:

$$\tan\beta, \tan\beta_R, \lambda_3, \lambda_S, \lambda_R, v_S, v_{R2}. \tag{39}$$

In the sector of the parameter space, the model accommodates a neutral Higgs with mass around 125 GeV. Taking $v_{R1} = 2.5$ TeV, $v_S = 5$ TeV, $\lambda_3 = 0.7, \lambda_R = 0.2$, and $\lambda_S = 0.9$, we plot the theoretical prediction on the mass of the lightest neutral Higgs versus the parameter $\tan\beta_R$ in Fig. 1(a), where the solid line corresponds to $\tan\beta = 10$, the dashed line corresponds to $\tan\beta = 20$, and the dotted line corresponds to $\tan\beta = 30$, respectively. Figures 1(b) and 1(c) also present the relationship between the mass of the lightest Higgs boson and v_{R1}, wherein the solid, dashed, and dotted lines represent increasing values of the parameters λ_3, λ_R, and λ_S, respectively. The numerical results indicate that there is parameter space to accommodate the 125 GeV Higgs in this model.

Figure 1 indicates that, by adjusting $\tan\beta, \tan\beta_R, v_{R1}, v_S, \lambda_3, \lambda_R$, and λ_S, suitable parameters can be found in the model to align the light Higgs particle mass with the observed value, providing a reference for constructing supersymmetric models consistent with experimental data. Because the mass of the lightest Higgs boson is influenced significantly in a complicated manner by $\tan\beta, \tan\beta_R, v_{R1}, v_S, \lambda_3, \lambda_R$, and λ_S, we scan the following parameter space:

$$\begin{aligned} &\tan\beta \in (2,50), \quad \tan\beta_R \in (0.8,1.5), \\ &v_{R1} \in (2,3)\,\text{TeV}, \quad v_S \in (4,6)\,\text{TeV}, \\ &\lambda_S \in (0.6,1.0), \quad \lambda_3 \in (0.6,1.0), \quad \lambda_R \in (0,0.4). \end{aligned} \tag{40}$$

To comprehensively explore the collective influence of $\tan\beta, \tan\beta_R, v_{R1}, v_S, \lambda_S, \lambda_3$, and λ_R on the signal strength of the 125 GeV Higgs boson, while maintaining m_{h_1} in the vicinity of 125 GeV during the scan, we specified in Eq. (40) that $\tan\beta$ varies between 2 and 50, $\tan\beta_R$ ranges from 0.8 to 1.5, λ_3 ranges from 0.6 to 1.0, λ_R from 0 to 0.4, and λ_S from 0.6 to 1.0.

With our assumption on the parameter space, it can be readily observed that the distribution of points in the figure is essentially consistent for the case where m_{h_1} lies within the 122–128 GeV interval and the case where it is constrained to the 124–126 GeV interval. As the scanned mass range of m_{h_1} becomes narrower, the number of corresponding points in the figure decreases. We present the signal strength $\mu_{\text{NP}}^{\gamma\gamma}$ versus $\tan\beta$ in Fig. 2(a), the signal strength $\mu_{\text{NP}}^{\tau^+\tau^-}$ versus $\tan\beta$ in Fig. 2(b), the signal strength μ_{NP}^{WW} versus $\tan\beta$ in Fig. 2(c), μ_{NP}^{ZZ} versus $\tan\beta$ in Fig. 2(d), and $\mu_{\text{NP}}^{b\bar{b}}$ versus $\tan\beta$ in Fig. 2(e), respectively. With the increase of $\tan\beta$, the signal strength for each decay channel approaches a certain value and coincides with the experimental data at large $\tan\beta$.

Figure 2(f) shows the relationship between the mixing matrix elements $|Z_{12}^H|^2$ and $\tan\beta$, where $|Z_{12}^H|^2$ represents the contribution of the ϕ_2 component. The horizontal axis represents $|Z_{12}^H|^2$, and the vertical axis represents $\tan\beta$. As

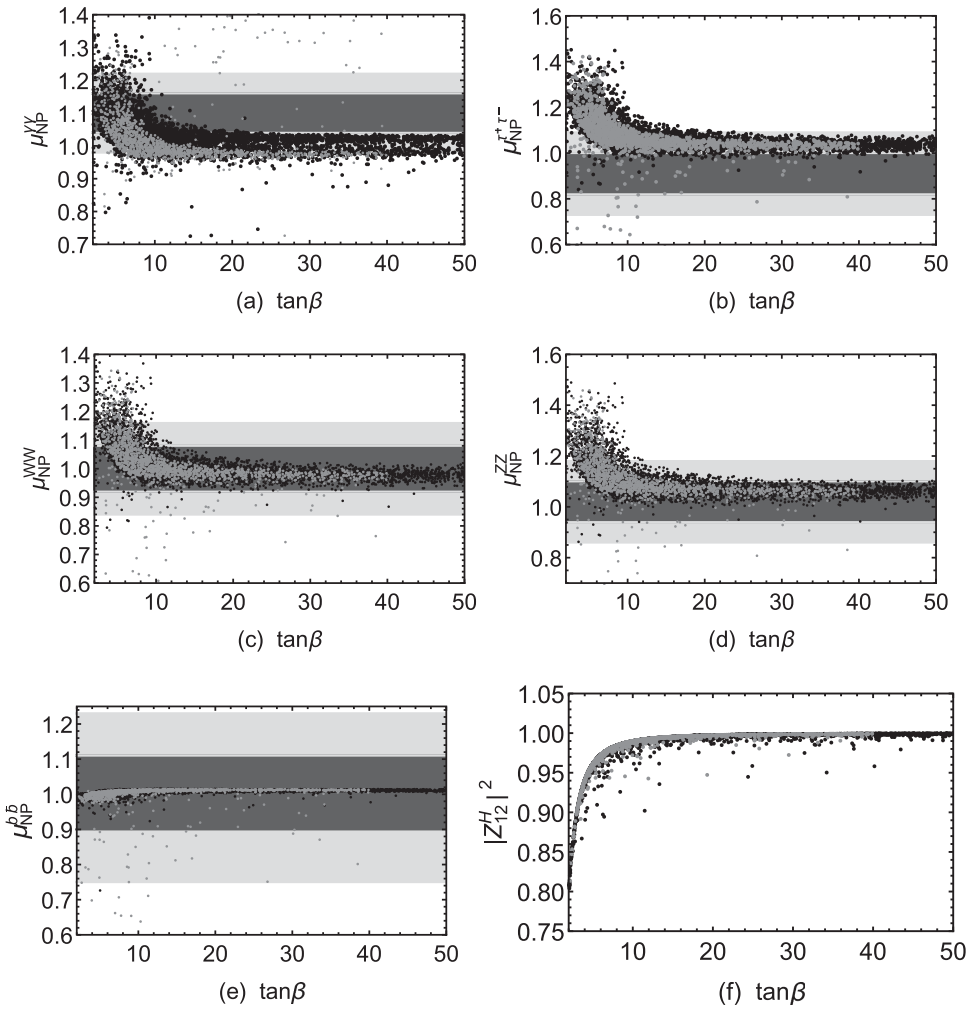


FIG. 2. A scan was performed in the parameter space provided by Eq. (40), by ensuring that m_{h1} lies within the range of 124–126 GeV. (a)–(e) Results of signal strengths $\mu^{\gamma\gamma}_{\rm NP}, \mu^{\tau^+\tau^-}_{\rm NP}, \mu^{WW}_{\rm NP}, \mu^{ZZ}_{\rm NP}$, and $\mu^{b\bar{b}}_{\rm NP}$, respectively, where $\tan\beta$ on the horizontal axis and the normalized signal strength for various decay channels on the vertical axis. The dark gray shaded areas represent the experimental 1σ range, and the light gray areas represent the experimental 2σ range. (f) Displays the relationship between the mixing matrix elements $\tan\beta$ and $|Z^H_{12}|^2$ for the two Higgs bosons. The gray points denote values of m_{h_1} within the range of 124–126 GeV, while the black points correspond to masses of m_{h_1} in the interval of 122–128 GeV.

$\tan\beta$ increases, $|Z^H_{12}|^2$ approaches unity. From Fig. 2(f), it can be observed that $|Z^H_{12}|^2$ is distributed around values close to 1, indicating that the ϕ_2 component dominates the contribution to the 125 GeV Higgs boson. Moreover, the numerical result indicates that when $|Z^H_{12}|^2$ approaches 1, the composition of the Higgs boson is consistent with the expectations of the SM, making the physical properties of the 125 GeV Higgs boson similar in the LRSSM to the SM-like Higgs boson.

As $\tan\beta$ increases, the ratios for both channels approach unity in the LRSSM, but the gray points slightly exceed 1, indicating that the LRSSM predicts a larger signal strength than the standard model in this regime.

Figure 3(a) presents the mass of the lightest doubly charged Higgs boson within the parameter space of the model. In the LRSSM, the tree-level squared mass of the lightest doubly charged Higgs boson, denoted as $m^2_{H^{\pm\pm}_{R_1}}$, is permitted to be negative and exhibits a strong dependence on $\tan\beta_R$. As $\tan\beta_R$ approaches unity, the value of $m_{H^{\pm\pm}_{R_1}}$ tends toward zero. The explicit functional relationship between $m_{H^{\pm\pm}_{R_1}}$ and $\tan\beta_R$ is detailed in Appendix F. As clearly illustrated in Fig. 3(a), the correlation between $m_{H^{\pm\pm}_{R_1}}$ and $\tan\beta_R$ is readily observable. According to the latest results from the LHC, the lower mass limit for $m_{H^{\pm\pm}_{R_1}}$ is set at 1.3 TeV [110–112]. In our calculation of the one-loop effective potential corrections to $m_{H^{\pm\pm}_{R_1}}$, the contributions from right-handed neutrinos dominate, while the effects from other particles are minimal and can be largely neglected. Employing the parameters from Fig. 1 with $\tan\beta = 20$, $\tan\beta_R = 1.01$, $v_{R1} = 2.5$ TeV, $v_S = 5$ TeV,

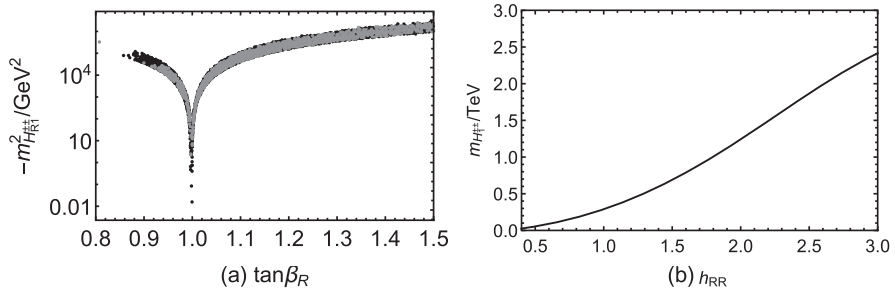


FIG. 3. (a) Shows the negative doubly charged Higgs mass square as a function of $\tan\beta_R$ at the tree level. (b) Illustrates the doubly charged Higgs mass as a function of h_{RR} after incorporating one-loop effective potential corrections.

$\lambda_3 = 0.7$, $\lambda_R = 0.2$, and $\lambda_S = 0.9$, the mass of the doubly charged Higgs boson $m_{H^{\pm\pm}_{R_1}}$ after one-loop effective potential corrections exhibits a positive correlation with the coupling parameter h_{RR}. The expression for the right-handed neutrino mass is $m_{\nu_R} = \frac{1}{\sqrt{2}} h_{RR} v_{R1}$. Simultaneously, the mass of the right-handed neutrino increases with larger values of h_{RR}. Consequently, it is straightforward to conclude that higher right-handed neutrino masses facilitate $m_{H^{\pm\pm}_{R_1}}$ more easily satisfying the experimental lower limit.

B. Signal strengths of the 95 and 125 GeV Higgs bosons

In our discussion of Higgs bosons where the lightest mass is 95 GeV and the second lightest is 125 GeV, the parameter space differs slightly from that of the previous section, which considered only the existence of a Higgs boson with a mass of 125 GeV. Similarly, we adopt the following assumption on the parameter space:

$$\begin{aligned} T_S &= 3000\ \text{GeV}, \qquad T_R = -2500\ \text{GeV}, \\ T_3 &= 4000\ \text{GeV}, \qquad T^1_Q = T^2_Q = -1000\ \text{GeV}, \\ M_1 &= 1000\ \text{GeV}, \qquad M_{2L} = M_{2R} = 5000\ \text{GeV}, \\ m^2_{Q_R} &= m^2_{Q_L} = 4\times 10^6\ \text{GeV}^2, \qquad \xi_F = -5500\ \text{GeV}^2, \\ m^2_{L_R} &= m^2_{L_L} = 4\times 10^6\ \text{GeV}^2. \end{aligned} \tag{41}$$

In this parameter space, it is possible to simultaneously have Higgs bosons with masses around 95 and 125 GeV. Taking $v_{R1} = 1.5$ TeV, $v_S = 9.5$ TeV, $\lambda_3 = 0.1$, $\lambda_R = 0.04$, and $\lambda_S = 0.9$, we plot the theoretical prediction of the mass of the lightest and the second-lightest neutral Higgs bosons versus the parameter $\tan\beta$, where the solid line corresponds to $\tan\beta_R = 0.988$, the dashed line corresponds to $\tan\beta_R = 0.990$, and the dotted line corresponds to $\tan\beta_R = 0.992$, respectively. We also plot the relationships between the lightest and second-lightest CP-even Higgs bosons and v_{R1} for different values of λ_3, λ_R, and λ_S. In Figs. 4(b)–4(d), the solid and dashed lines represent increasing values of the parameters λ_3, λ_R, and λ_S, respectively. The numerical results shown in Fig. 4 indicate that there is parameter space to accommodate the 95 GeV Higgs boson in this model.

We scanned the parameter space with

$$\begin{aligned} &\tan\beta \in (2,10), \quad \tan\beta_R \in (0.98,1.00), \\ &v_{R1} \in (2,3)\ \text{TeV}, \quad v_S \in (9,11)\ \text{TeV}, \\ &\lambda_S \in (0.9,1.0), \quad \lambda_3 \in (0,0.5), \quad \lambda_R \in (0.03,0.04). \end{aligned} \tag{42}$$

With the above assumption on the parameter space, we investigate the signal strengths of 95 and 125 GeV simultaneously. Obviously, the explanation of the 95 and 125 GeV Higgs boson particles and their signal strengths imposes stronger constraints on the parameter space of the model concerned here. For example, the scanning ranges for $\tan\beta_R$ and λ_R are significantly smaller, and the signal of the Higgs with a mass of 125 GeV must also conform to experimental findings. In the CP-even Higgs sector of the LRSSM, the lightest Higgs boson has a mass of 95 GeV, while the next-lightest Higgs boson has a mass of 125 GeV. In the scanned parameter space, we first analyze the signal strength of the 125 GeV Higgs boson.

We selected the signal strength that matches the 125 GeV Higgs boson as provided by the PDG [109]. Under the aforementioned conditions, we calculated the signal strengths of the 95 GeV Higgs boson for its final states of diphoton and $b\bar{b}$.

With our assumption on the parameter space, we present the signal strength $\mu^{\gamma\gamma}_{\text{NP}}$ versus v_{R2} in Fig. 5(a), the signal strength $\mu^{\tau^+\tau^-}_{\text{NP}}$ versus v_{R1} in Fig. 5(b), the signal strength μ^{WW}_{NP} versus v_{R1} in Fig. 5(c), the signal strength μ^{ZZ}_{NP} versus v_{R2} in Fig. 5(d), and the signal strength $\mu^{b\bar{b}}_{\text{NP}}$ versus v_{R2} in Fig. 5(e), respectively. In Figs. 5(a)–5(e), the dark gray regions correspond to the 1σ signal strength range of the 125 GeV Higgs boson, while the light gray areas represent the 2σ signal strength range. In Figs. 5–7, the gray points denote benchmarks where the next-to-lightest Higgs mass lies in 124–126 GeV, while the black points denote those with the next-to-lightest Higgs mass in 122–128 GeV. As can be readily observed in Fig. 5, under the condition that both the $\gamma\gamma$ and $b\bar{b}$ signal strengths of the lightest Higgs boson at 95 GeV and those of the second-lightest Higgs boson at 125 GeV largely fall within the 1σ confidence level, the majority of the parameter points are concentrated

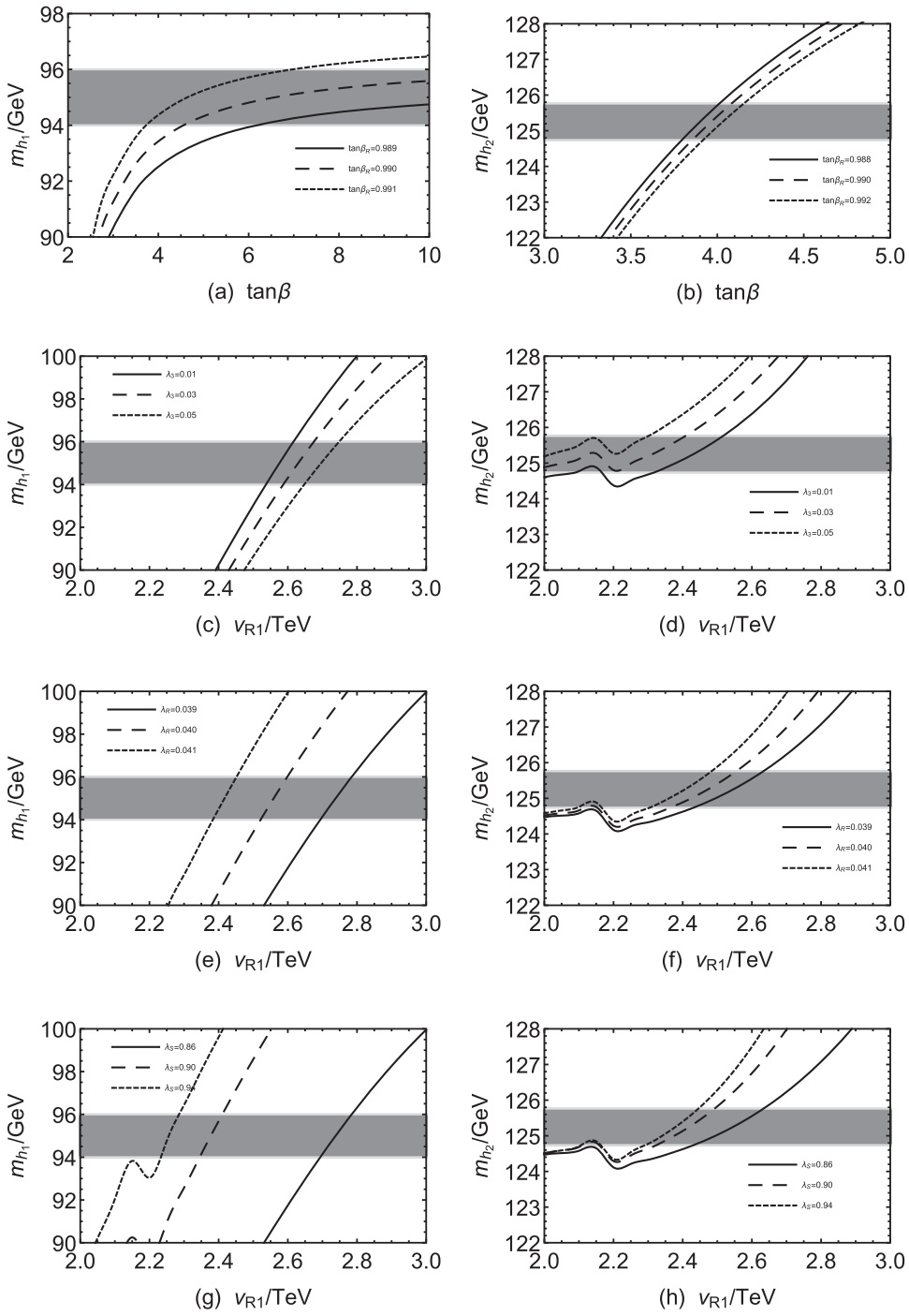


FIG. 4. (a),(b) The lightest and second-lightest CP-even Higgs bosons masses versus $\tan\beta$, respectively. (c),(e),(g) The dependence of the lightest CP-even Higgs-boson mass on v_{R1}. (d),(f),(h) The corresponding variation of the second-lightest CP-even Higgs-boson mass with v_{R1}. (a),(c),(e),(g) The horizontal gray band marks the 94–96 GeV mass window; (b),(d),(f),(h) The horizontal gray band represents the 3σ interval of Eq. (37).

in the range of $2 < v_{R1} < 3$ TeV. We also present the correlation between the $b\bar{b}$ and $\gamma\gamma$ signal strengths of the 95 GeV Higgs boson in this parameter space, as shown in Fig. 5(f). We considered the experimental constraints on the charged Higgs boson sector by applying the latest lower mass bounds from LHC searches [113]. Although certain marginal points in the preliminary scan exhibited enhanced signal strengths due to the presence of a lighter $H_1^{\pm}$, these have been effectively excluded after enforcing this stringent limit. The plots in Figs. 6(a) and 6(b) show the signal strength distributions of the 95 GeV Higgs boson in the $\gamma\gamma$ and $b\bar{b}$ decay channels, respectively, as functions of the

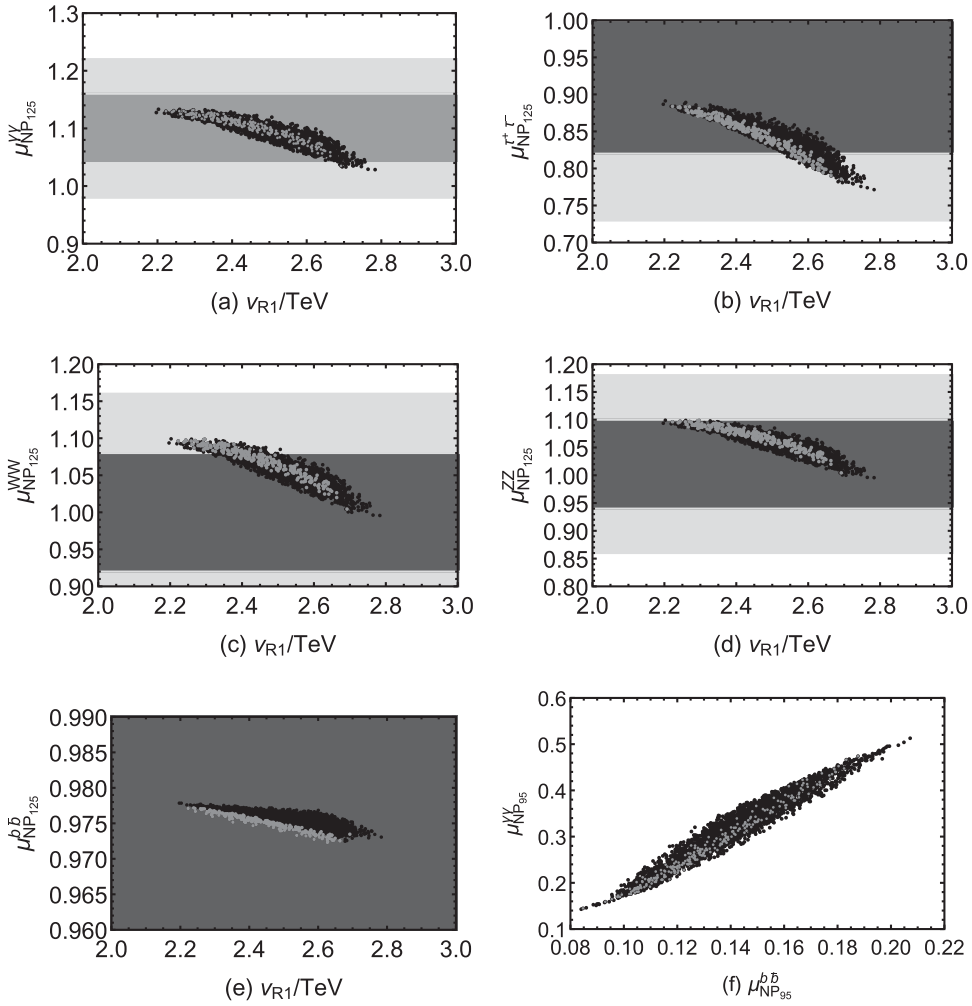


FIG. 5. (a)–(e) The signal strength of the 125 GeV Higgs boson in different decay channels as a function of the right-handed Higgs vacuum expectation value v_{R1}, with the dark and light gray regions indicating the 1σ and 2σ experimental ranges, respectively. (f) The 95 GeV Higgs boson signal strengths of $\gamma\gamma$ ($\mu^{\gamma\gamma}_{\mathrm{NP}_{95}}$) and $b\bar{b}$ ($\mu^{b\bar{b}}_{\mathrm{NP}_{95}}$) decay channels. Gray and black points denote benchmarks with the next-to-lightest Higgs mass in 124–126 and 122–128 GeV, respectively.

parameter v_{R1} in the LRSSM. To simultaneously explain the 95 and 125 GeV Higgs bosons, the parameter v_{R1} is constrained to the range of 2–3 TeV.

Figure 7(a) illustrates the correlation between $\tan\beta$ and $\tan\beta_R$. As can be seen from Fig. 7(a), the values of $\tan\beta_R$ approach but do not equal unity, clustering predominantly within the range of 0.986–0.992. This indicates that, for the condition of satisfying the 95 GeV signal strength within the 1σ range, the value of $\tan\beta_R$ cannot be strictly equal to 1 but is slightly deviated from it. In the analytical approximation presented in Appendix F for $m_{H_1^{\pm}}$ and its dependence on $\tan\beta_R$, it can be seen that, when $\tan\beta_R = 1$, the mass of the charged Higgs boson becomes very small, nearly approaching zero, which cannot satisfy the experimental constraints. For the doubly charged Higgs boson, the negative value of its mass squared is also small when $\tan\beta_R$ is close to 1, but because it is negative, it can easily be corrected to yield a positive mass squared. Therefore, the mass of the doubly charged Higgs is more easily adjusted to meet experimental requirements through one-loop corrections in the model when $\tan\beta_R$ is near 1, which is also the reason for choosing $\tan\beta_R$ around 1. As similarly demonstrated for $m_{H^{\pm\pm}_{R1}}$ in the previous section, the one-loop effective potential correction leads to a consistent

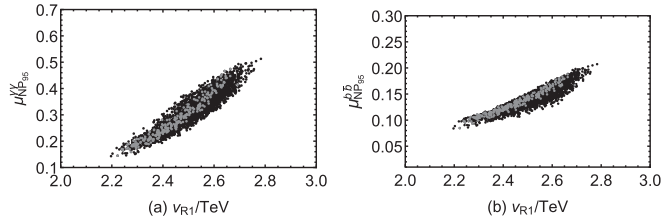


FIG. 6. $\mu^{\gamma\gamma}_{\mathrm{NP}_{95}}$ and $\mu^{b\bar{b}}_{\mathrm{NP}_{95}}$ as functions of v_{R1}/TeV are plotted in (a) and (b), respectively. Gray points denote benchmarks with the next-to-lightest Higgs mass in 124–126 GeV and black points for those in 122–128 GeV.

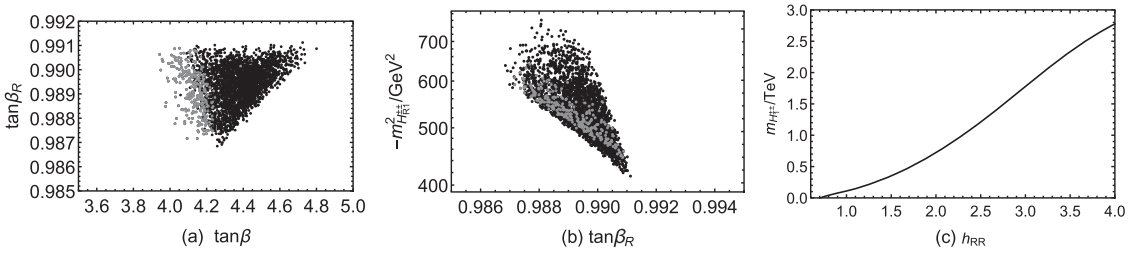


FIG. 7. (a) Shows the relationship between $\tan\beta$ and $\tan\beta_R$. (b) Shows the negative doubly charged Higgs mass square as a function of $\tan\beta_R$. Gray points denote benchmarks with the next-to-lightest Higgs mass in 124–126 GeV and black points for those in 122–128 GeV. (c) Illustrates the relationship between the lightest doubly charged Higgs mass and the parameter h_{RR} after incorporating the one-loop effective potential corrections.

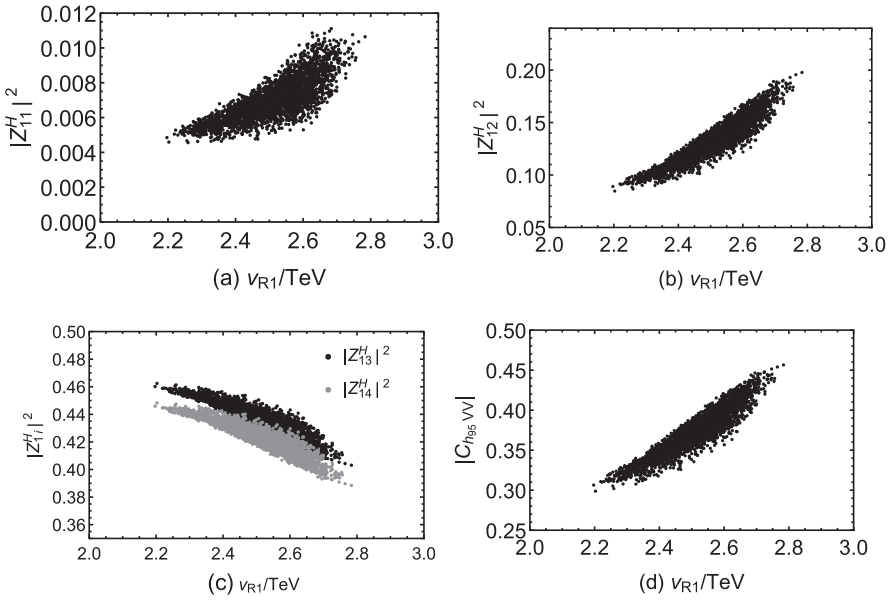


FIG. 8. (a) $|Z^H_{11}|^2$, (b) $|Z^H_{12}|^2$, (c) $|Z^H_{13}|^2$ (black points) and $|Z^H_{14}|^2$ (gray points), and (d) $|C_{h_95VV}|$ as functions of v_{R1} are plotted. The points represent the parameter benchmarks from the prior signal strength calculation.

conclusion. The corrected mass of $m_{H^{\pm\pm}_{R1}}$ exhibits a positive correlation with the mass of the right-handed neutrino. Specifically, larger right-handed neutrino masses render it easier for $m_{H^{\pm\pm}_{R1}}$ to satisfy the experimental lower limit. The numerical results are obtained under the current parameter space with $\tan\beta = 4.5$, $\tan\beta_R = 0.99$, $v_{R1} = 2.5$ TeV, $v_S = 9.5$ TeV, $\lambda_3 = 0.2$, $\lambda_R = 0.04$, and $\lambda_S = 0.95$. This ensures that the masses of the Higgs bosons in the model comply with the existing experimental limits.

We also perform an analysis of the mass-squared matrix structure and components of different Higgs states in the LRSSM and explore the components of various gauge eigenstates in the 95 and 125 GeV Higgs mass eigenstates, as shown in Figs. 8 and 9. Specifically, the 125 GeV Higgs

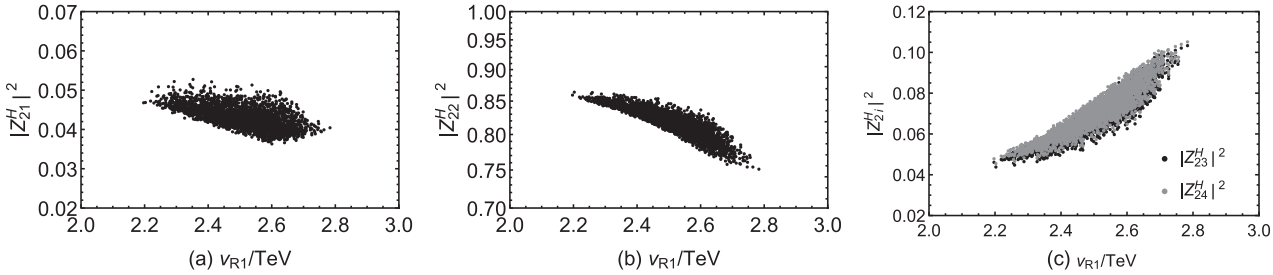


FIG. 9. (a) $|Z^H_{21}|^2$, (b) $|Z^H_{22}|^2$, (c) $|Z^H_{23}|^2$ (black points) and $|Z^H_{24}|^2$ (gray points) as functions of v_{R1} are plotted. The points represent the parameter benchmarks from the prior signal strength calculation.

boson is primarily composed of the Φ_2 field. In contrast, the 95 GeV Higgs boson is primarily composed of the δ_R and Δ_R fields. In the LRSSM, these two fields belong to the right-handed Higgs triplet and are associated with the breaking of right-handed gauge symmetry. This association causes the 95 GeV Higgs state to primarily originate from the mixing of δ_R and Δ_R. From Fig. 8(b), one can see that $|Z_{12}^H|^2$ lies in the range $0.1-0.2$, indicating that the 95 GeV Higgs state contains a $10\%-20\%$ component from Φ_2. From Eq. (36), it follows straightforwardly that the vertex $|C_{h_{95}VV}|$ depends on $|Z_{12}^H|^2$. The numerical values of $|C_{h_{95}VV}|$ are shown in Fig. 8(d). The distribution of the squared values of the matrix elements in the figure allows us to see that different Higgs mass states reflect the complex field contributions and interactions behind them.

V. SUMMARY

After considering the two-loop radiative corrections to the effective potential, we analyze the pole mass squared of the *CP*-even Higgs boson in the LRSSM. The numerical results show that, within the framework of this model, there exists a parameter space that can simultaneously account for the signal excesses of 95 and 125 GeV observed in the experiments. The dominant component of the 125 GeV Higgs boson comes from the bidoublet Φ_2, whereas the 95 GeV state is dominantly a mixture of the two triplets δ_R, Δ_R and a portion of the bidoublet Φ_2.

ACKNOWLEDGMENTS

This work was supported by the National Natural Science Foundation of China (No. 12235008), the Natural Science Foundation of Guangxi Autonomous Region (No. 2022GXNSFDA035068), the Hebei Natural Science Foundation (No. A2022201017, No. A2023201041), and the youth top-notch talent support program of the Hebei Province.

DATA AVAILABILITY

The data that support the findings of this article are available from the authors upon reasonable request.

APPENDIX A: THE HIGGS MASS MATRIX

The minimization of the scalar potential proceeds as

$$\begin{aligned}\frac{\partial V_0}{\partial H_{12}^0}=\frac{1}{8}(&8m_1^2v_1+g_L^2v_1(v_1^2-v_2^2)\\&+g_R^2v_1^2(v_1^2-v_2^2+2v_{R1}^2-2v_{R2}^2)-4\sqrt{2}T_3v_2v_S\\&+4\lambda_3^2v_1v_S^2+4\lambda_3v_2(\lambda_3v_1v_2\\&-\lambda_Rv_{R1}v_{R2}-3\lambda_Sv_S^2-2\xi_F)),\end{aligned}\tag{A1}$$

$$\begin{aligned}\frac{\partial V_0}{\partial H_{21}^0}=\frac{1}{8}(&8m_2^2v_2-g_R^2v_1^2v_2+g_R^2v_2^3+g_L^2(-v_1^2v_2+v_2^3)-2g_R^2v_2v_{R1}^2+2g_R^2v_2v_{R2}^2-4\sqrt{2}T_3v_1v_S\\&+4\lambda_3^2v_1^2v_2+4\lambda_3^2v_S^2v_2-4\lambda_S\lambda_Rv_1v_{R1}v_{R2}-12\lambda_3\lambda_Sv_1v_S^2-8\lambda_3\xi_Fv_1),\end{aligned}\tag{A2}$$

$$\begin{aligned}\frac{\partial V_0}{\partial H_{\Delta_R}^0}=\frac{1}{4}(&4m_{\Delta_R}^2v_{R1}+g_R^2v_{R1}(v1^2-v_2^2+2v_{R2}^2-2v_{R2}^2)+2(g_B(v_{R1}^3-v_{R1}^2v_{R2}^2)\\&+\sqrt{2}T_Rv_{R2}v_S+\lambda_R(-\lambda_3v_1v_2v_{R2}+\lambda_Rv_{R1}(v_{R2}^2+v_S^2)+v_{R2}(3\lambda_Sv_S^2+2\xi_F)))),\end{aligned}\tag{A3}$$

$$\begin{aligned}\frac{\partial V_0}{\partial H_{\delta_R}^0}=\frac{1}{4}(&4m_{\Delta_R}^2v_{R2}+2g_B^2v_{R2}(-v_{R1}^2+v_{R2}^2)+g_R^2v_{R2}(-v_1^2+v_2^2-2v_{R1}^2+2v_{R2}^2)\\&+2\sqrt{2}T_Rv_{R1}v_S+2\lambda_R^2v_S^2v_{R2}+2\lambda_Rv_{R1}(-\lambda_3v_1v_2+\lambda_Rv_{R1}v_{R2}+\lambda_Sv_S^2+2\xi_F)),\end{aligned}\tag{A4}$$

$$\begin{aligned}\frac{\partial V_0}{\partial H_S^0}=\frac{1}{2}(&-\sqrt{2}T_3v_1v_2+\sqrt{2}T_Rv_{R1}v_{R2}+2m_S^2v_S+3\sqrt{2}T_Sv_S^2+\lambda_3^2v_1^2v_S+\lambda_3^2v_2^2v_S\\&+\lambda_R^2v_{R1}^2v_S+\lambda_R^2v_{R2}^2v_S-6\lambda_S\lambda_3v_1v_2v_S+6\lambda_R\lambda_Sv_{R1}v_{R2}v_S+18\lambda_Sv_S^3+12\lambda_S\xi_Fv_S).\end{aligned}\tag{A5}$$

The 2×2 mass-squared matrix for these fields in the basis $(\mathrm{Re}[H_{11}^0],\mathrm{Re}[H_{22}^0])$

$$m_{H_1^0}^2=\begin{pmatrix}m_{H_{11}^0H_{11}^0}^2 & m_{H_{11}^0H_{22}^0}^2\\ m_{H_{22}^0H_{11}^0}^2 & m_{H_{22}^0H_{22}^0}^2\end{pmatrix}.\tag{A6}$$

The matrix elements are defined as

$$
\begin{aligned}
m^2_{H^0_{11}H^0_{11}} &= m_1^2 - \frac{g_L^2}{4}\left(\frac{v_1^2}{2}-\frac{v_2^2}{2}\right) - \frac{g_R^2}{4}\left(\frac{v_1^2}{2}-\frac{v_2^2}{2}+v_{R1}^2-v_{R2}^2\right) + \frac{v_S^2\lambda_3^2}{2} + 2\lambda_4^2 v_1^2 + \frac{\lambda_4^2 v_S^2}{2},\\
m^2_{H^0_{11}H^0_{22}} &= m^2_{H^0_{22}H^0_{11}} = -T_3\frac{v_S}{\sqrt{2}} + 2\lambda_4\lambda_5 v_1 v_2 - \lambda_3\left(-\frac{\lambda_3 v_1 v_2}{2} + \frac{\lambda_R v_{R1} v_{R2}}{2} + 3\frac{\lambda_S v_S^2}{2} + 8\xi_F\right),\\
m^2_{H^0_{22}H^0_{22}} &= m_1^2 + \frac{g_L^2}{4}\left(\frac{v_1^2}{2}-\frac{v_2^2}{2}\right) + \frac{g_R^2}{4}\left(\frac{v_1^2}{2}+\frac{v_2^2}{2}+v_{R1}^2-v_{R2}^2\right) + \frac{v_S^2\lambda_3^2}{2} + 2\lambda_5^2 v_2^2 + \frac{v_S^2\lambda_5^2}{2}.
\end{aligned}
\tag{A7}
$$

The 2×2 mass-squared matrix for these fields in the basis $(\mathrm{Re}[\Delta_L^0], \mathrm{Re}[\delta_L^0])$

$$
m^2_{H_2^0} = \begin{pmatrix} m^2_{\Delta_L^0\Delta_L^0} & m^2_{\Delta_L^0\delta_L^0} \\ m^2_{\delta_L^0\Delta_L^0} & m^2_{\delta_L^0\delta_L^0} \end{pmatrix}.
\tag{A8}
$$

The matrix elements are defined as

$$
\begin{aligned}
m^2_{\Delta_L^0\Delta_L^0} &= m^2_{\delta_L} + \frac{1}{2}g_L^2\left(\frac{v_1^2}{2}-\frac{v_2^2}{2}\right) - g_B^2\left(\frac{v_{R1}^2}{2}+\frac{v_{R2}^2}{2}\right) + \frac{\lambda_5^2 v_S^2}{2},\\
m^2_{\Delta_L^0\delta_L^0} &= m^2_{\delta_L^0\Delta_L^0} = \frac{T_L v_S}{\sqrt{2}} + \lambda_L\left(-\frac{1}{2}\lambda_3 v_1 v_2 + \frac{\lambda_5}{2}v_{R1}v_{R2} + \frac{3\lambda_5 v_S^2}{2} + \xi_F\right),\\
m^2_{\delta_L^0\delta_L^0} &= m^2_{\delta_L} - \frac{1}{2}g_L^2\left(\frac{v_1^2}{2}-\frac{v_2^2}{2}\right) + g_B^2\left(\frac{v_{R2}^2}{2}-\frac{v_{R1}^2}{2}\right) + \frac{\lambda_L^2 v_S^2}{2}.
\end{aligned}
\tag{A9}
$$

Similarly, in the LRSSM, the imaginary parts of the neutral Higgs fields generate pseudoscalar (CP-odd) states. Their mass-squared matrix is provided in the gauge basis $(\mathrm{Im}[H^0_{12}], \mathrm{Im}[H^0_{21}], \mathrm{Im}[H^0_{\Delta_R}], \mathrm{Im}[H^0_{\delta_R}], \mathrm{Im}[H^0_S])$

$$
m^2_{A_1} = \begin{pmatrix}
m^2_{\sigma^0_{12}\sigma^0_{12}} & m^2_{\sigma^0_{12}\sigma^0_{21}} & -\frac{1}{2}\lambda_3\lambda_R v_2 v_{R2} & -\frac{1}{2}\lambda_3\lambda_R v_2 v_{R1} & m^2_{\sigma^0_{12}\sigma^0_S} \\
m^2_{\sigma^0_{21}\sigma^0_{12}} & m^2_{\sigma^0_{21}\sigma^0_{21}} & -\frac{1}{2}\lambda_3\lambda_R v_1 v_{R2} & -\frac{1}{2}\lambda_3\lambda_R v_1 v_{R1} & m_{\sigma^0_{21}\sigma^0_S} \\
-\frac{1}{2}\lambda_3\lambda_R v_2 v_{R2} & -\frac{1}{2}\lambda_3\lambda_R v_1 v_{R2} & m^2_{\sigma^0_{\Delta_R}\sigma^0_{\Delta_R}} & m^2_{\sigma^0_{\Delta_R}\sigma^0_{\delta_R}} & m^2_{\sigma^0_{\Delta_R}\sigma^0_S} \\
-\frac{1}{2}\lambda_3\lambda_R v_2 v_{R1} & -\frac{1}{2}\lambda_3\lambda_R v_1 v_{R1} & m^2_{\sigma^0_{\delta_R}\sigma^0_{\Delta_R}} & m^2_{\sigma^0_{\delta_R}\sigma^0_{\delta_R}} & m^2_{\sigma^0_{\delta_R}\sigma^0_S} \\
m^2_{\sigma^0_S\sigma^0_{12}} & m^2_{\sigma^0_S\sigma^0_{21}} & m^2_{\sigma^0_S\sigma^0_{\Delta_R}} & m^2_{\sigma^0_S\sigma^0_{\delta_R}} & m^2_{\sigma^0_S\sigma^0_S}
\end{pmatrix}.
\tag{A10}
$$

The matrix elements are defined as

$$
\begin{aligned}
m^2_{\sigma^0_{12}\sigma^0_{21}} &= m^2_{\sigma^0_{21}\sigma^0_{12}} = \frac{1}{2}(\sqrt{2}T_3 v_s + \lambda_3(2\xi_F + \lambda_R v_{R1} v_{R2} + 3\lambda_s v_s^2)),\\
m^2_{\sigma^0_{12}\sigma^0_{12}} &= \frac{1}{8}(8m_1^2 + g_R^2 v_1^2 - g_R v_2^2 + g_L^2(v_1^2 - v_2^2) + 2g_R^2 v_{R1}^2 - 2g_R^2 v_{R2}^2 + 4\lambda_3^2 v_2^2 + 4\lambda_3^2 v_S^2 + 4\lambda_4 v_S^2),\\
m^2_{\sigma^0_{21}\sigma^0_{21}} &= \frac{1}{8}(g_L^2(v_2^2 - v_1^2) - g_R^2 v_1^2 + g_R^2 v_2^2 - 2g_R^2 v_{R1}^2 + 2g_R^2 v_{R2}^2 + 8m_2^2 + 4\lambda_3^2 v_1^2 + 4\lambda_3^2 v_s^2 + 4\lambda_5^2 v_s^2),\\
m^2_{\sigma^0_{\Delta_R}\sigma^0_{\Delta_R}} &= \frac{1}{4}(2g_B^2(v_{R1}^2 - v_{R2}^2) + g_R^2(v_1^2 - v_2^2 + 2v_{R1}^2 - 2v_{R2}^2) + 4m_{\Delta_R}^2 + 2\lambda_R^2(v_{R2}^2 + v_s^2)),
\end{aligned}
$$

$$
\begin{aligned}
m^2_{\sigma^0_{\delta_R}\sigma^0_{\delta_R}} &= \frac{1}{4}(2g_B^2(v_{R2}^2 - v_{R1}^2) + g_R^2(-v_1^2 + v_2^2 - 2v_{R1}^2 + 2v_{R2}^2) + 4m_{\delta_R}^2 + 2\lambda_R^2(v_{R1}^2 + v_s^2)),\\
m^2_{\sigma^0_{\Delta_R}\sigma^0_{\delta_R}} &= m_{\sigma^0_{\delta_R}\sigma^0_{\Delta_R}} = \frac{1}{2}(\lambda_R(-2\xi_F + \lambda_3 v_1 v_2 - 3\lambda_s v_s^2) - \sqrt{2}T_R v_s),\\
m^2_{\sigma^0_S\sigma^0_S} &= \frac{1}{2}(-12\lambda_s\xi_F + 2m_s^2 - 6\sqrt{2}T_S v_s + \lambda_3^2 v_1^2 + \lambda_4^2 v_1^2 + 6\lambda_3\lambda_s v_1 v_2 + \lambda_3^2 v_2^2 + \lambda_5^2 v_2^2 + \lambda_R^2 v_{R1}^2\\
&\quad - 6\lambda_R\lambda_s v_{R1} v_{R2} + \lambda_R^2 v_{R2}^2 + 18\lambda_s^2 v_s^2),\\
m^2_{\sigma^0_S\sigma^0_{12}} &= m^2_{\sigma^0_{12}\sigma^0_S} = \frac{T_3 v_2}{\sqrt{2}} - 3\lambda_3\lambda_s v_2 v_s, \qquad m^2_{\sigma^0_S\sigma^0_{21}} = m^2_{\sigma^0_{21}\sigma^0_S} = \frac{T_3 v_1}{\sqrt{2}} - 3\lambda_3\lambda_s v_1 v_s,\\
m^2_{\sigma^0_S\sigma^0_{\Delta_R}} &= m^2_{\sigma^0_{\Delta_R}\sigma^0_S} = 3\lambda_R\lambda_s v_{R2} v_s - \frac{T_R v_{R2}}{\sqrt{2}}, \qquad m^2_{\sigma^0_S\sigma^0_{\delta_R}} = m^2_{\sigma^0_{\delta_R}\sigma^0_S} = 3\lambda_R\lambda_s v_{R1} v_s - \frac{T_R v_{R1}}{\sqrt{2}}.
\end{aligned}
\tag{A11}
$$

By diagonalizing the matrix into physical mass eigenstates using the rotation matrix Z^A, three physical particles with definite masses, A_1, A_2, and A_3, are obtained. Meanwhile, the remaining two neutral states G_1^0 and G_2^0 become massless Goldstone bosons, which are absorbed by the corresponding gauge bosons Z and Z_R, giving them mass. The form of the transpose matrix is given as

$$
Z^A = \begin{pmatrix}
c_\beta & -s_\beta & 0 & 0 & 0\\
s_\beta & c_\beta & 0 & 0 & 0\\
0 & 0 & c_{\beta_R} & -s_{\beta_R} & 0\\
0 & 0 & s_{\beta_R} & c_{\beta_R} & 0\\
0 & 0 & 0 & 0 & 1
\end{pmatrix},
\tag{A12}
$$

where $c_\beta = \frac{v_1}{\sqrt{v_1^2+v_2^2}}$, $s_\beta = \frac{v_2}{\sqrt{v_1^2+v_2^2}}$, $c_{\beta_R} = \frac{v_{R1}}{\sqrt{v_{R1}^2+v_{R2}^2}}$, and $s_{\beta_R} = \frac{v_{R2}}{\sqrt{v_{R1}^2+v_{R2}^2}}$. Similarly, in the LRSSM, there are also two 2×2 *CP*-odd Higgs boson mass matrices, one of which has a basis of $(\mathrm{Im}[H_{11}^0], \mathrm{Im}[H_{22}^0])$

$$
m^2_{A_2} = \begin{pmatrix}
m^2_{\sigma^0_{11}\sigma^0_{11}} & m^2_{\sigma^0_{11}\sigma^0_{22}}\\
m^2_{\sigma^0_{22}\sigma^0_{11}} & m^2_{\sigma^0_{22}\sigma^0_{22}}
\end{pmatrix}.
\tag{A13}
$$

The various forms of the matrix elements are, respectively,

$$
\begin{aligned}
m^2_{\sigma^0_{11}\sigma^0_{22}} &= m^2_{\sigma^0_{22}\sigma^0_{11}} = \frac{T_3 v_s}{\sqrt{2}} + 2\lambda_4\lambda_5 v_1 v_2 + \lambda_3\left(\xi_F - \frac{\lambda_3 v_1 v_2}{2} + \frac{\lambda_R v_{R1} v_{R2}}{2} + \frac{3\lambda_s v_s^2}{2}\right),\\
m^2_{\sigma^0_{11}\sigma^0_{11}} &= -\frac{1}{4}g_L^2\left(\frac{v_1^2}{2} - \frac{v_2^2}{2}\right) - \frac{1}{4}g_R^2\left(\frac{v_1^2}{2} - \frac{v_2^2}{2} + v_{R1}^2 - v_{R2}^2\right) + m_1^2 + 2\lambda_4^2 v_1^2 + \frac{\lambda_3^2 v_s^2}{2} + \frac{\lambda_4^2 v_s^2}{2},\\
m^2_{\sigma^0_{22}\sigma^0_{22}} &= \frac{1}{4}g_L^2\left(\frac{v_1^2}{2} - \frac{v_2^2}{2}\right) + \frac{1}{4}g_R^2\left(\frac{v_1^2}{2} - \frac{v_2^2}{2} + v_{R1}^2 - v_{R2}^2\right) + m_2^2 + 2\lambda_5^2 v_2^2 + \frac{\lambda_3^2 v_s^2}{2} + \frac{\lambda_5^2 v_s^2}{2}.
\end{aligned}
\tag{A14}
$$

The basis of the other 2×2 *CP*-odd Higgs boson mass matrix is $(\mathrm{Im}[\Delta_L^0], \mathrm{Im}[\delta_L^0])$

$$
m^2_{A_3} = \begin{pmatrix}
m^2_{\sigma^0_{\Delta_L}\sigma^0_{\Delta_L}} & m^2_{\sigma^0_{\Delta_L}\sigma^0_{\delta_L}}\\
m^2_{\sigma^0_{\delta_L}\sigma^0_{\Delta_L}} & m^2_{\sigma^0_{\delta_L}\sigma^0_{\delta_L}}
\end{pmatrix}.
\tag{A15}
$$

The matrix elements are defined as

$$
\begin{aligned}
m^2_{\sigma^0_{\Delta_L}\sigma^0_{\Delta_L}} &= -g_B^2\left(\frac{v_{R2}^2}{2}-\frac{v_{R1}^2}{2}\right)+\frac{1}{2}g_L^2\left(\frac{v_1^2}{2}-\frac{v_2^2}{2}\right)+m^2_{\Delta_L}+\frac{\lambda_L^2 v_s^2}{2},\\
m^2_{\sigma^0_{\delta_L}\sigma^0_{\delta_L}} &= g_B^2\left(\frac{v_{R2}^2}{2}-\frac{v_{R1}^2}{2}\right)-\frac{1}{2}g_L^2\left(\frac{v_1^2}{2}-\frac{v_2^2}{2}\right)+m^2_{\delta_L}+\frac{\lambda_L^2 v_s^2}{2},\\
m^2_{\sigma^0_{\Delta_L}\sigma^0_{\delta_L}} &= m_{\sigma^0_{\delta_L}\sigma^0_{\Delta_L}} = -\frac{T_L v_s}{\sqrt{2}}-\lambda_L\left(\xi_F-\frac{\lambda_3 v_1 v_2}{2}+\frac{\lambda_R v_{R1} v_{R2}}{2}+\frac{3\lambda_s v_s^2}{2}\right).
\end{aligned}
\tag{A16}
$$

The mass-squared matrix for the singly charged Higgs bosons in the basis $(\Phi^{\pm}_{12},\Phi^{\pm}_{21},\Delta^{\pm}_R,\delta^{\pm}_R)$ is given as follows:

$$
m^2_{H_1^{\pm}}=\begin{pmatrix}
m^2_{\phi^+_{12}\phi^-_{12}} & m^2_{\phi^+_{12}\phi^-_{21}} & m^2_{\phi^+_{12}\Delta^-_R} & m^2_{\phi^+_{12}\delta^-_R}\\
m^2_{\phi^+_{21}\phi^-_{12}} & m^2_{\phi^+_{21}\phi^-_{21}} & m^2_{\phi^+_{21}\Delta^-_R} & m^2_{\phi^+_{21}\delta^-_R}\\
m^2_{\Delta^+_R\phi^-_{12}} & m^2_{\Delta^+_R\phi^-_{21}} & m^2_{\Delta^+_R\Delta^-_R} & m^2_{\Delta^+_R\delta^-_R}\\
m^2_{\delta^+_R\phi^-_{12}} & m^2_{\delta^+_R\phi^-_{21}} & m^2_{\delta^+_R\Delta^-_R} & m^2_{\delta^+_R\delta^-_R}
\end{pmatrix}.
\tag{A17}
$$

The matrix elements are defined as

$$
\begin{aligned}
m^2_{\phi^+_{12}\phi^-_{12}} &= \frac{1}{8}(g_L^2(v_1^2+v_2^2)+g_R^2v_1^2+g_R^2v_2^2-2g_R^2v_{R1}^2+2g_R^2v_{R2}^2+8m_1^2+4\lambda_3^2v_s^2+4\lambda_4^2v_s^2),\\
m^2_{\phi^+_{12}\phi^-_{21}} &= m_{\phi^+_{21}\phi^-_{12}} = \frac{1}{4}(g_L^2v_1v_2+g_R^2v_1v_2+4\lambda_3\xi_F+2\sqrt{2}T_3v_s-2\lambda_3^2v_1v_2+2\lambda_3\lambda_Rv_{R1}v_{R2}+6\lambda_3\lambda_sv_s^2),\\
m^2_{\phi^+_{21}\phi^-_{21}} &= \frac{1}{8}(g_L^2(v_1^2+v_2^2)+g_R^2v_1^2+g_R^2v_2^2+2g_R^2v_{R1}^2-2g_R^2v_{R2}^2+8m_2^2+4\lambda_3^2v_s^2+4\lambda_5^2v_s^2),\\
m^2_{\phi^+_{21}\Delta^-_R} &= m_{\Delta^+_R\phi^-_{21}} = \frac{g_R^2v_2v_{R2}}{2\sqrt{2}},\qquad m_{\phi^+_{12}\Delta^-_R} = m_{\Delta^+_R\phi^-_{12}} = -\frac{g_R^2v_2v_{R1}}{2\sqrt{2}},\\
m^2_{\phi^+_{21}\delta^-_R} &= m_{\delta^+_R\phi^-_{21}} = \frac{g_R^2v_1v_{R2}}{2\sqrt{2}},\qquad m_{\phi^+_{12}\delta^-_R} = m_{\delta^+_R\phi^-_{12}} = -\frac{g_R^2v_1v_{R1}}{2\sqrt{2}},\\
m^2_{\Delta^+_R\Delta^-_R} &= \frac{1}{2}(g_B^2(v_{R1}^2-v_{R2}^2)+g_R^2v_{R1}^2+2m^2_{\Delta_R}+\lambda_R^2v_s^2),\\
m^2_{\Delta^+_R\delta^-_R} &= m_{\delta^+_R\Delta^-_R} = \frac{1}{2}(-g_R^2v_{R1}v_{R2}+\sqrt{2}T_Rv_s+\lambda_R(2\xi_F-\lambda_3v_1v_2+\lambda_Rv_{R1}v_{R2}+3\lambda_sv_s^2)),\\
m^2_{\delta^+_R\delta^-_R} &= \frac{1}{2}(g_B^2(v_{R2}^2-v_{R1}^2)+g_R^2v_{R2}^2+2m^2_{\delta_R}+\lambda_R^2v_s^2).
\end{aligned}
\tag{A18}
$$

The basis of the other 2×2 charged Higgs boson mass matrix is $(\Phi^{\pm}_{11},\Phi^{\pm}_{22})$

$$
m^2_{H_2^{\pm}}=\begin{pmatrix}
m^2_{\phi^+_{11}\phi^-_{11}} & m^2_{\phi^+_{11}\phi^-_{22}}\\
m^2_{\phi^+_{22}\phi^-_{11}} & m^2_{\phi^+_{22}\phi^-_{22}}
\end{pmatrix}.
\tag{A19}
$$

The matrix elements are defined as

$$
\begin{aligned}
m^2_{\phi^+_{11}\phi^-_{11}} &= \frac{1}{8}(g_L^2(v_1^2-v_2^2)+g_R^2v_1^2-g_R^2v_2^2+2g_R^2v_{R1}^2-2g_R^2v_{R2}^2+8m_1^2+4\lambda_3^2v_s^2+4\lambda_4^2v_s^2),\\
m^2_{\phi^+_{22}\phi^-_{22}} &= \frac{1}{8}(g_L^2(v_2^2-v_1^2)-g_R^2v_1^2+g_R^2v_2^2-2g_R^2v_{R1}^2+2g_R^2v_{R2}^2+8m_2^2+4\lambda_3^2v_s^2+4\lambda_5^2v_s^2),\\
m^2_{\phi^+_{22}\phi^-_{11}} &= m^2_{\phi^+_{11}\phi^-_{22}} = \frac{1}{2}(\sqrt{2}T_3v_s+\lambda_3(2\xi_F-\lambda_3v_1v_2+\lambda_Rv_{R1}v_{R2}+3\lambda_sv_s^2)).
\end{aligned}
\tag{A20}
$$

The basis of the other 2×2 charged Higgs boson mass matrix is $(\Delta^{\pm}_L,\delta^{\pm}_L)$

$$m^2_{H_3^\pm} = \begin{pmatrix} m^2_{\Delta_L^+\Delta_L^-} & m^2_{\Delta_L^+\delta_L^-} \\ m^2_{\delta_L^+\Delta_L^-} & m^2_{\delta_L^+\delta_L^-} \end{pmatrix}. \tag{A21}$$

The various forms of the matrix elements are, respectively,

$$\begin{aligned} m^2_{\Delta_L^+\Delta_L^-} &= \frac{1}{2}(g_B^2(v_{R1}^2 - v_{R2}^2) + 2m^2_{\Delta_L} + \lambda_L^2 v_s^2), \\ m^2_{\delta_L^+\delta_L^-} &= \frac{1}{2}(g_B^2(v_{R2}^2 - v_{R1}^2) + 2m^2_{\delta_L} + \lambda_L^2 v_s^2), \\ m^2_{\Delta_L^+\delta_L^-} &= m^2_{\delta_L^+\Delta_L^-} = \frac{1}{2}\Big(\sqrt{2}T_L v_s + \lambda_L(2\xi_F - \lambda_3 v_1 v_2 \\ &\quad + \lambda_R v_{R1} v_{R2} + 3\lambda_s v_s^2)\Big). \end{aligned} \tag{A22}$$

In the LRSSM, the mass matrices $m^2_{H_1^\pm}$ and $m^2_{H_2^\pm}$ each contain a charged Goldstone boson, which, after electroweak symmetry breaking, is absorbed into the corresponding gauge bosons $W^\pm$ and $W_R^\pm$, imparting mass to these bosons. The mass matrix of the doubly charged Higgs bosons in the LRSSM is relatively simple, consisting of only two 2×2 matrices. The basis of the doubly charged Higgs boson mass matrix is $(\Delta_R^{\pm\pm}, \delta_R^{\pm\pm})$ and $(\Delta_L^{\pm\pm}, \delta_L^{\pm\pm})$. We denote them as $m^2_{H_1^{\pm\pm}}$ and $m^2_{H_2^{\pm\pm}}$, and their matrix forms are given below,

$$m^2_{H_1^{\pm\pm}} = \begin{pmatrix} m^2_{\Delta_R^{++}\Delta_R^{--}} & m^2_{\Delta_R^{++}\delta_R^{--}} \\ m^2_{\delta_R^{++}\Delta_R^{--}} & m^2_{\delta_R^{++}\delta_R^{--}} \end{pmatrix}, \tag{A23}$$

$$\begin{aligned} m^2_{\Delta_R^{++}\Delta_R^{--}} &= \frac{1}{4}(2g_B^2(v_{R1}^2 - v_{R2}^2) + g_R^2(-v_1^2 + v_2^2 - 2v_{R1}^2 + 2v_{R2}^2) + 4m^2_{\Delta_R} + 2\lambda_R^2 v_s^2), \\ m^2_{\delta_R^{++}\delta_R^{--}} &= \frac{1}{4}(-2g_B^2(v_{R1}^2 - v_{R2}^2) + g_R^2(v_1^2 - v_2^2 + 2v_{R1}^2 - 2v_{R2}^2) + 4m^2_{\delta_R} + 2\lambda_R^2 v_s^2), \\ m^2_{\Delta_R^{++}\delta_R^{--}} &= m^2_{\delta_R^{++}\Delta_R^{--}} = \frac{1}{2}\Big(\sqrt{2}T_R v_s + \lambda_R(2\xi_F - \lambda_3 v_1 v_2 + \lambda_R v_{R1} v_{R2} + 3\lambda_s v_s^2)\Big), \end{aligned} \tag{A24}$$

$$m^2_{H_2^{\pm\pm}} = \begin{pmatrix} m^2_{\Delta_L^{++}\Delta_L^{--}} & m^2_{\Delta_L^{++}\delta_L^{--}} \\ m^2_{\delta_L^{++}\Delta_L^{--}} & m^2_{\delta_L^{++}\delta_L^{--}} \end{pmatrix}, \tag{A25}$$

$$\begin{aligned} m^2_{\Delta_L^{++}\Delta_L^{--}} &= \frac{1}{4}(2g_B^2(v_{R1}^2 - v_{R2}^2) + g_L^2(v_2^2 - v_1^2) + 4m^2_{\Delta_L} + 2\lambda_L^2 v_s^2), \\ m^2_{\delta_L^{++}\delta_L^{--}} &= \frac{1}{4}(-2g_B^2 v_{R1}^2 + 2g_B^2 v_{R2}^2 + g_L^2(v_1^2 - v_2^2) + 4m^2_{\delta_L} + 2\lambda_L^2 v_s^2), \\ m^2_{\Delta_L^{++}\delta_L^{--}} &= m^2_{\delta_L^{++}\Delta_L^{--}} = \frac{1}{2}\Big(\sqrt{2}T_L v_s + \lambda_L(2\xi_F - \lambda_3 v_1 v_2 + \lambda_R v_{R1} v_{R2} + 3\lambda_s v_s^2)\Big). \end{aligned} \tag{A26}$$

The mass-squared matrix $m^2_{H_1^{\pm\pm}}$ of this doubly charged Higgs boson, when diagonalized, produces a negative eigenvalue, which is physically unreasonable as it would result in a tachyonic state. However, by incorporating radiative corrections into the mass of the doubly charged Higgs boson, this issue can be resolved, turning the eigenvalue positive [58,114].

APPENDIX B: SFERMION SECTORS, NEUTRALINOS, AND CHARGINOS

1. Sfermion sectors

In the LRSSM, fermions include scalar superpartners of up- and down-type quarks, as well as charged and neutral leptons. Because of the extended gauge symmetry in this model, the existence of right-handed neutrinos and their superpartners is ensured, making all fermion mass-squared matrices (including the sneutrinos) typically 6×6 matrices. We calculated the mass-squared matrices for scalar down-type squarks, up-type squarks, charged sleptons, and sneutrinos, which are represented in the gauge basis of $(\tilde{d}_L, \tilde{d}_R)$, $(\tilde{u}_L, \tilde{u}_R)$, $(\tilde{e}_L, \tilde{e}_R)$, and $(\tilde{\nu}_L, \tilde{\nu}_R)$. Therefore, we can express the mass-squared matrix of the squarks in the following form:

$$\mathbf{m}^2_{\tilde{d}} = \begin{pmatrix} m^2_{\tilde{d}_L\tilde{d}_L^*} & m^2_{\tilde{d}_L\tilde{d}_R^*} \\ m^2_{\tilde{d}_R\tilde{d}_L^*} & m^2_{\tilde{d}_R\tilde{d}_R^*} \end{pmatrix}, \qquad \mathbf{m}^2_{\tilde{u}} = \begin{pmatrix} m^2_{\tilde{u}_L\tilde{u}_L^*} & m^2_{\tilde{u}_L\tilde{u}_R^*} \\ m^2_{\tilde{u}_R\tilde{u}_L^*} & m^2_{\tilde{u}_R\tilde{u}_R^*} \end{pmatrix}. \tag{B1}$$

Each matrix element itself is a 3×3 matrix,

$$
\begin{aligned}
m^2_{\tilde{d}_L\tilde{d}^*_L} &= \frac{1}{3}g_B^2\left(\frac{v_{R2}^2}{2}-\frac{v_{R1}^2}{2}\right)+\left(\frac{1}{4}g_L^2\left(\frac{v_2^2}{2}-\frac{v_1^2}{2}\right)+m^2_{Q_L}+\frac{v_1^2(Y_Q^1)^2}{2}\right)\delta_{\alpha_1\beta_1},\\
m^2_{\tilde{d}_R\tilde{d}^*_R} &= -\frac{1}{3}g_B^2\left(\frac{v_{R2}^2}{2}-\frac{v_{R1}^2}{2}\right)+\left(\frac{1}{4}g_R^2\left(-\frac{v_1^2}{2}+\frac{v_2^2}{2}+v_{R1}^2-v_{R2}^2\right)+m^2_{Q_R}+\frac{v_1^2(Y_Q^1)^2}{2}\right)\delta_{\alpha_2\beta_2},\\
m^2_{\tilde{d}_L\tilde{d}^*_R} &= m^2_{\tilde{d}_R\tilde{d}^*_L}=\left(-\frac{T_Q^1 v_1}{\sqrt{2}}-\frac{1}{2}\lambda_3 v_2 v s Y_Q^1\right)\delta_{\alpha_1\beta_2},\\
m^2_{\tilde{u}_L\tilde{u}^*_L} &= \frac{1}{3}g_B^2\left(-\frac{v_{R1}^2}{2}+\frac{v_{R2}^2}{2}\right)+\left(m^2_{Q_L}+\frac{1}{4}g_L^2\left(\frac{v_1^2}{2}-\frac{v_2^2}{2}\right)+\frac{v_2^2(Y_Q^2)^2}{2}\right)\delta_{\alpha_1\beta_1},\\
m^2_{\tilde{u}_R\tilde{u}^*_R} &= -\frac{1}{3}g_B^2\left(-\frac{v_{R1}^2}{2}+\frac{v_{R2}^2}{2}\right)+\left(m^2_{Q_R}-\frac{1}{4}g_R^2\left(-\frac{v_1^2}{2}+\frac{v_2^2}{2}+v_{R1}^2-v_{R2}^2\right)+\frac{v_2^2(Y_Q^2)^2}{2}\right)\delta_{\alpha_2\beta_2},\\
m^2_{\tilde{u}_L\tilde{u}^*_R} &= m^2_{\tilde{u}_R\tilde{u}^*_L}=\left(\frac{T_Q^2 v_2}{\sqrt{2}}+\frac{1}{2}v_1 v_s Y_Q^2\lambda_3\right)\delta_{\alpha_1\beta_2}.
\end{aligned}
\tag{B2}
$$

Here α_1, α_2, β_1, and β_2 denote color indices. In general, these 3×3 matrices can be nondiagonal, allowing off-diagonal elements to enable mixing between different flavors. In our study, we do not consider flavor-violating processes; therefore, for simplicity, we assume that the matrices are diagonal and their elements are real. Likewise, the mass-squared matrix of the slepton is expressed as follows:

$$
\mathbf{m}^2_{\tilde{e}}=\begin{pmatrix} m^2_{\tilde{e}_L\tilde{e}^*_L} & m^2_{\tilde{e}_L\tilde{e}^*_R}\\ m^2_{\tilde{e}_R\tilde{e}^*_L} & m^2_{\tilde{e}_R\tilde{e}^*_R}\end{pmatrix},\qquad \mathbf{m}^2_{\tilde{\nu}}=\begin{pmatrix} m^2_{\tilde{\nu}_L\tilde{\nu}^*_L} & m^2_{\tilde{\nu}_L\tilde{\nu}^*_R}\\ m^2_{\tilde{\nu}_R\tilde{\nu}^*_L} & m^2_{\tilde{\nu}_R\tilde{\nu}^*_R}\end{pmatrix},
\tag{B3}
$$

with the matrix elements in the slepton sector being

$$
\begin{aligned}
m^2_{\tilde{e}_L\tilde{e}^*_L} &= \frac{g_B^2}{2}(v_{R2}^2-v_{R1}^2)+\frac{g_L^2}{2}(v_1^2-v_2^2)+(Y_L^1)^2v_2^2+m^2_{L_L},\\
m^2_{\tilde{e}_R\tilde{e}^*_R} &= \frac{g_B^2}{2}(v_{R1}^2-v_{R2}^2)+\frac{g_R^2}{4}(2v_{R2}^2-2v_{R1}^2-v_2^2+v_1^2)+v_2^2(Y_L^1)^2+m^2_{L_R},\\
m^2_{\tilde{e}_L\tilde{e}^*_R} &= m^2_{\tilde{e}_R\tilde{e}^*_L}=Y_L^1\lambda_3 v_s v_1-v_2T_L^1,\\
m^2_{\tilde{\nu}_L\tilde{\nu}^*_L} &= \frac{g_B^2}{2}(v_{R2}^2-v_{R1}^2)+\frac{g_L^2}{2}(v_2^2-v_1^2)+(Y_L^1)^2v_1^2+m^2_{L_L},\\
m^2_{\tilde{\nu}_R\tilde{\nu}^*_R} &= v_{R2}^2h_{RR}^2+\left(\frac{g_B^2}{2}(v_{R1}^2-v_{R2}^2)+\frac{g_R^2}{4}(2v_{R1}^2-2v_{R2}^2-v_1^2+v_1^2)+v_1^2(Y_L^1)^2+m^2_{L_R}\right),\\
m^2_{\tilde{\nu}_L\tilde{\nu}^*_R} &= m^2_{\tilde{\nu}_R\tilde{\nu}^*_L}=-Y_L^1\lambda_3 v_s v_1+v_1T_L^1.
\end{aligned}
\tag{B4}
$$

2. Neutralinos and charginos

This model contains 12 neutral fermions, with their mass matrix decomposed into three independent blocks: two 2×2 blocks that describe the mixing of the $\tilde{\delta}_L/\tilde{\Delta}_L$ and $\tilde{\Phi}^0_{22}/\tilde{\Phi}^0_{11}$ fields, respectively, and an 8×8 block involving the mixing of the other eight neutral Higgsinos and gauginos. These two 2×2 blocks are represented in the bases of $(\tilde{\delta}_L, \tilde{\Delta}^0_L)$ and $(\tilde{\Phi}^0_{22}, \tilde{\Phi}^0_{11})$,

$$
M_{\tilde{\chi}_\delta}=\begin{pmatrix}0 & \mu_L\\ \mu_L & 0\end{pmatrix}\quad\text{and}\quad M_{\tilde{\chi}_\Phi}=\begin{pmatrix}0 & -\mu_{\text{eff}}\\ -\mu_{\text{eff}} & 0\end{pmatrix},
\tag{B5}
$$

while the last 8×8 block reads, in the basis of $(\tilde{\Phi}^0_{12}, \tilde{\Phi}^0_{21}, \tilde{\delta}^0_R, \tilde{\Delta}^0_R, \tilde{S}, \tilde{B}, \tilde{W}^0_L, \tilde{W}^0_R)$,

$$M_{\chi^0}=\begin{pmatrix} 0 & -\mu_{\rm eff} & 0 & 0 & -\mu_2 & 0 & \frac{g_L v_1}{\sqrt{2}} & -\frac{g_R v_1}{\sqrt{2}} \\ -\mu_{\rm eff} & 0 & 0 & 0 & -\mu_1 & -\frac{g_L v_2}{\sqrt{2}} & \frac{g_R v_2}{\sqrt{2}} & 0 \\ 0 & 0 & 0 & \mu_R & \frac{\lambda_R v_{R1}}{\sqrt{2}} & g_R v_{R1} & 0 & -g_R v_{R1} \\ 0 & 0 & \mu_R & 0 & \frac{\lambda_R v_{R2}}{\sqrt{2}} & -g_R v_{R2} & 0 & -g_R v_{R2} \\ -\mu_2 & -\mu_1 & \frac{\lambda_R v_{R1}}{\sqrt{2}} & \frac{\lambda_R v_{R2}}{\sqrt{2}} & \mu_S & 0 & 0 & 0 \\ 0 & -\frac{g_L v_2}{\sqrt{2}} & g_R v_{R1} & -g_R v_{R2} & 0 & M_1 & 0 & 0 \\ \frac{g_L v_1}{\sqrt{2}} & \frac{g_L v_2}{\sqrt{2}} & 0 & 0 & 0 & 0 & M_{2L} & 0 \\ -\frac{g_R v_1}{\sqrt{2}} & \frac{g_R v_2}{\sqrt{2}} & -g_R v_{R1} & -g_R v_{R2} & 0 & 0 & 0 & M_{2R} \end{pmatrix}. \tag{B6}$$

We have defined $\mu_{\rm eff}=\lambda_3\frac{v_s}{\sqrt{2}},\mu_S=\lambda_S\frac{v_s}{\sqrt{2}},\mu_{L,R}=\lambda_{L,R}\frac{v_s}{\sqrt{2}}$, and $\mu_{1,2}=\lambda_3\frac{v_{1,2}}{\sqrt{2}}$. In the charged sector, the model has six singly charged charginos whose mass matrix can be written, in the bases of $(\tilde{\delta}_L^+,\tilde{\delta}_R^+,\tilde{\Phi}_{11}^+,\tilde{\Phi}_{21}^+,\tilde{W}_L^+,\tilde{W}_R^+)$ and $(\tilde{\Delta}_L^-,\tilde{\Delta}_R^-,\tilde{\Phi}_{12}^-,\tilde{\Phi}_{22}^-,\tilde{W}_L^-,\tilde{W}_R^-)$,

$$M_{\tilde{\chi}^\pm}=\begin{pmatrix} \lambda_L v_s/\sqrt{2} & 0 & 0 & 0 & 0 & 0 \\ 0 & \lambda_R v_s/\sqrt{2} & 0 & 0 & 0 & -g_R v_{R1} \\ 0 & 0 & 0 & \mu_{\rm eff} & g_L v_1/\sqrt{2} & 0 \\ 0 & 0 & \mu_{\rm eff} & 0 & 0 & -g_R v_2/\sqrt{2} \\ 0 & 0 & 0 & g_L v_2/\sqrt{2} & M_{2L} & 0 \\ 0 & g_R v_{R2} & -g_R v_1/\sqrt{2} & 0 & 0 & M_{2R} \end{pmatrix}. \tag{B7}$$

APPENDIX C: THE EXPRESSIONS FOR HIGGS DECAYS IN THE LRSSM

The concrete expressions that are present in the LRSSM are specifically discussed in the following:

(1) *CP*-even Higgs-W boson-W boson contribution

$$\begin{aligned} g_{h_i W_{L\mu}^+ W_{L\nu}^-} &= \frac{i}{2} g_{\mu\nu} g_L^2 (v_1 Z_{i1}^H + v_2 Z_{i2}^H), \\ g_{h_i W_{R\mu}^+ W_{R\nu}^-} &= \frac{i}{2} g_{\mu\nu} g_R^2 (v_1 Z_{i1}^H + v_2 Z_{i2}^H + 2v_{R1} Z_{i3}^H + 2v_{R2} Z_{i3}^H). \end{aligned} \tag{C1}$$

(2) *CP*-even Higgs-Z boson-Z boson contribution

$$\begin{aligned} g_{h_i Z_{L\mu} Z_{L\nu}} &= \frac{i}{2} g_{\mu\nu} \frac{g_L^2}{4\cos\theta_W} (v_1 Z_{i1}^H + v_2 Z_{i2}^H), \\ g_{h_i Z_{R\mu} Z_{R\nu}} &= \frac{i}{2} g_{\mu\nu} (g_R^2 + g_B^2)(4\cos\theta_R (v_1 Z_{i1}^H + v_2 Z_{i2}^H) + 4v_{R1} Z_{i3}^H + 4v_{R2} Z_{i3}^H). \end{aligned} \tag{C2}$$

(3) *CP*-even Higgs-charged Higgs-charged Higgs contribution

$$\begin{aligned} g_{h_i h_j^+ h_k^-} = {} & \frac{1}{8}(g_L^2 v_1 Z_{i1}^H + g_R^2 v_1 Z_{i1}^H + g_L^2 v_2 Z_{i2}^H + g_R^2 v_2 Z_{i2}^H - 2g_R^2 v_{R1} Z_{i3}^H + 2g_R^2 v_{R2} Z_{i4}^H \\ & + 4v_S Z_{i5}^H \lambda_3^2 + 4v_S Z_{i5}^H \lambda_4^2) Z_{j1}^+ Z_{k1}^+ + \frac{1}{8}(g_L^2 v_1 Z_{i1}^H + g_R^2 v_1 Z_{i1}^H + g_L^2 v_2 Z_{i2}^H \\ & + g_R^2 v_2 Z_{i2}^H + 2g_R^2 v_{R1} Z_{i3}^H - 2g_R^2 v_{R2} Z_{i4}^H + 4v_S Z_{i5}^H \lambda_3^2 + 4v_S Z_{i5}^H \lambda_4^2) Z_{j2}^+ Z_{k2}^+ \\ & + \frac{1}{2}(g_R^2 v_{R1} Z_{i3}^H + g_B^2 (v_{R1} Z_{i3}^H - v_{R2} Z_{i4}^H) + v_S Z_{i5}^H \lambda_R^2) Z_{j3}^+ Z_{k3}^+ + \frac{1}{2}(g_R^2 v_{R2} Z_{i4}^H \end{aligned}$$

$$
\begin{aligned}
&+ g_B^2(-v_{R1}Z_{i3}^H + v_{R2}Z_{i4}^H) + v_S Z_{i5}^H \lambda_R^2) Z_{j4}^+ Z_{k4}^+ + \frac{1}{4}(g_L^2(v_1 Z_{i2}^H + v_2 Z_{i1}^H) \\
&+ g_R^2(v_1 Z_{i2}^H + v_2 Z_{i1}^H) + 2\sqrt{2}T_3 Z_{i5}^H - 2(v_1 Z_{i2}^H + v_2 Z_{i1}^H)\lambda_3^2 + 2(v_{R1}Z_{i4}^H + v_{R2}Z_{i3}^H)\lambda_3\lambda_R \\
&+ 6v_S Z_{i5}^H \lambda_3 \lambda_S) Z_{j1}^+ Z_{k2}^+ - \frac{1}{2\sqrt{2}} g_R^2 (v_1 Z_{i3}^H + v_{R1} Z_{i1}^H) Z_{j1}^+ Z_{k3}^+ \\
&- \frac{1}{2\sqrt{2}} g_R^2 (v_1 Z_{i4}^H + v_{R2} Z_{i1}^H) Z_{j1}^+ Z_{k4}^+ - \frac{1}{2\sqrt{2}} g_R^2 (v_2 Z_{i3}^H + v_{R1} Z_{i2}^H) Z_{j2}^+ Z_{k3}^+ \\
&- \frac{1}{2\sqrt{2}} g_R^2 (v_2 Z_{i4}^H + v_{R2} Z_{i2}^H) Z_{j2}^+ Z_{k4}^+ + \frac{1}{2}(-g_R^2(v_{R1}Z_{i4}^H + v_{R2}Z_{i3}^H) + \sqrt{2}T_R Z_{i5}^H \\
&+ \lambda_R(-(v_1 Z_{i2}^H + v_2 Z_{i1}^H)\lambda_3 + (v_{R1}Z_{i4}^H + v_{R2}Z_{i3}^H)\lambda_R + 3v_S Z_{i5}^H \lambda_S)) Z_{j3}^+ Z_{k4}^+ .
\end{aligned} \tag{C3}
$$

(4) *CP*-even Higgs-squark-up squark contribution

$$
\begin{aligned}
g_{h_i \tilde{u}_j \tilde{u}_k} = -\frac{i}{12}\Bigg(&\sum_{a=1}^{3} Z_{j3+a}^U Z_{k3+a}^U (2(-3g_R^2 + g_B^2)(v_{1R}Z_{i3}^H - v_{2R}Z_{i4}^H) + 3g_R^2 v_1 Z_{i1}^H \\
&- 3g_R^2 v_2 Z_{i2}^H) + \sum_{a=1}^{3} Z_{ja}^U Z_{ka}^U (2g_B^2(-v_{1R}Z_{i3}^H + v_{2R}Z_{i4}^H) + 3g_L^2 v_1 Z_{i1}^H - 3g_L^2 v_2 Z_{i2}^H) \\
&- 6\Bigg(2\sqrt{2}m_{\Phi_1} \sum_{b=1}^{3} Z_{kb}^U \sum_{a=1}^{3} Y_{Q1,ab}^* Z_{j3+a}^U Z_{i1}^H + 2\sqrt{2}\mu_4^* \sum_{b=1}^{3} Z_{jb}^U \sum_{a=1}^{3} Z_{k3+a}^U Y_{Q1,ab} Z_{i1}^H\Bigg) \\
&+ \lambda_3 v_S \sum_{b=1}^{3} Z_{jb}^U \sum_{a=1}^{3} Z_{k3+a}^U Y_{Q2,ab} Z_{i1}^H - \sqrt{2} \sum_{b=1}^{3} Z_{jb}^U \sum_{c=1}^{3} Z_{kc}^U \sum_{a=1}^{3} Z_{j3+a}^U T_{Q2,ac} Z_{i2}^H \\
&- 2v_2 \sum_{b=1}^{3} Z_{jb}^U \sum_{c=1}^{3} Z_{kc}^U \sum_{a=1}^{3} Z_{j3+a}^U Y_{Q2,ac}^* Z_{i2}^H + \lambda_3 v_S \sum_{b=1}^{3} Z_{jb}^U \sum_{a=1}^{3} Z_{k3+a}^U Y_{Q2,ab} Z_{i5}^H\Bigg) Z_{j3}^D Z_{k3}^D .
\end{aligned} \tag{C4}
$$

(5) *CP*-even Higgs-down squark-down squark contribution

$$
\begin{aligned}
g_{h_i \tilde{d}_j \tilde{d}_k} = \frac{i}{12}\Bigg(&\sum_{a=1}^{3} Z_{ja}^D Z_{ka}^D (2g_B^2(v_{R1}Z_{i3}^H - v_{R2}Z_{i4}^H) + 3g_L^2 v_1 Z_{i1}^H - 3g_L^2 v_2 Z_{i2}^H) \\
&+ \sum_{a=1}^{3} Z_{j3+a}^D Z_{k3+a}^D (-2(3g_R^2 + g_B^2)(v_{R1}Z_{i3}^H - v_{R2}Z_{i4}^H) + 3g_R^2 v_1 Z_{i1}^H - 3g_R^2 v_2 Z_{i2}^H) \\
&- 6\Bigg(\sqrt{2} \sum_{b=1}^{3} Z_{kb}^D \sum_{a=1}^{3} T_{Q1,ab}^* Z_{j3+a}^D Z_{i1}^H + \sqrt{2} \sum_{b=1}^{3} Z_{jb}^D \sum_{a=1}^{3} Z_{k3+a}^D T_{Q1,ab} Z_{i1}^H\Bigg) \\
&+ 2v_1 \sum_{c=1}^{3} Z_{kc}^D \sum_{b=1}^{3} Z_{jb}^D \sum_{a=1}^{3} Y_{Q1,ac}^* Z_{j3+a}^D Z_{i1}^H + 2v_1 \sum_{c=1}^{3} Z_{jc}^D \sum_{b=1}^{3} Z_{k3+b}^D \sum_{a=1}^{3} Y_{Q1,ca} Y_{Q1,ba} Z_{i1}^H \\
&- \lambda_3 v_S \sum_{b=1}^{3} Z_{jb}^D \sum_{a=1}^{3} Z_{k3+a}^D Y_{Q1,ab} Z_{i2}^H - 2\sqrt{2}m_{\Phi_2} \sum_{b=1}^{3} Z_{kb}^D \sum_{a=1}^{3} Y_{Q2,ab} Z_{j3+a}^D Z_{i2}^H \\
&- \lambda_3 v_S \sum_{b=1}^{3} Z_{jb}^D \sum_{a=1}^{3} Z_{k3+a}^D Y_{Q2,ab} Z_{i5}^H - 2v_2 \sum_{b=1}^{3} Z_{jb}^D \sum_{a=1}^{3} Z_{k3+a}^D Y_{Q1,ab} Z_{i5}^H\Bigg).
\end{aligned} \tag{C5}
$$

(6) *CP*-even Higgs-slepton-slepton contribution

$$
\begin{aligned}
g_{h_i\tilde{l}_j\tilde{l}_k} = \frac{i}{4}\Bigg(&\sum_{a=1}^{3} Z^E_{j3+a}Z^E_{k3+a}(2(-g_R^2+g_B^2)(v_{R1}Z^H_{i3}-v_{R2}Z^H_{i4})+g_R^2 v_1 Z^H_{i1}-g_R^2 v_2 Z^H_{i2})\\
&+\sum_{a=1}^{3} Z^E_{ja}Z^E_{ka}(2g_B^2(-v_{R1}Z^H_{i3}+v_{R2}Z^H_{i4})+g_L^2 v_1 Z^H_{i1}-g_L^2 v_2 Z^H_{i2})\\
&+2\Bigg(-\sqrt{2}\sum_{b=1}^{3} Z^E_{kb}\sum_{a=1}^{3} T^*_{L1,ab}Z^E_{j3+a}Z^H_{i1}-\sqrt{2}\sum_{b=1}^{3} Z^E_{jb}\sum_{a=1}^{3} Z^E_{k3+a}T_{L1,ab}Z^H_{i1}\Bigg)\\
&-2v_1\sum_{c=1}^{3} Z^E_{kc}\sum_{b=1}^{3} Z^E_{jb}\sum_{a=1}^{3} Y^*_{L1,ac}Z^E_{j3+a}Z^H_{i1}-2v_1\sum_{c=1}^{3} Z^E_{jc}\sum_{b=1}^{3} Z^E_{k3+b}\sum_{a=1}^{3} Y_{L1,ca}Y_{L1,ba}Z^H_{i1}\\
&+\lambda_3 v_S\sum_{b=1}^{3} Z^E_{jb}\sum_{a=1}^{3} Z^E_{k3+a}Y_{L1,ab}Z^H_{i2}+\lambda_3 v_S\sum_{b=1}^{3} Z^E_{jb}\sum_{a=1}^{3} Z^E_{k3+a}Y_{L1,ab}Z^H_{i2}\\
&+2\sqrt{2}m_{\Phi_2}\sum_{b=1}^{3} Z^E_{kb}\sum_{a=1}^{3} Y_{L2,ab}Z^E_{j3+a}Z^H_{i2}+2\sqrt{2}m^*_{\Phi_2}\sum_{b=1}^{3} Z^E_{jb}\sum_{a=1}^{3} Z^E_{k3+a}Y_{L2,ab}Z^H_{i2}\\
&+3\lambda_3 v_2\sum_{b=1}^{3} Z^E_{jb}\sum_{a=1}^{3} Z^E_{k3+a}Y_{L1,ab}Z^H_{i5}\Bigg).
\end{aligned}
\tag{C6}
$$

(7) *CP*-even Higgs-double charged Higgs-double charged Higgs contribution

$$
\begin{aligned}
g_{h_i H^{++}_{R,j}H^{--}_{R,k}} = -\frac{i}{2}\Big(&U^{--}_{j2}(U^{--}_{k2}(-g_R^2 v_1 Z^H_{i1}+g_R^2 v_2 Z^H_{i2}+2g_B^2 v_{R1}Z^H_{i3}+2g_R^2 v_{R1}Z^H_{i3}+2g_B^2 v_{R2}Z^H_{i4}\\
&-2g_R^2 v_{R2}Z^H_{i4})+2\lambda_R^2 v_S Z^H_{i5})+U^{--}_{k1}(-\lambda_3\lambda_R v_2 Z^H_{i1}-\lambda_3\lambda_R v_1 Z^H_{i2}+\lambda_R^2 v_{R2}Z^H_{i3}\\
&+\lambda_R^2 v_{R1}Z^H_{i4}+2\lambda_R v_S Z^H_{i5}+\sqrt{2}T_R Z^H_{i5})+U^{--}_{j1}(g_R^2 v_1 Z^H_{i1}-g_R^2 v_2 Z^H_{i2}+2g_B^2 v_{R1}Z^H_{i3}\\
&-2g_R^2 v_{R1}Z^H_{i3}-2g_R^2 v_{R2}Z^H_{i4}+2g_R^2 v_{R2}Z^H_{i4}+2\lambda_R^2 v_S Z^H_{i5})+U^{--}_{k2}(-\lambda_3\lambda_R v_2 Z^H_{i1}\\
&-\lambda_3\lambda_R v_1 Z^H_{i2}+\lambda_R^2 v_{R2}Z^H_{i3}+\lambda_R^2 v_{R1}Z^H_{i4}+2\lambda_R v_S Z^H_{i5}+\sqrt{2}T_R Z^H_{i5})\Big),
\end{aligned}
\tag{C7}
$$

$$
\begin{aligned}
g_{h_i H^{++}_{L,j}H^{--}_{L,k}} = -\frac{i}{2}\Big(&U^{--}_{L,j2}(U^{--}_{L,k2}(-2g_B^2 v_{R1}Z^H_{k3}+2g_B^2 v_{R2}Z^H_{k4}+2\lambda_L^2 v_S Z^H_{k5}+g_L^2 v_1 Z^H_{k1}-g_L^2 v_2 Z^H_{k2})\\
&+U^{--}_{L,k1}(-\lambda_3\lambda_L v_2 Z^H_{k1}-\lambda_3\lambda_L v_1 Z^H_{k2}+\lambda_L\lambda_R v_{R2}Z^H_{k3}+\lambda_L\lambda_R v_{R1}Z^H_{k4}+2\lambda_L\lambda_S v_S Z^H_{k5})\\
&+\sqrt{2}T_L Z^H_{k5}))+U^{--}_{L,j1}(U^{--}_{L,k1}(2g_B^2 v_{R1}Z^H_{k3}-2g_B^2 v_{R2}Z^H_{k4}+2\lambda_L^2 v_S Z^H_{k5}-g_L^2 v_1 Z^H_{k1}\\
&+g_L^2 v_2 Z^H_{k2})+U^{--}_{L,k2}(-\lambda_3\lambda_L v_2 Z^H_{k1}-\lambda_3\lambda_L v_1 Z^H_{k2}+\lambda_L\lambda_R v_{R2}Z^H_{k3}+\lambda_L\lambda_R v_{R1}Z^H_{k4}\\
&+2\lambda_L\lambda_S v_S Z^H_{k5})+\sqrt{2}T_L Z^H_{k5})\Big).
\end{aligned}
\tag{C8}
$$

(8) *CP*-even Higgs chargino chargino contribution

$$
\begin{aligned}
g_{h_i\chi^+_j\chi^-_k} = -\frac{i}{2}&(\sqrt{2}g_L U^+_{k_1}U^{-,*}_{j_4}Z^H_{i_1}+\sqrt{2}g_L U^+_{k_3}U^{-,*}_{j_1}Z^H_{i_2}-\sqrt{2}g_R U^+_{k_2}U^{-,*}_{j_3}Z^H_{i_2})\\
&-2g_R U^+_{k_2}U^{-,*}_{j_6}Z^H_{i_3}+2g_R U^+_{k_4}U^{-,*}_{j_2}Z^H_{i_4}+\sqrt{2}\lambda_L U^+_{k_5}U^{-,*}_{j_3}Z^H_{i_5}\\
&+\sqrt{2}\lambda_R U^+_{k_6}U^{-,*}_{j_6}Z^H_{i_5}+\sqrt{2}U^+_{k_4}(-g_R U^{-,*}_{j_2}Z^H_{i_1}+\lambda_3 U^{-,*}_{j_3}Z^H_{i_5})\left(\frac{1-\gamma_5}{2}\right)
\end{aligned}
$$

$$
\begin{aligned}
&+\frac{-i}{2}(\sqrt{2}g_L U^+_{j_1}U^-_{k_4}Z^H_{i_1}+\sqrt{2}g_L U^+_{j_3}U^-_{k_1}Z^H_{i_2}-\sqrt{2}g_R U^+_{j_2}U^-_{k_2}Z^H_{i_2})\\
&+2g_R U^+_{j_6}U^-_{k_2}Z^H_{i_4}+\sqrt{2}\lambda_3 U^+_{j_4}U^-_{k_3}Z^H_{i_5}+\sqrt{2}\lambda_R U^+_{j_6}U^-_{k_5}Z^H_{i_5}\\
&+\sqrt{2}U^+_{j_4}(-g_R U^-_{k_2}Z^H_{i_2}+\lambda_3 U^-_{k_3}Z^H_{i_5})\left(\frac{1+\gamma_5}{2}\right).
\end{aligned}
\tag{C9}
$$

(9) *CP*-even-Higgs-neutralino-neutralino contribution

$$
\begin{aligned}
g_{h_i\chi^0_j\chi^0_k}=&-\frac{i}{2}(g_L Z^{0,*}_{k_1}Z^{0,*}_{j_6}Z^H_{i_1}-g_R Z^{0,*}_{k_2}Z^{0,*}_{j_6}Z^H_{i_1}-\sqrt{2}\lambda_3 Z^{0,*}_{k_5}Z^{0,*}_{j_{12}}Z^H_{i_1})\\
&-g_L Z^{0,*}_{k_5}Z^{0,*}_{j_1}Z^H_{i_2}+g_R Z^{0,*}_{k_2}Z^{0,*}_{j_7}Z^H_{i_2}-g_L Z^{0,*}_{k_1}1Z^{0,*}_{j_5}Z^H_{i_2}+g_R Z^{0,*}_{k_6}Z^{0,*}_{j_5}Z^H_{i_2}\\
&+2g_R Z^{0,*}_{k_1}Z^{0,*}_{j_2}Z^H_{i_3}-2g_B Z^{0,*}_{k_3}Z^{0,*}_{j_4}Z^H_{i_3}+2g_R Z^{0,*}_{k_5}Z^{0,*}_{j_2}Z^H_{i_4}-2g_B Z^{0,*}_{k_3}Z^{0,*}_{j_9}Z^H_{i_4}\\
&+\sqrt{2}\lambda_R Z^{0,*}_{k_9}Z^{0,*}_{j_8}Z^H_{i_3}-2g_R Z^{0,*}_{k_1}0Z^{0,*}_{j_6}Z^H_{i_4}+2g_B Z^{0,*}_{k_1}1Z^{0,*}_{j_9}Z^H_{i_4}-2g_R Z^{0,*}_{k_1}2Z^{0,*}_{j_1}0Z^H_{i_5}\\
&+2g_B Z^{0,*}_{k_1}3Z^{0,*}_{j_6}Z^H_{i_5}+\sqrt{2}\lambda_3 Z^{0,*}_{k_4}Z^{0,*}_{j_2}Z^H_{i_4}-\sqrt{2}\lambda_3 Z^{0,*}_{k_3}Z^{0,*}_{j_4}Z^H_{i_4}+\sqrt{2}\lambda_R Z^{0,*}_{k_8}Z^{0,*}_{j_5}Z^H_{i_5}\\
&-\sqrt{2}\lambda_3 Z^{0,*}_{k_7}Z^{0,*}_{j_6}Z^H_{i_4}+\sqrt{2}\lambda_R Z^{0,*}_{k_1}2Z^{0,*}_{j_1}0Z^H_{i_5}+\sqrt{2}\lambda_R Z^{0,*}_{k_1}3Z^{0,*}_{j_1}0Z^H_{i_6}+\sqrt{2}\lambda_3 Z^{0,*}_{k_4}Z^{0,*}_{j_3}Z^H_{i_6}\\
&+\sqrt{2}\lambda_R Z^{0,*}_{k_8}Z^{0,*}_{j_9}Z^H_{i_6}+\sqrt{2}Z^{0,*}_{k_9}Z^{0,*}_{j_8}Z^H_{i_3}+\sqrt{2}\lambda_3 Z^{0,*}_{k_7}Z^{0,*}_{j_6}Z^H_{i_4}\left(\frac{1-\gamma_5}{2}\right)\\
&+\frac{-i}{2}(g_L Z^0_{k_1}Z^0_{j_6}Z^H_{i_1}-g_R Z^0_{k_2}Z^0_{j_6}Z^H_{i_1}-\sqrt{2}\lambda_3 Z^0_{k_5}Z^0_{j_{12}}Z^H_{i_1}-g_L Z^0_{k_5}Z^0_{j_1}Z^H_{i_2})\\
&+g_R Z^0_{k_5}Z^0_{j_2}Z^H_{i_2}-g_L Z^0_{k_1}Z^0_{j_5}Z^H_{i_2}+g_R Z^0_{k_{11}}Z^0_{j_2}Z^H_{i_3}+2g_R Z^0_{k_1}Z^0_{j_2}Z^H_{i_3}\\
&-2g_B Z^0_{k_3}Z^0_{j_4}Z^H_{i_3}+2g_R Z^0_{k_5}Z^0_{j_2}Z^H_{i_4}-2g_B Z^0_{k_3}Z^0_{j_9}Z^H_{i_4}+\sqrt{2}\lambda_R Z^0_{k_9}Z^0_{j_{12}}Z^H_{i_3}\\
&-2g_R Z^0_{k_9}Z^0_{j_2}Z^H_{i_4}+2g_B Z^0_{k_3}Z^0_{j_9}Z^H_{i_4}-2g_R Z^0_{k_{12}}Z^0_{j_{10}}Z^H_{i_5}+2g_B Z^0_{k_{13}}Z^0_{j_6}Z^H_{i_5}\\
&+\sqrt{2}\lambda_R Z^0_{k_{11}}Z^0_{j_{12}}Z^H_{i_4}-\sqrt{2}\lambda_3 Z^0_{k_7}Z^0_{j_4}Z^H_{i_5}-\sqrt{2}\lambda_3 Z^0_{k_5}Z^0_{j_6}Z^H_{i_5}+\sqrt{2}\lambda_L Z^0_{k_{10}}Z^0_{j_8}Z^H_{i_5}\\
&+\sqrt{2}\lambda_R Z^0_{k_{11}}Z^0_{j_9}Z^H_{i_5}+\sqrt{2}\lambda_L Z^0_{k_{10}}Z^0_{j_{11}}Z^H_{i_5}+\sqrt{2}\lambda_R Z^0_{k_{11}}Z^0_{j_9}Z^H_{i_5}\\
&+\sqrt{2}Z^0_{k_{12}}(2\lambda_S Z^0_{j_{12}}Z^H_{i_5}-\lambda_3 Z^0_{j_5}Z^H_{i_2}-\lambda_3 Z^0_{j_6}Z^H_{i_4}+\lambda_R Z^0_{j_{11}}Z^H_{i_4}+\lambda_R Z^0_{j_9}Z^H_{i_3})\\
&+Z^0_{k_6}(g_L Z^0_{j_1}Z^H_{i_1}-g_R Z^0_{j_2}Z^H_{i_1}-\sqrt{2}\lambda_3(Z^0_{j_{12}}Z^H_{i_2}+Z^0_{j_5}Z^H_{i_5}))\left(\frac{1+\gamma_5}{2}\right).
\end{aligned}
\tag{C10}
$$

(10) *CP*-even Higgs-up quark-up quark contribution

$$
g_{h_i\bar{u}u}=-i\frac{1}{\sqrt{2}}\sum_{b=1}^{3}U^{u,*}_{L,jb}\sum_{a=1}^{3}U^{u,*}_{R,ka}Y_{Q2,ab}Z^H_{i_2}\left(\frac{1-\gamma_5}{2}\right)-i\frac{1}{\sqrt{2}}\sum_{b=1}^{3}\sum_{a=1}^{3}Y^*_{Q2,ab}U^u_{R,ja}U^u_{L,kb}Z^H_{i_2}\left(\frac{1+\gamma_5}{2}\right).
\tag{C11}
$$

(11) *CP*-even Higgs-down quark-down quark contribution

$$
g_{h_i\bar{d}d}=-i\frac{1}{\sqrt{2}}\sum_{b=1}^{3}\sum_{a=1}^{3}U^{d,*}_{L,jb}U^{d,*}_{R,ka}Y_{Q1,ab}Z^H_{i_1}\left(\frac{1-\gamma_5}{2}\right)-i\frac{1}{\sqrt{2}}\sum_{b=1}^{3}\sum_{a=1}^{3}Y^*_{Q1,ab}U^d_{R,ja}U^d_{L,kb}Z^H_{i_1}\left(\frac{1+\gamma_5}{2}\right).
\tag{C12}
$$

(12) *CP*-even Higgs-lepton-lepton contribution

$$
g_{h_i\bar{l}l}=-i\frac{1}{\sqrt{2}}\sum_{b=1}^{3}\sum_{a=1}^{3}U^{e,*}_{L,jb}U^{e,*}_{R,ka}Y_{L1,ab}Z^H_{i_1}\left(\frac{1-\gamma_5}{2}\right)+-i\frac{1}{\sqrt{2}}\sum_{b=1}^{3}\sum_{a=1}^{3}Y^*_{L1,ab}U^e_{R,ja}U^e_{L,kb}Z^H_{i_1}\left(\frac{1+\gamma_5}{2}\right).
\tag{C13}
$$

APPENDIX D: THE RADIATIVE CORRECTIONS TO THE *CP*-EVEN NEUTRAL HIGGS MASS MATRIX

In the LRSSM, the forms of the mass-squared matrices for the top squark and bottom quark are, respectively, as follows:

$$m_{\tilde{t}}^2 = \begin{pmatrix} m_{\tilde{t}_L}^2 & m_{\tilde{t}_{12}}^2 \\ m_{\tilde{t}_{21}}^2 & m_{\tilde{t}_R}^2 \end{pmatrix}, \qquad m_{\tilde{b}}^2 = \begin{pmatrix} m_{\tilde{b}_L}^2 & m_{\tilde{b}_{12}}^2 \\ m_{\tilde{b}_{21}}^2 & m_{\tilde{b}_R}^2 \end{pmatrix}, \tag{D1}$$

where

$$\begin{aligned}
m_{\tilde{b}_L}^2 &= \frac{1}{3}g_B^2\left(\frac{v_{R2}^2}{2}-\frac{v_{R1}^2}{2}\right)+\left(\frac{1}{4}g_L^2\left(\frac{v_2^2}{2}-\frac{v_1^2}{2}\right)+m_{Q_L}^2+\frac{v_1^2(Y_Q^1)^2}{2}\right),\\
m_{\tilde{b}_R}^2 &= -\frac{1}{3}g_B^2\left(\frac{v_{R2}^2}{2}-\frac{v_{R1}^2}{2}\right)+\left(\frac{1}{4}g_R^2\left(-\frac{v_1^2}{2}+\frac{v_2^2}{2}+v_{R1}^2-v_{R2}^2\right)+m_{Q_R}^2+\frac{v_1^2(Y_Q^1)^2}{2}\right),\\
m_{\tilde{b}_{12}}^2 &= m_{\tilde{b}_{21}}^2 = \left(-\frac{T_Q^1 v_1}{\sqrt{2}}-\frac{1}{2}\lambda_3 v_2 v s Y_Q^1\right),\\
m_{\tilde{t}_L}^2 &= \frac{1}{3}g_B^2\left(-\frac{v_{R1}^2}{2}+\frac{v_{R2}^2}{2}\right)+\left(m_{Q_L}^2+\frac{1}{4}g_L^2\left(\frac{v_1^2}{2}-\frac{v_2^2}{2}\right)+\frac{v_2^2(Y_Q^2)^2}{2}\right),\\
m_{\tilde{t}_R}^2 &= -\frac{1}{3}g_B^2\left(-\frac{v_{R1}^2}{2}+\frac{v_{R2}^2}{2}\right)+\left(m_{Q_R}^2-\frac{1}{4}g_R^2\left(-\frac{v_1^2}{2}+\frac{v_2^2}{2}+v_{R1}^2-v_{R2}^2\right)+\frac{v_2^2(Y_Q^2)^2}{2}\right),\\
m_{\tilde{t}_{12}}^2 &= m_{\tilde{t}_{21}}^2 = \left(\frac{T_Q^2 v_2}{\sqrt{2}}+\frac{1}{2}v_1 v_s Y_Q^2\lambda_3\right).
\end{aligned} \tag{D2}$$

Then, the mass eigenvalues of stop and bottom quarks will be given by

$$m_{\tilde{t}_{1,2}}^2 = \frac{1}{2}(m_{\tilde{t}_L}^2+m_{\tilde{t}_R}^2)\pm\frac{1}{2}[(m_{\tilde{t}_L}^2-m_{\tilde{t}_R}^2)^2+4m_{\tilde{t}_{12}}^4]^{\frac{1}{2}}, \tag{D3}$$

$$m_{\tilde{b}_{1,2}}^2 = \frac{1}{2}(m_{\tilde{b}_L}^2+m_{\tilde{b}_R}^2)\pm\frac{1}{2}[(m_{\tilde{b}_L}^2-m_{\tilde{b}_R}^2)^2+4m_{\tilde{b}_{12}}^4]^{\frac{1}{2}}. \tag{D4}$$

Therefore, the radiative corrections $\Delta\Pi^1$ from the one-loop zero temperature effective potential will be deduced as

$$\begin{aligned}
\Delta\Pi_{ii}^1 &= \left[-\frac{1}{\phi_i}\frac{\partial V_1}{\partial\phi_i}+\frac{\partial^2 V_1}{\partial\phi_i^2}\right]_{\phi_i=v_i},\\
\Delta\Pi_{ij}^1 &= \left[\frac{\partial^2 V_1}{\partial\phi_i\partial\phi_j}\right]_{\phi_i=v_i},
\end{aligned} \tag{D5}$$

where

$$\begin{aligned}
\Delta\Pi_{ij}^{(1)} &= \sum_\ell \frac{n_\ell}{32\pi^2}\left[\ln\frac{m_\ell^2}{Q^2}\frac{\partial m_\ell^2}{\partial\phi_i}\frac{\partial m_\ell^2}{\partial\phi_j}+m_\ell^2\left(\ln\frac{m_\ell^2}{Q^2}-1\right)\frac{\partial^2 m_\ell^2}{\partial\phi_i\partial\phi_j}\right](i\neq j),\\
\Delta\Pi_{ii}^{(1)} &= \sum_\ell \frac{n_\ell}{32\pi^2}\left[\ln\frac{m_\ell^2}{Q^2}\left(\frac{\partial m_\ell^2}{\partial\phi_i}\right)^2+m_\ell^2\left(\ln\frac{m_\ell^2}{Q^2}-1\right)\frac{\partial^2 m_\ell^2}{\partial\phi_i^2}\right]\\
&\quad -\frac{1}{v_i}\sum_\ell \frac{n_\ell}{32\pi^2}\left[m_\ell^2\left(\ln\frac{m_\ell^2}{Q^2}-1\right)\frac{\partial m_\ell^2}{\partial\phi_i}\right].
\end{aligned} \tag{D6}$$

Here, $i=1,2,R1,R2,S$ and $\ell = t,b,\tau,\nu_R,\tilde{u}_i,\tilde{d}_i,\tilde{e}_i,\tilde{\nu}_i,W_R,W_L,Z_R,Z_L,\chi_i^0,H_i^\pm,\chi_i^0$, Q is the new physics scale, and we take $Q=m_W$ in the following numerical discussion. In the one-loop effective potential, the numerically dominant contributions come from the top/stop and bottom/sbottom sectors, together with the heavy gauge and right-handed neutrino

states, namely, V_t, $V_{\tilde{t}_i}$ $(i=1,2)$, V_b, $V_{\tilde{b}_i}$, V_{W_R}, V_{Z_R}, and V_{ν_R}. All remaining terms are subleading. Below, we present the explicit expressions for the derivatives of the field-dependent masses with respect to ϕ_i that enter these dominant contributions.

The two-loop effective potential corrections to the CP-even neutral Higgs mass matrix are given by

$$\Delta\Pi^2_{ii} = \left[-\frac{1}{\phi_i}\frac{\partial V_2}{\partial\phi_i} + \frac{\partial^2 V_2}{\partial\phi_i^2}\right]_{\phi_i=v_i},$$
$$\Delta\Pi^2_{ij} = \left[\frac{\partial^2 V_2}{\partial\phi_i\partial\phi_j}\right]_{\phi_i=v_i}, \tag{D7}$$

where

$$\frac{\partial V_2}{\partial\phi_i} = \frac{\partial V_2}{\partial m_t^2}\frac{\partial m_t^2}{\partial\phi_i} + \frac{\partial V_2}{\partial m_{\tilde{t}_1}^2}\frac{\partial m_{\tilde{t}_1}^2}{\partial\phi_i} + \frac{\partial V_2}{\partial m_{\tilde{t}_2}^2}\frac{\partial m_{\tilde{t}_2}^2}{\partial\phi_i} + \frac{\partial V_2}{\partial c_{2\theta_t}^2}\frac{\partial c_{2\theta_t}^2}{\partial\phi_i}, \tag{D8}$$

$$\begin{aligned}\frac{\partial^2 V_2}{\partial\phi_i\partial\phi_j} = &\left[\left(\frac{\partial^2 V_2}{\partial m_t^2\partial m_t^2}\frac{\partial m_t^2}{\partial\phi_j} + \frac{\partial^2 V_2}{\partial m_t^2\partial m_{\tilde{t}_1}^2}\frac{\partial m_{\tilde{t}_1}^2}{\partial\phi_j} + \frac{\partial^2 V_2}{\partial m_t^2\partial m_{\tilde{t}_2}^2}\frac{\partial m_{\tilde{t}_2}^2}{\partial\phi_j} + \frac{\partial^2 V_2}{\partial m_t^2\partial c_{2\theta_t}^2}\frac{\partial c_{2\theta_t}^2}{\partial\phi_j}\right)\frac{\partial m_t^2}{\partial\phi_i}\right.\\
&+\left(\frac{\partial^2 V_2}{\partial m_{\tilde{t}_1}^2\partial m_t^2}\frac{\partial m_t^2}{\partial\phi_j} + \frac{\partial^2 V_2}{\partial m_{\tilde{t}_1}^2\partial m_{\tilde{t}_1}^2}\frac{\partial m_{\tilde{t}_1}^2}{\partial\phi_j} + \frac{\partial^2 V_2}{\partial m_{\tilde{t}_1}^2\partial m_{\tilde{t}_2}^2}\frac{\partial m_{\tilde{t}_2}^2}{\partial\phi_j} + \frac{\partial^2 V_2}{\partial m_{\tilde{t}_1}^2\partial c_{2\theta_t}^2}\frac{\partial c_{2\theta_t}^2}{\partial\phi_j}\right)\frac{\partial m_{\tilde{t}_1}^2}{\partial\phi_i}\\
&+\left(\frac{\partial^2 V_2}{\partial m_{\tilde{t}_2}^2\partial m_t^2}\frac{\partial m_t^2}{\partial\phi_j} + \frac{\partial^2 V_2}{\partial m_{\tilde{t}_2}^2\partial m_{\tilde{t}_1}^2}\frac{\partial m_{\tilde{t}_1}^2}{\partial\phi_j} + \frac{\partial^2 V_2}{\partial m_{\tilde{t}_2}^2\partial m_{\tilde{t}_2}^2}\frac{\partial m_{\tilde{t}_2}^2}{\partial\phi_j} + \frac{\partial^2 V_2}{\partial m_{\tilde{t}_2}^2\partial c_{2\theta_t}^2}\frac{\partial c_{2\theta_t}^2}{\partial\phi_j}\right)\frac{\partial m_{\tilde{t}_2}^2}{\partial\phi_i}\\
&+\left(\frac{\partial^2 V_2}{\partial c_{2\theta_t}^2\partial m_t^2}\frac{\partial m_t^2}{\partial\phi_j} + \frac{\partial^2 V_2}{\partial c_{2\theta_t}^2\partial m_{\tilde{t}_1}^2}\frac{\partial m_{\tilde{t}_1}^2}{\partial\phi_j} + \frac{\partial^2 V_2}{\partial c_{2\theta_t}^2\partial m_{\tilde{t}_2}^2}\frac{\partial m_{\tilde{t}_2}^2}{\partial\phi_j} + \frac{\partial^2 V_2}{\partial c_{2\theta_t}^2\partial c_{2\theta_t}^2}\frac{\partial c_{2\theta_t}^2}{\partial\phi_j}\right)\frac{\partial c_{2\theta_t}^2}{\partial\phi_i}\\
&\left.+\frac{\partial V_2}{\partial m_t^2}\frac{\partial^2 m_t^2}{\partial\phi_i\partial\phi_j} + \frac{\partial V_2}{\partial m_{\tilde{t}_1}^2}\frac{\partial^2 m_t^2}{\partial\phi_i\partial\phi_j} + \frac{\partial V_2}{\partial m_{\tilde{t}_2}^2}\frac{\partial^2 m_t^2}{\partial\phi_i\partial\phi_j} + \frac{\partial V_2}{\partial c_{2\theta_t}^2}\frac{\partial^2 m_t^2}{\partial\phi_i\partial\phi_j}\right].\end{aligned} \tag{D9}$$

We have

$$c_{2\theta_t}^2 = 1 - \frac{4|m_{\tilde{t}_{12}}^2|^2}{(m_{\tilde{t}_1}^2 - m_{\tilde{t}_2}^2)^2}, \tag{D10}$$

and the results of $\frac{\partial V^2}{\partial M^2}, \frac{\partial^2 V^2}{\partial M^2\partial M^2}$ with $M = m_t, m_{\tilde{t}_1}, m_{\tilde{t}_2}$ can be found in the Appendix of Ref. [68]. The derivatives of $m_t^2, m_{\tilde{t}_1}^2, m_{\tilde{t}_2}^2, c_{2\tilde{\theta}_t}^2$ over $\phi_i (i=1,2,R1,R2,S)$ can be written as

$$\frac{\partial c_{2\theta_t}^2}{\partial\phi_i} = \frac{2m_{\tilde{t}_{12}}^2}{(m_{\tilde{t}_1}^2 - m_{\tilde{t}_2}^2)^2}\frac{\partial m_{\tilde{t}_{12}}^2}{\partial\phi_i} + \frac{-2m_{\tilde{t}_{12}}^4}{(m_{\tilde{t}_1}^2 - m_{\tilde{t}_2}^2)^3}\left(\frac{\partial m_{\tilde{t}_1}^2}{\partial\phi_i} - \frac{\partial m_{\tilde{t}_2}^2}{\partial\phi_i}\right), \tag{D11}$$

$$\begin{aligned}\frac{\partial^2 c_{2\theta_t}^2}{\partial\phi_i\partial\phi_j} = &\left[\frac{2}{(m_{\tilde{t}_1}^2 - m_{\tilde{t}_2}^2)^2}\frac{\partial m_{\tilde{t}_{12}}^2}{\partial\phi_j} + \frac{2m_{\tilde{t}_{12}}^2}{(m_{\tilde{t}_1}^2 - m_{\tilde{t}_2}^2)^3}\left(\frac{\partial m_{\tilde{t}_1}^2}{\partial\phi_j} - \frac{\partial m_{\tilde{t}_2}^2}{\partial\phi_j}\right)\right]\frac{\partial m_{\tilde{t}_{12}}^2}{\partial\phi_i}\\
&+\frac{2m_{\tilde{t}_{12}}^2}{(m_{\tilde{t}_1}^2 - m_{\tilde{t}_2}^2)^2}\frac{\partial^2 m_{\tilde{t}_{12}}^2}{\partial\phi_i\partial\phi_j} + \left[\frac{-2m_{\tilde{t}_{12}}^2}{(m_{\tilde{t}_1}^2 - m_{\tilde{t}_2}^2)^3}\frac{\partial m_{\tilde{t}_{12}}^2}{\partial\phi_j}\right.\\
&\left.+\frac{-6m_{\tilde{t}_{12}}^4}{(m_{\tilde{t}_1}^2 - m_{\tilde{t}_2}^2)^4}\left(\frac{\partial m_{\tilde{t}_1}^2}{\partial\phi_j} - \frac{\partial m_{\tilde{t}_2}^2}{\partial\phi_j}\right)\right]\left(\frac{\partial m_{\tilde{t}_1}^2}{\partial\phi_i} - \frac{\partial m_{\tilde{t}_2}^2}{\partial\phi_i}\right)\\
&+\frac{-2m_{\tilde{t}_{12}}^4}{(m_{\tilde{t}_1}^2 - m_{\tilde{t}_2}^2)^3}\left(\frac{\partial^2 m_{\tilde{t}_1}^2}{\partial\phi_i\partial\phi_j} - \frac{\partial^2 m_{\tilde{t}_2}^2}{\partial\phi_i\partial\phi_j}\right),\end{aligned} \tag{D12}$$

$$\left.\frac{\partial m_{\tilde{k}}^2}{\partial\phi_i}\right|_{k=\tilde{t}_1,\tilde{t}_2,\tilde{b}_1,\tilde{b}_2} = \frac{1}{2}\left(\frac{\partial m_{\tilde{k}_L}^2}{\partial\phi_i}+\frac{\partial m_{\tilde{k}_R}^2}{\partial\phi_i}\right) \pm \frac{1}{4}\left[2\left(\frac{\partial m_{\tilde{k}_L}^2}{\partial\phi_i}-\frac{\partial m_{\tilde{k}_R}^2}{\partial\phi_i}\right)+8m_{\tilde{k}_{12}}^2\frac{\partial m_{\tilde{k}_{12}}^2}{\partial\phi_i}\right][(m_{\tilde{k}_L}^2-m_{\tilde{k}_R}^2)^2+4m_{\tilde{k}_{12}}^4]^{-\frac{1}{2}}, \tag{D13}$$

$$\begin{aligned}\left.\frac{\partial^2 m_{\tilde{k}}^2}{\partial\phi_i\partial\phi_j}\right|_{k=\tilde{t}_1,\tilde{t}_2,\tilde{b}_1,\tilde{b}_2} &= \frac{1}{2}\left(\frac{\partial^2 m_{\tilde{k}_L}^2}{\partial\phi_j\partial\phi_i}+\frac{\partial^2 m_{\tilde{k}_R}^2}{\partial\phi_j\partial\phi_i}\right) \pm \frac{1}{4}[(m_{\tilde{k}_L}^2-m_{\tilde{k}_R}^2)^2+4m_{\tilde{k}_{12}}^4]^{-\frac{1}{2}} \\ &\times\left\{2\left[\frac{\partial}{\partial\phi_j}(m_{\tilde{k}_L}^2-m_{\tilde{k}_R}^2)\right]\left[\frac{\partial}{\partial\phi_i}(m_{\tilde{k}_L}^2-m_{\tilde{k}_R}^2)\right]+2(m_{\tilde{k}_L}^2-m_{\tilde{k}_R}^2)\left(\frac{\partial^2 m_{\tilde{k}_L}^2}{\partial\phi_j\partial\phi_i}-\frac{\partial^2 m_{\tilde{k}_R}^2}{\partial\phi_j\partial\phi_i}\right)\right. \\ &\left.+8\frac{\partial m_{\tilde{k}_{12}}^2}{\partial\phi_i}\frac{\partial m_{\tilde{k}_{12}}^2}{\partial\phi_j}+8m_{\tilde{k}_{12}}^2\frac{\partial^2 m_{\tilde{k}_{12}}^2}{\partial\phi_j\partial\phi_i}\right\} \mp \frac{1}{8}[(m_{\tilde{k}_L}^2-m_{\tilde{k}_R}^2)^2+4m_{\tilde{k}_{12}}^4]^{-\frac{3}{2}} \\ &\times\left[2(m_{\tilde{k}_L}^2-m_{\tilde{k}_R}^2)\frac{\partial(m_{\tilde{k}_L}^2-m_{\tilde{k}_R}^2)}{\partial\phi_i}+8m_{\tilde{k}_{12}}^2\frac{\partial m_{\tilde{k}_{12}}^2}{\partial\phi_i}\right] \\ &\times\left[2(m_{\tilde{k}_L}^2-m_{\tilde{k}_R}^2)\frac{\partial(m_{\tilde{k}_L}^2-m_{\tilde{k}_R}^2)}{\partial\phi_j}+8m_{\tilde{k}_{12}}^2\frac{\partial m_{\tilde{k}_{12}}^2}{\partial\phi_j}\right].\end{aligned} \tag{D14}$$

In the preceding expressions, the derivatives of the matrix elements with $m_{\tilde{t}_L}^2, m_{\tilde{t}_R}^2, m_{\tilde{t}_12}^2, m_{\tilde{b}_L}^2, m_{\tilde{b}_R}^2$, and $m_{\tilde{b}_12}^2$ with respect to $\phi_{i(i=1,2,R1,R2,S)}$ are given as follows:

$$\begin{aligned}&\frac{\partial m_{\tilde{t}_R}^2}{\partial\phi_1}=-\frac{g_R^2}{4}\phi_1, \quad \frac{\partial m_{\tilde{t}_R}^2}{\partial\phi_2}=\frac{g_R^2}{4}\phi_2+(Y_Q^2)^2\phi_2, \quad \frac{\partial m_{\tilde{t}_R}^2}{\partial\phi_{R1}}=\left(\frac{g_B^2}{3}-\frac{g_R^2}{2}\right)\phi_{R1}, \\ &\frac{\partial m_{\tilde{t}_R}^2}{\partial\phi_{R2}}=\left(\frac{g_R^2}{2}-\frac{g_B^2}{3}\right)\phi_{R2}, \quad \frac{\partial m_{\tilde{t}_L}^2}{\partial\phi_1}=\frac{g_L^2}{4}\phi_1, \quad \frac{\partial m_{\tilde{t}_L}^2}{\partial\phi_2}=-\frac{g_L^2}{4}\phi_2+(Y_Q^2)^2\phi_2, \\ &\frac{\partial m_{\tilde{t}_L}^2}{\partial\phi_{R1}}=-\frac{g_B^2}{3}\phi_{R1}, \quad \frac{\partial m_{\tilde{t}_L}^2}{\partial\phi_{R2}}=\frac{g_B^2}{3}\phi_{R2}, \quad \frac{\partial m_{\tilde{t}_{12}}^2}{\partial\phi_1}=\frac{\lambda_3 Y_Q^2}{2}\phi_S, \\ &\frac{\partial m_{\tilde{t}_{12}}^2}{\partial\phi_2}=\frac{T_Q^2}{\sqrt{2}}, \quad \frac{\partial m_{\tilde{t}_{12}}^2}{\partial\phi_S}=\frac{\lambda_3 Y_Q^2}{2}\phi_1, \\ &\frac{\partial m_{\tilde{t}_L}^2}{\partial\phi_S}=\frac{\partial m_{\tilde{t}_R}^2}{\partial\phi_S}=\frac{\partial m_{\tilde{t}_{12}}^2}{\partial\phi_{R1}}= \quad \frac{\partial m_{\tilde{t}_{12}}^2}{\partial\phi_{R2}}=0\end{aligned} \tag{D15}$$

$$\begin{aligned}&\frac{\partial m_{\tilde{b}_R}^2}{\partial\phi_1}=\left(-\frac{g_R^2}{4}+(Y_Q^1)^2\right)\phi_1, \quad \frac{\partial m_{\tilde{b}_R}^2}{\partial\phi_2}=\frac{g_R^2}{4}\phi_2, \quad \frac{\partial m_{\tilde{b}_R}^2}{\partial\phi_{R1}}=\left(\frac{g_B^2}{2}+\frac{g_R^2}{2}\right)\phi_{R1}, \\ &\frac{\partial m_{\tilde{b}_R}^2}{\partial\phi_{R2}}=\left(\frac{g_R^2}{2}-\frac{g_B^2}{3}\right)\phi_{R2} \quad \frac{\partial m_{\tilde{b}_L}^2}{\partial\phi_1}=\left(-\frac{g_L^2}{4}+(Y_Q^1)^2\right)\phi_1, \quad \frac{\partial m_{\tilde{b}_L}^2}{\partial\phi_2}=\frac{g_L^2}{4}\phi_2, \\ &\frac{\partial m_{\tilde{b}_L}^2}{\partial\phi_{R1}}=-\frac{g_B^2}{3}\phi_{R1}, \quad \frac{\partial m_{\tilde{b}_L}^2}{\partial\phi_{R2}}=\frac{g_B^2}{3}\phi_{R2} \quad \frac{\partial m_{\tilde{b}_{12}}^2}{\partial\phi_1}=-\frac{T_Q^1}{\sqrt{2}}, \\ &\frac{\partial m_{\tilde{b}_{12}}^2}{\partial\phi_2}=-\frac{Y_Q^1\lambda_3}{2}\phi_S, \quad \frac{\partial m_{\tilde{b}_{12}}^2}{\partial\phi_S}=-\frac{Y_Q^1\lambda_3}{2}\phi_2, \\ &\frac{\partial m_{\tilde{b}_L}^2}{\partial\phi_S}=\frac{\partial m_{\tilde{b}_R}^2}{\partial\phi_S}=\frac{\partial m_{\tilde{b}_{12}}^2}{\partial\phi_{R1}}= \quad \frac{\partial m_{\tilde{b}_{12}}^2}{\partial\phi_{R2}}=0,\end{aligned} \tag{D16}$$

$$
\begin{aligned}
&\frac{\partial^2 m^2_{\tilde{t}_L}}{\partial\phi_1\partial\phi_1}=\frac{g_L^2}{4}, \quad \frac{\partial^2 m^2_{\tilde{t}_L}}{\partial\phi_1\partial\phi_2}=\frac{\partial^2 m^2_{\tilde{t}_L}}{\partial\phi_1\partial\phi_{R1}}=\frac{\partial^2 m^2_{\tilde{t}_L}}{\partial\phi_1\partial\phi_{R2}}=\frac{\partial^2 m^2_{\tilde{t}_L}}{\partial\phi_1\partial\phi_S}=0,\\
&\frac{\partial^2 m^2_{\tilde{t}_L}}{\partial\phi_2\partial\phi_2}=-\frac{g_L^2}{4}+(Y_Q^2)^2, \quad \frac{\partial^2 m^2_{\tilde{t}_L}}{\partial\phi_2\partial\phi_1}=\frac{\partial^2 m^2_{\tilde{t}_L}}{\partial\phi_2\partial\phi_{R1}}=\frac{\partial^2 m^2_{\tilde{t}_L}}{\partial\phi_2\partial\phi_{R2}}=\frac{\partial^2 m^2_{\tilde{t}_L}}{\partial\phi_2\partial\phi_S}=0,\\
&\frac{\partial^2 m^2_{\tilde{t}_L}}{\partial\phi_{R1}\partial\phi_{R1}}=-\frac{g_B^2}{3}, \quad \frac{\partial^2 m^2_{\tilde{t}_L}}{\partial\phi_{R1}\partial\phi_1}=\frac{\partial^2 m^2_{\tilde{t}_L}}{\partial\phi_{R1}\partial\phi_{R1}}=\frac{\partial^2 m^2_{\tilde{t}_L}}{\partial\phi_{R1}\partial\phi_{R2}}=\frac{\partial^2 m^2_{\tilde{t}_L}}{\partial\phi_{R1}\partial\phi_S}=0,\\
&\frac{\partial^2 m^2_{\tilde{t}_L}}{\partial\phi_{R2}\phi_{R2}}=-\frac{g_B^2}{3}, \quad \frac{\partial^2 m^2_{\tilde{t}_L}}{\partial\phi_{R2}\partial\phi_{R1}}=\frac{\partial^2 m^2_{\tilde{t}_L}}{\partial\phi_{R2}\partial\phi_{R1}}=\frac{\partial^2 m^2_{\tilde{t}_L}}{\partial\phi_{R2}\partial\phi_{R2}}=\frac{\partial^2 m^2_{\tilde{t}_L}}{\partial\phi_{R2}\partial\phi_S}=0,\\
&\frac{\partial^2 m^2_{\tilde{t}_L}}{\partial\phi_S\phi_S}=\frac{\partial^2 m^2_{\tilde{t}_L}}{\partial\phi_S\partial\phi_S}=\frac{\partial^2 m^2_{\tilde{t}_L}}{\partial\phi_S\partial\phi_{R1}}=\frac{\partial^2 m^2_{\tilde{t}_L}}{\partial\phi_S\partial\phi_{R2}}=0,\\
&\frac{\partial^2 m^2_{\tilde{t}_R}}{\partial\phi_1\partial\phi_1}=-\frac{g_R^2}{4}, \quad \frac{\partial^2 m^2_{\tilde{t}_R}}{\partial\phi_1\partial\phi_2}=\frac{\partial^2 m^2_{\tilde{t}_R}}{\partial\phi_1\partial\phi_{R1}}=\frac{\partial^2 m^2_{\tilde{t}_R}}{\partial\phi_1\partial\phi_{R2}}=\frac{\partial^2 m^2_{\tilde{t}_R}}{\partial\phi_1\partial\phi_S}=0,\\
&\frac{\partial^2 m^2_{\tilde{t}_R}}{\partial\phi_2\partial\phi_2}=-\frac{g_R^2}{4}+(Y_Q^2)^2, \quad \frac{\partial^2 m^2_{\tilde{t}_R}}{\partial\phi_2\partial\phi_1}=\frac{\partial^2 m^2_{\tilde{t}_R}}{\partial\phi_2\partial\phi_{R1}}=\frac{\partial^2 m^2_{\tilde{t}_R}}{\partial\phi_2\partial\phi_{R2}}=\frac{\partial^2 m^2_{\tilde{t}_R}}{\partial\phi_2\partial\phi_S}=0,\\
&\frac{\partial^2 m^2_{\tilde{t}_R}}{\partial\phi_{R1}\partial\phi_{R1}}=-\frac{g_B^2}{3}-\frac{g_R^2}{2}, \quad \frac{\partial^2 m^2_{\tilde{t}_R}}{\partial\phi_{R1}\partial\phi_1}=\frac{\partial^2 m^2_{\tilde{t}_R}}{\partial\phi_{R1}\partial\phi_{R1}}=\frac{\partial^2 m^2_{\tilde{t}_R}}{\partial\phi_{R1}\partial\phi_{R2}}=\frac{\partial^2 m^2_{\tilde{t}_R}}{\partial\phi_{R1}\partial\phi_S}=0,\\
&\frac{\partial^2 m^2_{\tilde{t}_R}}{\partial\phi_{R2}\partial\phi_{R2}}=-\frac{g_B^2}{3}+\frac{g_R^2}{2}, \quad \frac{\partial^2 m^2_{\tilde{t}_R}}{\partial\phi_{R2}\partial\phi_{R1}}=\frac{\partial^2 m^2_{\tilde{t}_R}}{\partial\phi_{R2}\partial\phi_{R1}}=\frac{\partial^2 m^2_{\tilde{t}_R}}{\partial\phi_{R2}\partial\phi_{R2}}=\frac{\partial^2 m^2_{\tilde{t}_R}}{\partial\phi_{R2}\partial\phi_S}=0,\\
&\frac{\partial^2 m^2_{\tilde{t}_R}}{\partial\phi_S\partial\phi_S}=\frac{\partial^2 m^2_{\tilde{t}_R}}{\partial\phi_S\partial\phi_S}=\frac{\partial^2 m^2_{\tilde{t}_R}}{\partial\phi_S\partial\phi_{R1}}=\frac{\partial^2 m^2_{\tilde{t}_R}}{\partial\phi_S\partial\phi_{R2}}=0,\\
&\frac{\partial^2 m^2_{\tilde{t}_{12}}}{\partial\phi_1\partial\phi_S}=\frac{Y_Q^2\lambda_3}{2}, \quad \frac{\partial^2 m^2_{\tilde{t}_{12}}}{\partial\phi_1\partial\phi_1}=\frac{\partial^2 m^2_{\tilde{t}_{12}}}{\partial\phi_1\partial\phi_2}-\frac{\partial^2 m^2_{\tilde{t}_{12}}}{\partial\phi_1\partial\phi_{R1}}-\frac{\partial^2 m^2_{\tilde{t}_{12}}}{\partial\phi_1\partial\phi_{R2}}=0,\\
&\frac{\partial^2 m^2_{\tilde{t}_{12}}}{\partial\phi_2\partial\phi_2}=\frac{\partial^2 m^2_{\tilde{t}_{12}}}{\partial\phi_2\partial\phi_{R1}}-\frac{\partial^2 m^2_{\tilde{t}_{12}}}{\partial\phi_2\partial\phi_{R2}}-\frac{\partial^2 m^2_{\tilde{t}_{12}}}{\partial\phi_2\partial\phi_S}=0,\\
&\frac{\partial^2 m^2_{\tilde{t}_{12}}}{\partial\phi_{R1}\partial\phi_{R1}}=\frac{\partial^2 m^2_{\tilde{t}_{12}}}{\partial\phi_{R1}\partial\phi_{R1}}-\frac{\partial^2 m^2_{\tilde{t}_{12}}}{\partial\phi_{R1}\partial\phi_{R2}}-\frac{\partial^2 m^2_{\tilde{t}_{12}}}{\partial\phi_{R1}\partial\phi_S}=0,\\
&\frac{\partial^2 m^2_{\tilde{t}_{12}}}{\partial\phi_S\partial\phi_1}=\frac{Y_Q^2\lambda_3}{2}, \quad \frac{\partial^2 m^2_{\tilde{t}_{12}}}{\partial\phi_{R2}\partial\phi_{R2}}=\frac{\partial^2 m^2_{\tilde{t}_{12}}}{\partial\phi_{R2}\partial\phi_{R1}}-\frac{\partial^2 m^2_{\tilde{t}_{12}}}{\partial\phi_{R2}\partial\phi_{R2}}-\frac{\partial^2 m^2_{\tilde{t}_{12}}}{\partial\phi_{R2}\partial\phi_S}=0,\\
&\frac{\partial^2 m^2_{\tilde{t}_{12}}}{\partial\phi_S\partial\phi_S}=\frac{\partial^2 m^2_{\tilde{t}_{12}}}{\partial\phi_S\partial\phi_1}-\frac{\partial^2 m^2_{\tilde{t}_{12}}}{\partial\phi_S\partial\phi_{R1}}-\frac{\partial^2 m^2_{\tilde{t}_{12}}}{\partial\phi_S\partial\phi_{R2}}=0,
\end{aligned}
\tag{D17}
$$

$$
\begin{aligned}
&\frac{\partial^2 m^2_{\tilde{b}_L}}{\partial\phi_1\partial\phi_1}=-\frac{g_L^2}{4}+(Y_Q^1)^2, \quad \frac{\partial^2 m^2_{\tilde{b}_L}}{\partial\phi_1\partial\phi_2}=\frac{\partial^2 m^2_{\tilde{b}_L}}{\partial\phi_1\partial\phi_{R1}}=\frac{\partial^2 m^2_{\tilde{b}_L}}{\partial\phi_1\partial\phi_{R2}}=\frac{\partial^2 m^2_{\tilde{b}_L}}{\partial\phi_1\partial\phi_S}=0,\\
&\frac{\partial^2 m^2_{\tilde{b}_L}}{\partial\phi_2\partial\phi_2}=\frac{g_L^2}{4}, \quad \frac{\partial^2 m^2_{\tilde{b}_L}}{\partial\phi_2\partial\phi_1}=\frac{\partial^2 m^2_{\tilde{b}_L}}{\partial\phi_2\partial\phi_{R1}}=\frac{\partial^2 m^2_{\tilde{b}_L}}{\partial\phi_2\partial\phi_{R2}}=\frac{\partial^2 m^2_{\tilde{b}_L}}{\partial\phi_2\partial\phi_S}=0,\\
&\frac{\partial^2 m^2_{\tilde{b}_L}}{\partial\phi_{R1}\partial\phi_{R1}}=-\frac{g_B^2}{3}, \quad \frac{\partial^2 m^2_{\tilde{b}_L}}{\partial\phi_{R1}\partial\phi_1}=\frac{\partial^2 m^2_{\tilde{b}_L}}{\partial\phi_{R1}\partial\phi_{R1}}=\frac{\partial^2 m^2_{\tilde{b}_L}}{\partial\phi_{R1}\partial\phi_{R2}}=\frac{\partial^2 m^2_{\tilde{b}_L}}{\partial\phi_{R1}\partial\phi_S}=0,\\
&\frac{\partial^2 m^2_{\tilde{b}_L}}{\partial\phi_{R2}\partial\phi_{R2}}=\frac{g_B^2}{3}, \quad \frac{\partial^2 m^2_{\tilde{b}_L}}{\partial\phi_{R2}\partial\phi_{R1}}=\frac{\partial^2 m^2_{\tilde{b}_L}}{\partial\phi_{R2}\partial\phi_{R1}}=\frac{\partial^2 m^2_{\tilde{b}_L}}{\partial\phi_{R2}\partial\phi_{R2}}=\frac{\partial^2 m^2_{\tilde{b}_L}}{\partial\phi_{R2}\partial\phi_S}=0,\\
&\frac{\partial^2 m^2_{\tilde{b}_L}}{\partial\phi_S\partial\phi_S}=\frac{\partial^2 m^2_{\tilde{b}_L}}{\partial\phi_S\partial\phi_S}=\frac{\partial^2 m^2_{\tilde{b}_L}}{\partial\phi_S\partial\phi_{R1}}=\frac{\partial^2 m^2_{\tilde{b}_L}}{\partial\phi_S\partial\phi_{R2}}=0,
\end{aligned}
$$

$$\frac{\partial^2 m^2_{\tilde{b}_R}}{\partial\phi_1\partial\phi_1} = -\frac{g_R^2}{4} + (Y_Q^1)^2, \qquad \frac{\partial^2 m^2_{\tilde{b}_R}}{\partial\phi_1\partial\phi_2} = \frac{\partial^2 m^2_{\tilde{b}_R}}{\partial\phi_1\partial\phi_{R1}} - \frac{\partial^2 m^2_{\tilde{b}_R}}{\partial\phi_1\partial\phi_{R2}} - \frac{\partial^2 m^2_{\tilde{b}_R}}{\partial\phi_1\partial\phi_S} = 0,$$
$$\frac{\partial^2 m^2_{\tilde{b}_R}}{\partial\phi_2\partial\phi_2} = \frac{g_R^2}{4}, \qquad \frac{\partial^2 m^2_{\tilde{b}_R}}{\partial\phi_2\partial\phi_1} = \frac{\partial^2 m^2_{\tilde{b}_R}}{\partial\phi_2\partial\phi_{R1}} - \frac{\partial^2 m^2_{\tilde{b}_R}}{\partial\phi_2\partial\phi_{R2}} - \frac{\partial^2 m^2_{\tilde{b}_R}}{\partial\phi_2\partial\phi_S} = 0,$$
$$\frac{\partial^2 m^2_{\tilde{b}_R}}{\partial\phi_{R1}\partial\phi_{R1}} = -\frac{g_B^2}{3} - \frac{g_R^2}{2}, \qquad \frac{\partial^2 m^2_{\tilde{b}_R}}{\partial\phi_{R1}\partial\phi_1} = \frac{\partial^2 m^2_{\tilde{b}_R}}{\partial\phi_{R1}\partial\phi_{R1}} - \frac{\partial^2 m^2_{\tilde{b}_R}}{\partial\phi_{R1}\partial\phi_{R2}} - \frac{\partial^2 m^2_{\tilde{b}_R}}{\partial\phi_{R1}\partial\phi_S} = 0,$$
$$\frac{\partial^2 m^2_{\tilde{b}_R}}{\partial\phi_{R2}\partial\phi_{R2}} = -\frac{g_B^2}{3} + \frac{g_R^2}{2}, \qquad \frac{\partial^2 m^2_{\tilde{b}_R}}{\partial\phi_{R2}\partial\phi_{R1}} = \frac{\partial^2 m^2_{\tilde{b}_R}}{\partial\phi_{R2}\partial\phi_{R1}} - \frac{\partial^2 m^2_{\tilde{b}_R}}{\partial\phi_{R2}\partial\phi_{R2}} - \frac{\partial^2 m^2_{\tilde{b}_R}}{\partial\phi_{R2}\partial\phi_S} = 0,$$
$$\frac{\partial^2 m^2_{\tilde{b}_R}}{\partial\phi_S\partial\phi_S} = \frac{\partial^2 m^2_{\tilde{b}_R}}{\partial\phi_S\partial\phi_S} - \frac{\partial^2 m^2_{\tilde{b}_R}}{\partial\phi_S\partial\phi_{R1}} - \frac{\partial^2 m^2_{\tilde{b}_R}}{\partial\phi_S\partial\phi_{R2}} = 0,$$
$$\frac{\partial^2 m^2_{\tilde{b}_{12}}}{\partial\phi_S\partial\phi_1} = \frac{\partial^2 m^2_{\tilde{b}_{12}}}{\partial\phi_S\partial\phi_{R1}} = \frac{\partial^2 m^2_{\tilde{b}_{12}}}{\partial\phi_S\partial\phi_{R2}} = \frac{\partial^2 m^2_{\tilde{b}_{12}}}{\partial\phi_S\partial\phi_2} = 0,$$
$$\frac{\partial^2 m^2_{\tilde{b}_{12}}}{\partial\phi_2\partial\phi_1} = -\frac{Y_Q^1\lambda_3}{2}, \frac{\partial^2 m^2_{\tilde{b}_{12}}}{\partial\phi_2\partial\phi_2} = \frac{\partial^2 m^2_{\tilde{b}_{12}}}{\partial\phi_2\partial\phi_{R1}} = \frac{\partial^2 m^2_{\tilde{b}_{12}}}{\partial\phi_2\partial\phi_{R2}} = \frac{\partial^2 m^2_{\tilde{b}_{12}}}{\partial\phi_2\partial\phi_S} = 0,$$
$$\frac{\partial^2 m^2_{\tilde{b}_{12}}}{\partial\phi_{R1}\partial\phi_{R1}} = \frac{\partial^2 m^2_{\tilde{b}_{12}}}{\partial\phi_{R1}\partial\phi_{R1}} = \frac{\partial^2 m^2_{\tilde{b}_{12}}}{\partial\phi_{R1}\partial\phi_{R2}} = \frac{\partial^2 m^2_{\tilde{b}_{12}}}{\partial\phi_{R1}\partial\phi_S} = 0,$$
$$\frac{\partial^2 m^2_{\tilde{b}_{12}}}{\partial\phi_{R2}\partial\phi_{R2}} = \frac{\partial^2 m^2_{\tilde{b}_{12}}}{\partial\phi_{R2}\partial\phi_{R1}} = \frac{\partial^2 m^2_{\tilde{b}_{12}}}{\partial\phi_{R2}\partial\phi_{R2}} = \frac{\partial^2 m^2_{\tilde{b}_{12}}}{\partial\phi_{R2}\partial\phi_S} = 0,$$
$$\frac{\partial^2 m^2_{\tilde{b}_{12}}}{\partial\phi_S\partial\phi_2} = -\frac{Y_Q^1\lambda_3}{2}, \qquad \frac{\partial^2 m^2_{\tilde{b}_{12}}}{\partial\phi_S\partial\phi_S} = \frac{\partial^2 m^2_{\tilde{b}_{12}}}{\partial\phi_S\partial\phi_1} = \frac{\partial^2 m^2_{\tilde{b}_{12}}}{\partial\phi_S\partial\phi_{R1}} = \frac{\partial^2 m^2_{\tilde{b}_{12}}}{\partial\phi_S\partial\phi_{R2}} = 0. \tag{D18}$$

In our setup, the field-dependent masses satisfy $m_t = \frac{Y_t}{\sqrt{2}} v_1$ and $m_{\nu_R} = \frac{h_{RR}}{\sqrt{2}} v_{R1}$; that is, the top quark mass depends only on v_1, while the right-handed neutrino mass depends only on v_{R1}. The derivatives with respect to ϕ_i are provided as follows:

$$\frac{\partial m_t^2}{\partial\phi_1} = Y_t^2 v_1, \qquad \frac{\partial^2 m_t^2}{\partial\phi_1\partial\phi_1} = Y_t^2, \qquad \frac{\partial m^2_{\nu_R}}{\partial\phi_{R1}} = h^2_{RR} v_{R1}, \qquad \frac{\partial^2 m^2_{\nu_R}}{\partial\phi_{R1}\partial\phi_{R1}} = h^2_{RR}. \tag{D19}$$

For the right-handed gauge bosons, W_R and Z_R, the derivatives with respect to the ϕ_i are given as follows:

$$\frac{\partial m^2_{W_R}}{\partial\phi_1} = g_R^2 v_1, \qquad \frac{\partial m^2_{W_R}}{\partial\phi_2} = g_R^2 v_2, \qquad \frac{\partial m^2_{W_R}}{\partial\phi_{R1}} = 2g_R^2 v_{R1},$$
$$\frac{\partial m^2_{W_R}}{\partial\phi_{R2}} = 2g_R^2 v_{R2}, \qquad \frac{\partial^2 m^2_{W_R}}{\partial\phi_1\partial\phi_1} = g_R^2, \qquad \frac{\partial^2 m^2_{W_R}}{\partial\phi_1\partial\phi_1} = g_R^2,$$
$$\frac{\partial^2 m^2_{W_R}}{\partial\phi_{R1}\partial\phi_{R1}} = 2g_R^2, \qquad \frac{\partial^2 m^2_{W_R}}{\partial\phi_{R2}\partial\phi_{R2}} = 2g_R^2, \qquad \frac{\partial^2 m^2_{W_R}}{\partial\phi_S} = 0,$$
$$\frac{\partial^2 m^2_{W_R}}{\partial\phi_i\partial\phi_j} = 0 (i \neq j),$$
$$\frac{\partial m^2_{Z_R}}{\partial\phi_1} = \frac{g_R^4}{g_R^2 + g_B^2} v_1, \qquad \frac{\partial m^2_{Z_R}}{\partial\phi_2} = \frac{g_R^4}{g_R^2 + g_B^2} v_2, \qquad \frac{\partial m^2_{Z_R}}{\partial\phi_{R1}} = 4(g_R^2 + g_B^2)(v_{R1} + v_{R2}),$$

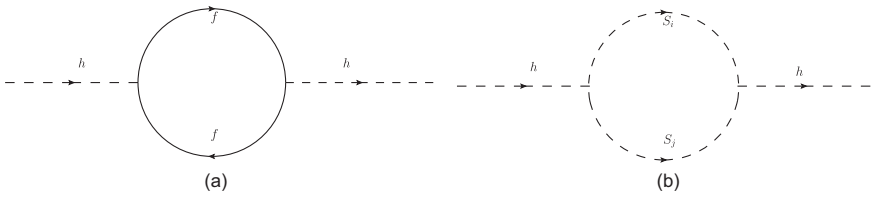


FIG. 10. One-loop diagrams that induce the radiative corrections to the lightest Higgs boson mass, where $f = t, b, \tilde{\chi}_i^0$ and $S_i = \tilde{t}_{1,2}, \tilde{b}_{1,2}$.

$$\frac{\partial m_{Z_R}^2}{\partial \phi_{R2}} = 4(g_R^2 + g_B^2)(v_{R1} + v_{R2}), \qquad \frac{\partial^2 m_{Z_R}^2}{\partial \phi_1 \partial \phi_1} = \frac{g_R^4}{g_R^2 + g_B^2}, \qquad \frac{\partial^2 m_{Z_R}^2}{\partial \phi_2 \partial \phi_2} = \frac{g_R^4}{g_R^2 + g_B^2},$$
$$\frac{\partial^2 m_{Z_R}^2}{\partial \phi_{R1} \partial \phi_{R1}} = 4(g_R^2 + g_B^2), \qquad \frac{\partial^2 m_{Z_R}^2}{\partial \phi_{R2} \partial \phi_{R2}} = 4(g_R^2 + g_B^2), \qquad \frac{\partial^2 m_{Z_R}^2}{\partial \phi_{R1} \partial \phi_{R2}} = 4(g_R^2 + g_B^2),$$
$$\frac{\partial^2 m_{Z_R}^2}{\partial \phi_S \partial \phi_S} = 0, \qquad \frac{\partial^2 m_{Z_R}^2}{\partial \phi_i \partial \phi_j} = 0|_{(i \neq j \text{ and } i,j=1,2)}. \tag{D20}$$

In order to get the pole mass of the lightest Higgs consistently, we write the explicit expressions for the self-energy diagrams. It is well known that the dominant corrections to the lightest Higgs mass originate from bottom, sbottom, top, and stop. The relevant diagrams are plotted in Fig. 10, and the corresponding corrections are given as follows:

$$\Delta\Pi_{hh}^{(1)} = \frac{-6C_{hff}^2}{(4\pi)^2}\left[(4m_f^2 - m_h^2)B(m_f, m_f, m_h) - 4m_f^2 \ln\frac{m_f^2}{Q^2}\right],$$
$$\Delta\Pi_{hh}^{(2)} = \frac{3C_{hs_i,s_j}^2}{(4\pi)^2}[B(m_{s_i}, m_{s_j}, m_h) - B(m_{s_i}, m_{s_j}, 0)]. \tag{D21}$$

The function B is defined as

$$B(m_1, m_2, m_3) = \int_0^1 dx \ln\frac{(1-x)m_1^2 + xm_2^2 + x(x-1)m_3^2}{Q^2}. \tag{D22}$$

APPENDIX E: APPROXIMATE RESULTS FOR m_{h_1}, m_{h_2}, $m_{H_1^\pm}$, AND $m_{H^{\pm\pm}}$

We performed an approximate analytical study of the lightest doubly charged Higgs and the lightest singly charged Higgs under the condition $\tan\beta_R = 1$, in order to more clearly reveal their relationship with $\tan\beta_R$. Since the mass matrix of the doubly charged Higgs is a 2×2 matrix, the mass of the lightest doubly charged Higgs can be expressed as

$$M_{H_1^{\pm\pm}}^2 = \frac{1}{2}\Big[m_{\Delta_R^{++}\Delta_R^{--}}^2 + m_{\delta_R^{++}\delta_R^{--}}^2 - \sqrt{(m_{\Delta_R^{++}\Delta_R^{--}}^2 - m_{\delta_R^{++}\delta_R^{--}}^2)^2 + 4m_{\Delta_R^{++}\delta_R^{--}}^4}\Big]. \tag{E1}$$

We begin by performing an approximate expansion around $\tan\beta_R = 1$. For this purpose, we define $\tan\beta_R = 1 + \delta$ and $v_1/v_{R1} = \sigma$. The squared mass of the lightest doubly charged Higgs, $M_{H^{\pm\pm}1}^2$, can thus be regarded as a function of δ and σ, denoted as $M_{H_1^{\pm\pm}}^2(\delta, \sigma)$. Expanding this function as a Taylor series around the point $\delta = 0$, $\sigma = 0$,

$$m_{H_1^{\pm\pm}}^2 = -\frac{4g_R^2 v_{R1}(-2g_R^2 v_{R1}^2 + \sqrt{2}T_R v_S + \lambda_R(\lambda_R v_{R1}^2 + 3\lambda_S v_S^2 + 2\xi_F))}{\sqrt{2}T_R v_S + \lambda_R(\lambda_R v_{R1}^2 + 3\lambda_S v_S^2 + 2\xi_F)}\delta^2. \tag{E2}$$

The calculation results show that the mass of the lightest doubly charged Higgs is strongly correlated with δ^2. Since the mass matrix of the lightest singly charged Higgs boson is 4×4, its approximation procedure is more complicated. To facilitate the calculation, we first divide the singly charged mass matrix $M^2_{H^\pm}$ by v_{R1} and then substitute $\tan\beta_R = 1+\delta$ and $v_1/v_{R1} = \sigma$. The resulting form of the matrix is

$$\frac{1}{v^2_{R1}} M^2_{H^\pm} = \begin{pmatrix} M^2_{1(2\times 2)} & M^2_{3(2\times 2)} \\ M^{\dagger 2}_{3(2\times 2)} & M^2_{2(2\times 2)} \end{pmatrix}, \tag{E3}$$

where

$$M^2_{3(2\times 2)} = \begin{pmatrix} -\frac{g^2_R \sigma}{2\sqrt{2}} & \frac{g^2_R(1+\delta)\sigma}{2\sqrt{2}} \\ -\frac{g^2_R t_\beta \sigma}{2\sqrt{2}} & \frac{g^2_R t_\beta(1+\delta)\sigma}{2\sqrt{2}} \end{pmatrix}. \tag{E4}$$

It is evident that all elements of the matrix $M^2_{3(2\times 2)}$ depend on δ and σ. Therefore, we treat $M^2_{3(2\times 2)}$ as a perturbation and perform an approximate treatment on $M^2_{1(2\times 2)}$. We have

$$M'^2_{1(2\times 2)} = M^2_{1(2\times 2)} + M^{2T}_{3(2\times 2)} (M^2_{1(2\times 2)} - M^2_{2(2\times 2)})^{-1} M^2_{3(2\times 2)}. \tag{E5}$$

We then similarly perform a Taylor expansion on the eigenvalues of $M'^2_{1(2\times 2)}$ as described above, yielding

$$m^2_{H^\pm_1} = \begin{cases} -\frac{g^2_R(t_\beta - 1)(1+t\beta)v^2_{R1}}{1+t^2_\beta}\delta & \text{if } \sqrt{2}T_3 + \lambda_3(\lambda_R v^2_{R1} + 3\lambda^2_S v^2_S + 2\xi_F) > 0 \\ \frac{g^2_R(t^2_\beta - 1)v^2_{R1}\delta}{1+t_\beta} + \frac{\lambda_3 \lambda_R v^2_{R1}\delta}{2t_\beta} & \text{if } \sqrt{2}T_3 + \lambda_3(\lambda_R v^2_{R1} + 3\lambda^2_S v^2_S + 2\xi_F) < 0. \end{cases} \tag{E6}$$

The calculation shows that only terms proportional to δ remain in the above expression, while all other terms vanish exactly. It is evident from the expressions for $m^2_{H^{\pm\pm}_1}$ and $m^2_{H^\pm_1}$ that both approach zero as $\tan\beta_R$ tends toward 1. We also performed an approximate analytical study of the dependence of the Higgs boson masses (m_{h_1} and m_{h_2}) on $\tan\beta$. Since the mass matrix of the CP-even Higgs bosons is a 5×5 matrix, the approximation process becomes significantly more complex. For simplicity, we define $\tan\beta_R = 1$ and $v_1/v_{R1} = \sigma$. We first perform a transformation on the CP-even mass matrix ($m^2_{H_3}$),

$$M^2_{H_{t1}} = U^\dagger_1 m^2_{H_3} U_1, \tag{E7}$$

where

$$U_1 = \begin{pmatrix} \frac{1}{\sqrt{1+\tan^2\beta}} & \frac{-\tan\beta}{\sqrt{1+\tan^2\beta}} & 0 & 0 & 0 \\ \frac{\tan\beta}{\sqrt{1+\tan^2\beta}} & \frac{1}{\sqrt{1+\tan^2\beta}} & 0 & 0 & 0 \\ 0 & 0 & \frac{1}{\sqrt{2}} & \frac{-1}{\sqrt{2}} & 0 \\ 0 & 0 & \frac{1}{\sqrt{2}} & \frac{1}{\sqrt{2}} & 0 \\ 0 & 0 & 0 & 0 & 1 \end{pmatrix}. \tag{E8}$$

This formulation is based on the following set of basis vectors:

$$U^\dagger_1 \begin{pmatrix} H^0_{12} \\ H^2_{21} \\ H^0_{\Delta_R} \\ H^0_{\delta_R} \\ H^0_S \end{pmatrix} = \begin{pmatrix} \frac{1}{\sqrt{1+\tan^2\beta}}(H^0_{12} + \tan\beta H^2_{21}) \\ \frac{1}{\sqrt{1+\tan^2\beta}}(H^0_{21} - \tan\beta H^2_{12}) \\ \frac{1}{\sqrt{2}}(H^0_{\Delta_R} + H^0_{\delta_R}) \\ \frac{1}{\sqrt{2}}(H^0_{\delta_R} - H^0_{\Delta_R}) \\ H^0_S \end{pmatrix}. \tag{E9}$$

The form of is $M^2_{H_{t1}}$ given by

$$M^2_{H_{t1}} = \begin{pmatrix} m^2_{11} & m^2_{12} & m^2_{13} & m^2_{14} & m^2_{15} \\ m^2_{21} & m^2_{22} & m^2_{23} & m^2_{24} & m^2_{25} \\ m^2_{31} & m^2_{32} & m^2_{33} & m^2_{34} & m^2_{35} \\ m^2_{41} & m^2_{42} & m^2_{43} & m^2_{44} & m^2_{45} \\ m^2_{51} & m^2_{52} & m^2_{53} & m^2_{54} & m^2_{55} \end{pmatrix}. \tag{E10}$$

The matrix entries are given by

$$
\begin{aligned}
m_{11}^2 &= \frac{v_1^2(g_L^2(-1+t_\beta^2)^2+g_R^2(-1+t_\beta^2)^2+8t_\beta^2\lambda_3^2)}{4(1+t_\beta^2)}, \qquad m_{12}^2 = m_{21}^2 = \frac{t_\beta(-1+t_\beta^2)v_1^2(g_L^2+g_R^2-2\lambda_3^2)}{2(1+t_\beta^2)},\\
m_{13}^2 &= m_{31}^2 = -\frac{\sqrt{2}t_\beta v_1 v_{R1}\lambda_3\lambda_R}{\sqrt{1+t_\beta^2}}, \qquad m_{14}^2 = m_{41}^2 = \frac{g_R^2(-1+t_\beta^2)v_1 v_{R1}}{\sqrt{2}\sqrt{1+t_\beta^2}},\\
m_{15}^2 &= m_{51}^2 = \frac{v_1\left(-\sqrt{2}T_3 t_\beta + v_S\lambda_3(\lambda_3+t_\beta^2\lambda_3-6t_\beta\lambda_S)\right)}{\sqrt{1+t_\beta^2}},\\
m_{22}^2 &= \frac{1}{2(t_\beta^3+t_\beta)}\Big(2g_L^2t_\beta^3v_1^2+2g_R^2t_\beta^3v_1^2+2\lambda_3\xi_F+\sqrt{2}T_3t_\beta^4v_S+2\sqrt{2}T_3t_\beta^2v_S+\sqrt{2}T_3v_S\\
&\quad+2\lambda_3\xi_Ft_\beta^4+4\lambda_3\xi_Ft_\beta^2-4\lambda_3^2t_\beta^3v_1^2+\lambda_3\lambda_Rt_\beta^4v_{R1}^2+2\lambda_3\lambda_Rt_\beta^2v_{R1}^2+3\lambda_3\lambda_St_\beta^4v_S^2\\
&\quad+6\lambda_3\lambda_St_\beta^2v_S^2+\lambda_3\lambda_Rv_{R1}^2+3\lambda_3\lambda_Sv_S^2\Big),\\
m_{23}^2 &= m_{32}^2 = \frac{\lambda_3\lambda_R(t_\beta^2-1)v_1v_{R1}}{\sqrt{2}\sqrt{t_\beta^2+1}}, \qquad m_{24}^2 = m_{42}^2 = \frac{\sqrt{2}g_R^2t_\beta v_1v_{R1}}{\sqrt{t_\beta^2+1}},\\
m_{25}^2 &= m_{52}^2 = \frac{(t_\beta^2-1)v_1\left(\sqrt{2}T_3+6\lambda_3\lambda_sv_s\right)}{2\sqrt{t_\beta^2+1}}, \qquad m_{33}^2 = \lambda_R^2v_{R1}^2, \qquad m_{34}^2 = m_{43}^2 = 0,\\
m_{35}^2 &= m_{53}^2 = v_{R1}\left(T_R+\sqrt{2}\lambda_Rv_s(\lambda_R+3\lambda_s)\right), \qquad m_{45}^2 = m_{54}^2 = 0,\\
m_{44}^2 &= 2g_B^2v_{R1}^2+2g_R^2v_{R1}^2-2\lambda_R\xi_F+\lambda_3\lambda_Rt_\beta v_1^2-\sqrt{2}T_Rv_s-\lambda_R^2v_{R1}^2-3\lambda_R\lambda_sv_s^2,\\
m_{55}^2 &= \frac{-2\sqrt{2}\xi_s+\sqrt{2}T_3t_\beta v_1^2-\sqrt{2}T_Rv_{R1}^2+3\sqrt{2}T_Sv_s^2+36\lambda_s^2v_s^3}{2v_s}.
\end{aligned}
\tag{E11}
$$

It is straightforward to observe that, when $\tan\beta_R = 1$, the Higgs boson with the basis state $\frac{1}{\sqrt{1+t_\beta^2}}(H_{21}^0 - t_\beta H_{12}^0)$ exhibits negligible mixing with the other Higgs bosons. Therefore, we decouple this particular Higgs state from the system. As a result, the original 5×5 mass matrix $M_{H_{t1}}^2$ is effectively reduced to a 4×4 matrix. We define the decoupled 4×4 matrix as $M_{H_{t2}}^2$, whose explicit form is given by

$$
M_{H_{t2}}^2 = \begin{pmatrix} (M_{t11}^2)_{2\times2} & (M_{t12}^2)_{2\times2} \\ (M_{t21}^2)_{2\times2} & (M_{t22}^2)_{2\times2} \end{pmatrix}, \tag{E12}
$$

where

$$
\begin{aligned}
M_{t11}^2 &= \begin{pmatrix} m_{11}^2 & m_{13}^2 \\ m_{31}^2 & m_{33}^2 \end{pmatrix}, \quad M_{t12}^2 = \begin{pmatrix} m_{14}^2 & m_{15}^2 \\ m_{24}^2 & m_{25}^2 \end{pmatrix},\\
M_{t21}^2 &= \begin{pmatrix} m_{41}^2 & m_{43}^2 \\ m_{51}^2 & m_{53}^2 \end{pmatrix}, \quad M_{t22}^2 = \begin{pmatrix} m_{44}^2 & m_{45}^2 \\ m_{54}^2 & m_{55}^2 \end{pmatrix},
\end{aligned}
\tag{E13}
$$

where the matrix elements m_{ij}^2 are the entries of $M_{H_{t1}}^2$. By substituting $v_1/v_{R1} = \sigma$ into $M_{H_{t2}}^2$, it is evident that both M_{t21}^2 and M_{t22}^2 exhibit strong dependence on σ. We therefore treat these terms as perturbations and apply a perturbative approximation to M_{t11}^2,

$$
M_\alpha^2 = M_{t11}^2 + M_{t12}^2(M_{t11}^2 - M_{t22}^2)^{-1}M_{t21}^2. \tag{E14}
$$

In the approximated matrix M_α, the lightest and next-to-lightest Higgs bosons from the original 5×5 matrix are preserved. Because of the exceedingly complex form of the expression, we provide only their general form here,

$$
M_\alpha^2 = \begin{pmatrix} m_{\alpha11}^2 & m_{\alpha12}^2 \\ m_{\alpha21}^2 & m_{\alpha22}^2 \end{pmatrix}. \tag{E15}
$$

The expressions for the lightest and next-to-lightest Higgs bosons are provided as

$$
\begin{aligned}
F_{h_1}^2(\sigma) &= \frac{1}{2}\left(m_{\alpha11}^2+m_{\alpha22}^2-\sqrt{(m_{\alpha11}^2-m_{\alpha22}^2)^2+4m_{\alpha12}^2m_{\alpha21}^2}\right),\\
F_{h_2}^2(\sigma) &= \frac{1}{2}\left(m_{\alpha11}^2+m_{\alpha22}^2+\sqrt{(m_{\alpha11}^2-m_{\alpha22}^2)^2+4m_{\alpha12}^2m_{\alpha21}^2}\right).
\end{aligned}
\tag{E16}
$$

Finally, we perform a Taylor expansion around $\sigma = 0$ to derive approximate solutions for the masses of the lightest and next-to-lightest Higgs bosons

$$m_{h_1}^2 = \frac{F_{h_1}^{(2)}(\sigma)}{2!}\sigma^2 + \frac{F_{h_1}^{(4)}(\sigma)}{4!}\sigma^4 + \frac{F_{h_1}^{(6)}(\sigma)}{6!}\sigma^6,$$
$$m_{h_2}^2 = F_{h_2}^2(0) + \frac{F_{h_2}^{(2)}(\sigma)}{2!}\sigma^2 + \frac{F_{h_2}^{(4)}(\sigma)}{4!}\sigma^4 + \frac{F_{h_2}^{(6)}(\sigma)}{6!}\sigma^6. \tag{E17}$$

The form of $F_{h_2}^2(0)$ is given by

$$F_{h_2}^2(0) = v_{R1}^2\left(\lambda_R^2 - \frac{2v_S(T_R + \sqrt{2}v_S\lambda_R(\lambda_R + 3\lambda_S))^2}{-\sqrt{2}T_R v_{R1}^2 + 3\sqrt{2}T_S v_S^2 + 36\lambda_S^2 v_S^2 - 2\sqrt{2}\xi_S}\right), \tag{E18}$$

where $f_i^{(n)}(\sigma)$ is $\frac{\partial^{(n)}F_{h_i}^2(\sigma)}{(\partial\sigma)^n}|_{\sigma=0,i=1,2}$. Because of the complexity of the explicit analytical expressions, we refrain from providing the detailed forms of $f_i^{(n)}(\sigma)$. Under the parameter choices considered in this analysis, the zeroth-order term in the expansion of $m_{h_1}^2$ around $\sigma = 0$ is zero, whereas the zeroth-order term for $m_{h_2}^2$ is nonzero and constitutes the dominant contribution. Additionally, $f_1^{(4)}(\sigma)$ and $f_1^{(6)}(\sigma)$ are both negative, while $f_1^{(2)}(\sigma)$, $f_2^{(2)}(\sigma)$, $f_2^{(4)}(\sigma)$, and $f_2^{(6)}(\sigma)$ are all positive. The parameter σ is inversely proportional to $\tan\beta$. As $\tan\beta$ increases, the mass m_{h_1} exhibits an initial rise followed by a gradual leveling off, while m_{h_2} shows an initial decrease and then asymptotically stabilizes. This behavior is consistent with the analysis presented in the text.

APPENDIX F: NEUTRINO MASSES AND MIXING IN LRSSM

In the paper, the right-handed neutrinos can make important contributions to the mass correction of the 95 GeV Higgs particle, while the effect on the 125 GeV Higgs particle is minimal. Therefore, we present simple analysis of the neutrino sector in the LRSSM. The form of the neutrino mass matrix in the LRSSM is given by

$$M_\nu = \begin{pmatrix} 0 & m_{\nu_L\nu_R} \\ m_{\nu_R\nu_L} & m_{\nu_R\nu_R} \end{pmatrix}, \tag{F1}$$

where

$$m_{\nu_L\nu_R} = \frac{Y_\nu}{\sqrt{2}}v_1, \quad m_{\nu_R\nu_L} = \frac{Y_\nu^\dagger}{\sqrt{2}}v_1, \quad m_{\nu_R\nu_R} = \frac{h_{RR}}{\sqrt{2}}v_{R1}. \tag{F2}$$

The lightest 95 GeV Higgs is primarily composed of Δ_R and δ_R. In this case, in addition to the contributions from top quark and top squark particles, the contributions from right-handed bosons and right-handed neutrinos also become important. It is straightforward to obtain the masses of the left-handed and right-handed neutrinos as follows:

$$M_{\nu_L} \approx -\frac{v_1^2}{2}Y_\nu^\dagger m_{\nu_R\nu_R}^{-1}Y_\nu,$$
$$M_{\nu_R} \approx \frac{h_{RR}}{\sqrt{2}}v_{R1}. \tag{F3}$$

The form of Y_ν is given by

$$Y_\nu = \sqrt{2}\frac{1}{v_1}\sqrt{M_{\nu_R}^{\rm dig}}R\sqrt{M_{\nu_L}^{\rm dig}}U_{\rm PMNS}^\dagger. \tag{F4}$$

The form of the Pontecorvo-Maki-Nakagawa-Sakata (PMN-S) matrix $U_{\rm PMNS}$ is given by

$$U_{\rm PMNS} = \begin{pmatrix} c_{12}c_{13} & s_{12}c_{13} & s_{13}e^{-i\delta} \\ -s_{12}c_{23} - c_{12}s_{23}s_{13}e^{i\delta} & c_{12}c_{23} - s_{12}s_{23}s_{13}e^{i\delta} & s_{23}c_{13} \\ s_{12}s_{23} - c_{12}c_{23}s_{13}e^{i\delta} & -c_{12}s_{23} - s_{12}c_{23}s_{13}e^{i\delta} & c_{23}c_{13} \end{pmatrix}, \tag{F5}$$

where $s_{ij} = \sin(\theta_{ij})_{i,j=1,2,3}$, $c_{ij} = \cos(\theta_{ij})_{i,j=1,2,3}$, and

$$\sin^2(\theta_{12}) = 0.307 \pm 0.012,$$
$$\sin^2(\theta_{23}) = 0.537 \pm 0.020 \quad \text{(inverted order)},$$
$$\sin^2(\theta_{23}) = 0.534^{+0.015}_{-0.019} \quad \text{(normal order)},$$
$$\sin^2(\theta_{13}) = (2.16 \pm 0.06) \times 10^{-2}. \tag{F6}$$

The neutrino mass differences are provided as

$$\begin{aligned}
\Delta m^2_{21} &= (7.50 \pm 0.19) \times 10^{-5}\ \text{eV}^2, \\
\Delta m^2_{32} &= (-2.527 \pm 0.034) \times 10^{-3}\ \text{eV}^2 \quad (\text{inverted order}), \\
\Delta m^2_{32} &= (2.451 \pm 0.026) \times 10^{-3}\ \text{eV}^2 \quad (\text{normal order}), \\
\delta, CP\text{-violating phase} &= 1.21^{+0.19}_{-0.22}\pi\ \text{rad} \quad (S = 1.2), \\
\langle \Delta m^2_{21} - \Delta m^2_{21} \rangle &< 1.1 \times 10^{-4}\ \text{eV}^2, \text{CL} = 99.7\%, \\
\langle \Delta m^2_{32} - \Delta m^2_{32} \rangle &= (-0.12 \pm 0.25) \times 10^{-3}\ \text{eV}^2.
\end{aligned} \tag{F7}$$

We have calculated Y_{NO} and Y_{IO} for two scenarios: one with the lightest Higgs boson mass at 125 GeV, and the other with the lightest Higgs boson mass at 95 GeV and the next-to-lightest at 125 GeV, respectively. In both cases, δ is taken as 1.21π. In the case of inverted order (IO), we set the mass of the lightest neutrino m_{v_1} to be 0.01 eV. In the case of normal order (NO), we set the mass of the lightest neutrino m_{v_1} to be 0.0509 eV. In the scenario where the lightest Higgs boson mass is 125 GeV, the parameter values we used are $\tan\beta = 20$, $\tan\beta_R = 1.1$, $v_{R1} = 2.5$ TeV, and $h_{RR} = 2.0$. The results for $Y^{h_{125}}_{\nu(\text{NO})}$ and $Y^{h_{125}}_{\nu(\text{IO})}$ are given by

$$Y^{h_{125}}_{\nu(\text{NO})} = \begin{pmatrix} 1.262 \times 10^{-5} & -4.473 \times 10^{-6} - 7.918 \times 10^{-7} i & 7.372 \times 10^{-6} - 7.046 \times 10^{-7} i \\ 9.302 \times 10^{-6} & 1.026 \times 10^{-5} - 5.844 \times 10^{-7} i & -9.791 \times 10^{-6} - 5.214 \times 10^{-7} i \\ -4.214 \times 10^{-6} - 2.864 \times 10^{-6} i & 2.544 \times 10^{-5} & 2.638 \times 10^{-5} \end{pmatrix}, \tag{F8}$$

$$Y^{h_{125}}_{\nu(\text{IO})} = \begin{pmatrix} 2.843 \times 10^{-4} & -1.092 \times 10^{-4} - 1.786 \times 10^{-6} i & 1.663 \times 10^{-4} - 1.590 \times 10^{-5} i \\ 1.905 \times 10^{-4} & 2.104 \times 10^{-4} - 1.970 \times 10^{-6} i & -2.005 \times 10^{-4} - 1.065 \times 10^{-6} i \\ -1.873 \times 10^{-6} - 1.273 \times 10^{-6} i & 1.308 \times 10^{-5} & 1.006 \times 10^{-4} \end{pmatrix}. \tag{F9}$$

In the scenario where the lightest Higgs boson mass is 95 GeV and the next to lightest is 125 GeV, we adopt the following parameter values: $\tan\beta = 20$, $\tan\beta_R = 0.99$, $v_{R1} = 4$ TeV, and $h_{RR} = 2.0$. The resulting values for $Y^{h_{95}}_{\nu(\text{NO})}$ and $Y^{h_{95}}_{\nu(\text{IO})}$ are

$$Y^{h_{95}}_{\nu(\text{NO})} = \begin{pmatrix} 2.267 \times 10^{-5} & -8.109 \times 10^{-6} - 1.417 \times 10^{-6} i & 1.321 \times 10^{-5} - 1.274 \times 10^{-6} i \\ 1.674 \times 10^{-5} & 1.852 \times 10^{-5} - 1.046 \times 10^{-6} i & -1.759 \times 10^{-5} - 9.404 \times 10^{-7} i \\ -7.577 \times 10^{-6} - 5.149 \times 10^{-6} i & 4.553 \times 10^{-5} & 4.093 \times 10^{-5} \end{pmatrix}, \tag{F10}$$

$$Y^{h_{95}}_{\nu(\text{IO})} = \begin{pmatrix} 5.111 \times 10^{-5} & -1.814 \times 10^{-5} - 3.211 \times 10^{-6} i & 2.990 \times 10^{-5} - 2.858 \times 10^{-6} i \\ 3.425 \times 10^{-5} & 3.776 \times 10^{-5} - 2.152 \times 10^{-6} i & -3.605 \times 10^{-5} - 1.915 \times 10^{-6} i \\ -3.368 \times 10^{-6} - 2.289 \times 10^{-6} i & 2.033 \times 10^{-5} & 1.809 \times 10^{-5} \end{pmatrix}. \tag{F11}$$

In summary, while our primary goal is to account for the ~95 GeV hints in the diphoton and b-jet channels under the Higgs and collider constraints, we have now made explicit the realization of the neutrino sector consistent with our benchmarks.

[1] G. Aad *et al.* (ATLAS Collaboration), Observation of a new particle in the search for the standard model Higgs boson with the ATLAS detector at the LHC, Phys. Lett. B **716**, 1 (2012).

[2] S. Chatrchyan *et al.* (CMS Collaboration), Observation of a new boson at a mass of 125 GeV with the CMS Experiment at the LHC, Phys. Lett. B **716**, 30 (2012).

[3] G. Abbiendi *et al.* (OPAL Collaboration), Decay mode independent searches for new scalar bosons with the OPAL detector at LEP, Eur. Phys. J. C **27**, 311 (2003).

[4] R. Barate *et al.* (LEP Working Group for Higgs boson searches, ALEPH, DELPHI, L3 and OPAL Collaborations), Search for the standard model Higgs boson at LEP, Phys. Lett. B **565**, 61 (2003).

[5] S. Schael *et al.* (ALEPH, DELPHI, L3, OPAL Collaborations and LEP Working Group for Higgs Boson Searches), Search for neutral MSSM Higgs bosons at LEP, Eur. Phys. J. C **47**, 547 (2006).

[6] T. Biekötter, S. Heinemeyer, and G. Weiglein, The CMS di-photon excess at 95 GeV in view of the LHC Run 2 results, Phys. Lett. B **846**, 138217 (2023).

[7] CMS Collaboration, Search for new resonances in the diphoton final state in the mass range between 80 and 115 GeV in pp collisions at $\sqrt{s} = 8$ TeV, CMS-PAS-HIG-14-037, 2015.

[8] A. M. Sirunyan *et al.* (CMS Collaboration), Search for a standard model-like Higgs boson in the mass range between 70 and 110 GeV in the diphoton final state in proton-proton collisions at $\sqrt{s} = 8$ and 13 TeV, Phys. Lett. B **793**, 320 (2019).

[9] A. Hayrapetyan *et al.* (CMS Collaboration), Search for a standard model-like Higgs boson in the mass range between 70 and 110 GeV in the diphoton final state in proton-proton collisions at $\sqrt{s} = 13$ TeV, Phys. Lett. B **860**, 139067 (2025).

[10] S. Moretti and S. Munir, Di-photon Higgs signals at the LHC in the next-to-minimal supersymmetric standard model, Eur. Phys. J. C **47**, 791 (2006).

[11] U. Ellwanger, Enhanced di-photon Higgs signal in the next-to-minimal supersymmetric standard model, Phys. Lett. B **698**, 293 (2011).

[12] J. Cao, Z. Heng, T. Liu, and J. M. Yang, Di-photon Higgs signal at the LHC: A comparative study in different supersymmetric models, Phys. Lett. B **703**, 462 (2011).

[13] D. Albornoz Vasquez, G. Belanger, C. Boehm, J. Da Silva, P. Richardson, and C. Wymant, The 125 GeV Higgs in the NMSSM in light of LHC results and astrophysics constraints, Phys. Rev. D **86**, 035023 (2012).

[14] U. Ellwanger and C. Hugonie, Higgs bosons near 125 GeV in the NMSSM with constraints at the GUT scale, Adv. High Energy Phys. **2012**, 625389 (2012).

[15] F. Boudjema and G. D. La Rochelle, Supersymmetric Higgses beyond the MSSM: An update with flavour and dark matter constraints, Phys. Rev. D **86**, 115007 (2012).

[16] K. Schmidt-Hoberg and F. Staub, Enhanced $h \to \gamma\gamma$ rate in MSSM singlet extensions, J. High Energy Phys. 10 (2012) 195.

[17] M. Badziak, M. Olechowski, and S. Pokorski, New regions in the NMSSM with a 125 GeV Higgs, J. High Energy Phys. 06 (2013) 043.

[18] M. Badziak, M. Olechowski, and S. Pokorski, 125 GeV Higgs and enhanced diphoton signal of a light singlet-like scalar in NMSSM, Proc. Sci. EPS-HEP2013 (**2013**) 257.

[19] R. Barbieri, D. Buttazzo, K. Kannike, F. Sala, and A. Tesi, One or more Higgs bosons?, Phys. Rev. D **88**, 055011 (2013).

[20] J. W. Fan, J. Q. Tao, Y. Q. Shen, G. M. Chen, H. S. Chen, S. Gascon-Shotkin, M. Lethuillier, L. Sgandurra, and P. Soulet, Study of diphoton decays of the lightest scalar Higgs boson in the next-to-minimal supersymmetric standard model, Chin. Phys. C **38**, 073101 (2014).

[21] J. Cao, X. Jia, and J. Lian, Unified interpretation of the muon $g-2$ anomaly, the 95 GeV diphoton, and $b\bar{b}$ excesses in the general next-to-minimal supersymmetric standard model, Phys. Rev. D **110**, 115039 (2024).

[22] J. Cao, X. Jia, Y. Yue, H. Zhou, and P. Zhu, 96 GeV diphoton excess in seesaw extensions of the natural NMSSM, Phys. Rev. D **101**, 055008 (2020).

[23] T. Biekötter, M. Chakraborti, and S. Heinemeyer, The "96 GeV excess" in the N2HDM, arXiv:1910.06858.

[24] T. Biekötter, M. Chakraborti, and S. Heinemeyer, A 96 GeV Higgs boson in the N2HDM, Eur. Phys. J. C **80**, 2 (2020).

[25] T. Biekötter and M. O. Olea-Romacho, Reconciling Higgs physics and pseudo-Nambu-Goldstone dark matter in the S2HDM using a genetic algorithm, J. High Energy Phys. 10 (2021) 215.

[26] T. Biekötter, A. Grohsjean, S. Heinemeyer, C. Schwanenberger, and G. Weiglein, Possible indications for new Higgs bosons in the reach of the LHC: N2HDM and NMSSM interpretations, Eur. Phys. J. C **82**, 178 (2022).

[27] S. Heinemeyer, C. Li, F. Lika, G. Moortgat-Pick, and S. Paasch, Phenomenology of a 96 GeV Higgs boson in the 2HDM with an additional singlet, Phys. Rev. D **106**, 075003 (2022).

[28] T. Biekötter, S. Heinemeyer, and G. Weiglein, Mounting evidence for a 95 GeV Higgs boson, J. High Energy Phys. 08 (2022) 201.

[29] D. Sachdeva and S. Sadhukhan, Discussing 125 GeV and 95 GeV excess in light radion model, Phys. Rev. D **101**, 055045 (2020).

[30] T. Biekötter, S. Heinemeyer, and C. Muñoz, Precise prediction for the Higgs-boson masses in the $\mu\nu$SSM, Eur. Phys. J. C **78**, 504 (2018).

[31] T. Biekötter, S. Heinemeyer, and C. Muñoz, Precise prediction for the Higgs-Boson masses in the $\mu\nu$SSM with three right-handed neutrino superfields, Eur. Phys. J. C **79**, 667 (2019).

[32] C. X. Liu, Y. Zhou, X. Y. Zheng, J. Ma, T. F. Feng, and H. B. Zhang, 95 GeV excess in a CP-violating $\mu-$ from $-\nu$ SSM, Phys. Rev. D **109**, 056001 (2024).

[33] A. Azatov, R. Contino, and J. Galloway, Model-independent bounds on a light Higgs, J. High Energy Phys. 04 (2012) 127; 04 (2013) 140(E).

[34] S. Heinemeyer and T. Stefaniak, A Higgs boson at 96 GeV?!, Proc. Sci. CHARGED2018 (**2019**) 016.

[35] T. Mondal, S. Moretti, and P. Sanyal, On the CP nature of the '95 GeV' anomalies, Phys. Lett. B **872**, 140041 (2026).

[36] A. Khanna, S. Moretti, and A. Sarkar, Explaining 95 GeV anomalies in the 2-Higgs doublet model type-I, Nucl. Phys. **B1011**, 117229 (2026).

[37] R. N. Mohapatra and J. C. Pati, Left-right gauge symmetry and an isoconjugate model of CP violation, Phys. Rev. D **11**, 566 (1975).
[38] G. Senjanovic and R. N. Mohapatra, Exact left-right symmetry and spontaneous violation of parity, Phys. Rev. D **12**, 1502 (1975).
[39] K. Huitu, P. N. Pandita, and K. Puolamaki, Mass of the lightest Higgs boson in supersymmetric left-right models, Phys. Lett. B **423**, 97 (1998).
[40] K. Huitu, P. N. Pandita, and K. Puolamaki, Phenomenology of light Higgs bosons in supersymmetric left-right models, arXiv:hep-ph/9904388.
[41] A. Alloul, M. Frank, B. Fuks, and M. Rausch de Traubenberg, Chargino and neutralino production at the Large Hadron Collider in left-right supersymmetric models, J. High Energy Phys. 10 (2013) 033.
[42] R. M. Francis, M. Frank, and C. S. Kalman, Anomalous magnetic moment of the muon arising from the extensions of the supersymmetric standard model based on left-right symmetry, Phys. Rev. D **43**, 2369 (1991).
[43] M. Frank, Electric dipole moment of the electron in the left-right supersymmetric model, Phys. Rev. D **59**, 055006 (1999).
[44] M. Frank and S. Nie, $b^{\to}s\gamma$ in the left-right supersymmetric model, Phys. Rev. D **65**, 114006 (2002).
[45] M. Frank and S. q. Nie, $B^{\to}X_s l^+ l^-$ in the left-right supersymmetric model, Phys. Rev. D **66**, 055001 (2002).
[46] M. Frank and S. q. Nie, $B_d^0 - \overline{B}_d^0$ mixing and the $B_d \to J/\psi K_S$ asymmetry in the left-right supersymmetric model, Phys. Rev. D **67**, 075005 (2003).
[47] M. Frank, Leptogenesis in the left-right supersymmetric model, Phys. Rev. D **70**, 036004 (2004).
[48] M. Frank and I. Turan, $t \to cg, c\gamma, cZ$ in the left-right supersymmetric model, Phys. Rev. D **72**, 035008 (2005).
[49] M. Frank, D. K. Ghosh, K. Huitu, S. K. Rai, I. Saha, and H. Waltari, Left-right supersymmetry after the Higgs boson discovery, Phys. Rev. D **90**, 115021 (2014).
[50] A. Chatterjee, M. Frank, B. Fuks, K. Huitu, S. Mondal, S. K. Rai, and H. Waltari, Multileptonic signals of co-annihilating left-right supersymmetric dark matter, Phys. Rev. D **99**, 035017 (2019).
[51] M. Frank, B. Fuks, K. Huitu, S. Mondal, S. K. Rai, and H. Waltari, Left-right supersymmetric option at a high-energy upgrade of the LHC, Phys. Rev. D **101**, 115014 (2020).
[52] M. Frank, Neutrino masses in the left-right supersymmetric model, Phys. Lett. B **540**, 269 (2002).
[53] M. Frank, CP phases in the leptonic sector of LRSUSY and leptogenesis, Int. J. Mod. Phys. A **19**, 5377 (2004).
[54] M. Frank, Flavor violation from Z penguins in the left-right supersymmetric model, Mod. Phys. Lett. A **19**, 189 (2004).
[55] R. N. Mohapatra and G. Senjanovic, Neutrino mass and spontaneous parity nonconservation, Phys. Rev. Lett. **44**, 912 (1980).
[56] R. N. Mohapatra and A. Rasin, Simple supersymmetric solution to the strong CP problem, Phys. Rev. Lett. **76**, 3490 (1996).
[57] K. Huitu, A minimal supersymmetric left-right model, dark matter and signals at the LHC, Eur. Phys. J. Special Topics **229**, 3187 (2020).
[58] K. S. Babu and A. Patra, Higgs boson spectra in supersymmetric left-right models, Phys. Rev. D **93**, 055030 (2016).
[59] M. Frank, B. Fuks, K. Huitu, S. K. Rai, and H. Waltari, Resonant slepton production and right sneutrino dark matter in left-right supersymmetry, J. High Energy Phys. 05 (2017) 015.
[60] Y. Zhang, H. An, X. d. Ji, and R. N. Mohapatra, Light Higgs mass bound in SUSY left-right models, Phys. Rev. D **78**, 011302 (2008).
[61] M. Frank and B. Korutlu, Higgs Bosons in a minimal R-parity conserving left-right supersymmetric model, Phys. Rev. D **83**, 073007 (2011).
[62] G. Beall, M. Bander, and A. Soni, Constraint on the mass scale of a left-right symmetric electroweak theory from the $K_L - K_S$ mass difference, Phys. Rev. Lett. **48**, 848 (1982).
[63] P. Langacker and S. U. Sankar, Bounds on the mass of W_R and the $W_L - W_R$ mixing angle ξ in general $\mathrm{SU}(2)_L \times \mathrm{SU}(2)_R \times U(1)$ models, Phys. Rev. D **40**, 1569 (1989).
[64] P. Colangelo and G. Nardulli, Improved bound on W_R mass in left-right symmetric models from $K^0 - K^0$ mixing, Phys. Lett. B **253**, 154 (1991).
[65] R. J. Zhang, Two loop effective potential calculation of the lightest CP even Higgs boson mass in the MSSM, Phys. Lett. B **447**, 89 (1999).
[66] J. R. Espinosa and R. J. Zhang, MSSM lightest CP even Higgs boson mass to O(alpha(s) alpha(t)): The effective potential approach, J. High Energy Phys. 03 (2000) 026.
[67] G. Degrassi, P. Slavich, and F. Zwirner, On the neutral Higgs boson masses in the MSSM for arbitrary stop mixing, Nucl. Phys. **B611**, 403 (2001).
[68] G. Degrassi and P. Slavich, On the radiative corrections to the neutral Higgs boson masses in the NMSSM, Nucl. Phys. **B825**, 119 (2010).
[69] M. Quiros, Finite temperature field theory and phase transitions, arXiv:hep-ph/9901312.
[70] S. Gao, S. M. Zhao, S. Di, X. X. Dong, and T. F. Feng, A 95 GeV Higgs boson in the $U(1)_X$SSM, Nucl. Phys. B **1018**, 117026 (2025).
[71] B. O'Leary, W. Porod, and F. Staub, Mass spectrum of the minimal SUSY B-L model, J. High Energy Phys. 05 (2012) 042.
[72] D. M. Pierce, J. A. Bagger, K. T. Matchev, and R. j. Zhang, Precision corrections in the minimal supersymmetric standard model, Nucl. Phys. **B491**, 3 (1997).
[73] P. Slavich, S. Heinemeyer, E. Bagnaschi, H. Bahl, M. Goodsell, H. E. Haber, T. Hahn, R. Harlander, W. Hollik, G. Lee *et al.*, Higgs-mass predictions in the MSSM and beyond, Eur. Phys. J. C **81**, 450 (2021).
[74] E. A. R. R. and R. Fazio, High-precision calculations of the Higgs boson mass, Particles **5**, 53 (2022).
[75] M. Quiros, Constraints on the Higgs boson properties from the effective potential, Adv. Ser. Dir. High Energy Phys. **17**, 148 (1997).
[76] G. Degrassi, S. Heinemeyer, W. Hollik, P. Slavich, and G. Weiglein, Towards high precision predictions for the MSSM Higgs sector, Eur. Phys. J. C **28**, 133 (2003).
[77] S. P. Martin, Three-loop corrections to the lightest Higgs scalar boson mass in supersymmetry, Phys. Rev. D **75**, 055005 (2007).

[78] R. V. Harlander, P. Kant, L. Mihaila, and M. Steinhauser, Higgs boson mass in supersymmetry to three loops, Phys. Rev. Lett. **100**, 191602 (2008).
[79] S. Heinemeyer, O. Stal, and G. Weiglein, Interpreting the LHC Higgs search results in the MSSM, Phys. Lett. B **710**, 201 (2012).
[80] A. Arbey, M. Battaglia, A. Djouadi, and F. Mahmoudi, The Higgs sector of the phenomenological MSSM in the light of the Higgs boson discovery, J. High Energy Phys. 09 (2012) 107.
[81] K. J. Bae, Reconsidering the blind spots of neutralino dark matter: A perturbative approach, New Phys. Sae Mulli **72**, 573 (2022).
[82] M. A. Shifman, A. I. Vainshtein, M. B. Voloshin, and V. I. Zakharov, Low-energy theorems for Higgs boson couplings to photons, Sov. J. Nucl. Phys. **30**, 711 (1979).
[83] L. Bergstrom and G. Hulth, Induced Higgs couplings to neutral bosons in e^+e^- collisions, Nucl. Phys. **B259**, 137 (1985); **B276**, 744(E) (1986).
[84] A. Djouadi, The anatomy of electro-weak symmetry breaking. II. The Higgs bosons in the minimal supersymmetric model, Phys. Rep. **459**, 1 (2008).
[85] G. Cacciapaglia, A. Deandrea, and J. Llodra-Perez, $H \to \gamma\gamma$ beyond the standard model, J. High Energy Phys. 06 (2009) 054.
[86] W. Bernreuther, P. Gonzalez, and M. Wiebusch, Pseudoscalar Higgs bosons at the LHC: Production and decays into electroweak gauge bosons revisited, Eur. Phys. J. C **69**, 31 (2010).
[87] P. Gonzalez, S. Palmer, M. Wiebusch, and K. Williams, Heavy MSSM Higgs production at the LHC and decays to WW,ZZ at higher orders, Eur. Phys. J. C **73**, 2367 (2013).
[88] L. Resnick, M. K. Sundaresan, and P. J. S. Watson, Is there a light scalar boson?, Phys. Rev. D **8**, 172 (1973).
[89] A. Arbey, A. Deandrea, F. Mahmoudi, and A. Tarhini, Anomaly mediated supersymmetric models and Higgs data from the LHC, Phys. Rev. D **87**, 115020 (2013).
[90] ATLAS Collaboration, Search for diphoton resonances in the 66 to 110 GeV mass range using 140 fb^{-1} of 13 TeV pp collisions collected with the ATLAS detector, CERN Report No. ATLAS-CONF-2023-035, 2023.
[91] J. Cao, X. Jia, J. Lian, and L. Meng, 95 GeV diphoton and $b\bar{b}$ excesses in the general next-to-minimal supersymmetric standard model, Phys. Rev. D **109**, 075001 (2024).
[92] F. Richard, Search for a light radion at HL-LHC and ILC250, arXiv:1712.06410.
[93] U. Haisch and A. Malinauskas, Let there be light from a second light Higgs doublet, J. High Energy Phys. 03 (2018) 135.
[94] D. Liu, J. Liu, C. E. M. Wagner, and X. P. Wang, A light Higgs at the LHC and the B-anomalies, J. High Energy Phys. 06 (2018) 150.
[95] J. M. Cline and T. Toma, Pseudo-Goldstone dark matter confronts cosmic ray and collider anomalies, Phys. Rev. D **100**, 035023 (2019).
[96] J. A. Aguilar-Saavedra and F. R. Joaquim, Multiphoton signals of a (96 GeV?) stealth boson, Eur. Phys. J. C **80**, 403 (2020).
[97] S. Bhattacharya, G. Coloretti, A. Crivellin, S. E. Dahbi, Y. Fang, M. Kumar, and B. Mellado, Growing excesses of new scalars at the electroweak scale, arXiv:2306.17209.
[98] S. Banik, G. Coloretti, A. Crivellin, and B. Mellado, Uncovering new Higgses in the LHC analyses of differential $t\bar{t}$ cross sections, J. High Energy Phys. 01 (2025) 155.
[99] G. Coloretti, A. Crivellin, and B. Mellado, Combined explanation of LHC multi-lepton, di-photon and top-quark excesses, Phys. Rev. D **110**, 073001 (2024).
[100] A. Tumasyan *et al.* (CMS Collaboration), Searches for additional Higgs bosons and for vector leptoquarks in $\tau\tau$ final states in proton-proton collisions at $\sqrt{s} = 13$ TeV, J. High Energy Phys. 07 (2023) 073.
[101] D. Azevedo, T. Biekötter, and P. M. Ferreira, 2HDM interpretations of the CMS diphoton excess at 95 GeV, J. High Energy Phys. 11 (2023) 017.
[102] CMS Collaboration, Search for dilepton resonances from decays of (pseudo)scalar bosons produced in association with a massive vector boson or top quark anti-top quark pair at $\sqrt{s} = 13$ TeV, CERN Report No. CMS-PAS-EXO-21-018, 2022.
[103] S. Iguro, T. Kitahara, and Y. Omura, Scrutinizing the 95–100 GeV di-tau excess in the top associated process, Eur. Phys. J. C **82**, 1053 (2022).
[104] CMS Collaboration, Search for a standard model-like Higgs boson in the mass range between 70 and 110 GeV in the diphoton final state in proton-proton collisions at $\sqrt{s} = 13$ TeV, CMS-PAS-HIG-20-002, 2023.
[105] J. Cao, X. Guo, Y. He, P. Wu, and Y. Zhang, Diphoton signal of the light Higgs boson in natural NMSSM, Phys. Rev. D **95**, 116001 (2017).
[106] T. Biekötter, M. Chakraborti, and S. Heinemeyer, The "96 GeV excess" at the LHC, Int. J. Mod. Phys. A **36**, 2142018 (2021).
[107] A. Djouadi, The anatomy of electro-weak symmetry breaking. I: The Higgs boson in the standard model, Phys. Rep. **457**, 1 (2008).
[108] R. L. Workman *et al.* (Particle Data Group), Review of particle physics, Prog. Theor. Exp. Phys. **2022**, 083C01 (2022).
[109] S. Navas *et al.* (Particle Data Group), Review of particle physics, Phys. Rev. D **110**, 030001 (2024).
[110] Y. Horii (ATLAS Collaboration), Searches for singly- and doubly-charged Higgs bosons in ATLAS, Proc. Sci. ICHEP2024 (**2025**) 070.
[111] G. Aad *et al.* (ATLAS Collaboration), Search for doubly charged Higgs boson production in multi-lepton final states using 139 fb^{-1} of proton–proton collisions at $\sqrt{s} = 13$ TeV with the ATLAS detector, Eur. Phys. J. C **83**, 605 (2023).
[112] G. Aad *et al.* (ATLAS Collaboration), Search for doubly and singly charged Higgs bosons decaying into vector bosons in multi-lepton final states with the ATLAS detector using proton-proton collisions at $\sqrt{s} = 13$ TeV, J. High Energy Phys. 06 (2021) 146.
[113] A. M. Sirunyan *et al.* (CMS Collaboration), Search for charged Higgs bosons decaying into a top and a bottom quark in the all-jet final state of pp collisions at $\sqrt{s} = 13$ TeV, J. High Energy Phys. 07 (2020) 126.
[114] K. S. Babu and R. N. Mohapatra, Minimal supersymmetric left-right model, Phys. Lett. B **668**, 404 (2008).